Ex Vivo Gene Therapy Approaches for the Treatment of Globoid Cell Leukodystrophy

Thesis

UNRESTRICTED

Ilaria Visigalli

EX VIVO GENE THERAPY APPROACHES FOR THE TREATMENT OF GLOBOID CELL LEUKODYSTROPHY

PhD thesis in fulfillment of the requirements of the Open University for the degree of Doctor of Philosophy in Molecular and Cellular Biology

2009

Director of studies
Prof. Luigi Naldini

External Supervisor
Prof. Adrian Thrasher

Vita-Salute San Raffaele University
Telethon Institute for Gene Therapy (TIGET)
DIBIT, San Raffaele Scientific Institute,
Milan, Italy

Submission date: 23 January 2009
Date of award: 28 April 2009

ABSTRACT

Globoid cell leukodystrophy (GLD) is a rare lysosomal storage disorder (LSD) due to the deficiency of the lysosomal enzyme Galactocerebrosidase (GALC). The enzymatic deficiency results in intracellular storage of undegraded metabolites in the nervous system, leading to progressive dysmyelination. We are testing the feasibility and efficacy of a gene therapy strategy based on hematopoietic stem/progenitor cells (HSPC) and lentiviral vectors (LV) in the murine model of GLD. Differently from what observed with other lysosomal enzymes, GALC gene transfer and expression in HSPC causes apoptosis and functional impairment of the transduced cells due to an inbalance of the intracellular content in bioactive sphingolipids consequent to de novo enzyme expression. Differentiated cells of the myeloid and lymphoid lineages are not affected by GALC expression, suggesting a unique sensitivity of HSPC to enzyme toxicity.

To overcome this issue, we explored strategies aimed at de-targeting vector expression from HSPC, while permitting GALC over-expression in differentiated cells. The first approach aims at a transcriptional regulation of GALC expression by the microglia/macrophage specific promoter CD11b. The second strategy exploits endogenous microRNAs for post-transcriptional regulation of GALC expression. The use of LV containing the target sequence of miRNA126, expressed only in HSPC, allows expressing GALC only in the differentiated progeny of transduced HSPC. Although these two approaches proved to be very promising in protecting HSPC from enzyme toxicity both *in vitro* and *in vivo* in heterozygous GLD mice, gene-corrected HSPC failed to repopulate lethally irradiated homozygous GLD mice. This poor result might be explained by the existence of a niche defect in homozygous GLD mice, which might hamper the engraftment of HSPC.

LIST OF CONTENTS

1. Globoid Cell Leukodystrophy

1.1 Lysosomal Storage Disorders

Lysosomal storage disorders (LSDs) are a group of inherited disorders caused by defects in the genes which control the lysosomal degradation of naturally occurring proteins, glycoproteins, sphingolipids, glycosaminoglycans (GAGS) and carbohydrates, and the transport of certain smaller molecules from lysosomes. The likelihood of an individual being affected with an LSD is estimated to occur in about 1 in 5000-8000 births in the United States and Europe [1]. The majority of LSDs are caused by mutations in the genes coding for lysosomal enzymes and most are inherited in an autosomal recessive manner. Depending on the specificity of the enzyme and the nature of the mutation, there will be one or more substrates whose catabolism is affected by the deficiency. Tissues with no naturally present substrate will have little or no pathology, while the accumulation of undegraded material in cells where the substrate is physiologically present, usually results in cellular pathology. In addition to the pathology caused by engorging the lysosomes with undegraded storage products, possibly disrupting normal lysosomal functions, some undegraded products may be toxic to other organelles leading to the death of certain cell types.

Although the majority of LSDs are caused by defects in the lysosomal enzymes directly involved in catabolism, some LSDs are due to defects in the sphingolipid activator proteins, saposins which are required for interactions between sphingolipid substrates and the enzyme. In addition, a few other LSDs are caused by defects in the enzymes involved in post-translational modification of lysosomal enzymes.

1.2 Globoid Cell Leukodystrophy: clinical manifestation

Globoid Cell Leukodystrophy (GLD), or Krabbe disease, is an autosomal recessive LSD caused by deficiency of the lysosomal enzyme Galactocerebrosidase (GALC) which catalyzes the catabolism of galactosylceramide (GalCer). It is a rare LSD, with an incidence of 1 in 100,000 live births worldwide. GLD was first described in children as a syndrome that began during infancy and was characterized by tonic spasms, nystagmus, muscular rigidity, progressive quadriplegia and early death [2 3]. It affects both the central nervous system (CNS) and the peripheral nervous system (PNS) and the typical neuropathological finding includes generalized brain atrophy with the central white matter being replaced by gliotic tissue. Postmortem examination of affected individuals reveals loss of myelin, degeneration of long spinal tracts, gliosis and infiltration of characteristic globoid cells of macrophage-microglia origin. The prognosis is severe, leading to death a few years after diagnosis. Clinically, GLD is classified according to the patient's age at onset. Different forms of GLD exist: early infantile (EI), late infantile (LI), juvenile (J) and adult (AD). The most severe variant is the one with EI presentation, which accounts for over 90% of patients, becoming manifest within six months of age in most cases [4] and developing in four stages [3]:

Pre-symptomatic stage: infants are able to fix and follow visual targets and can reach for objects.

Stage 1 (3 to 4 months): photic and auditory sensitivity, extreme irritability, neurogenic fever, developmental arrest followed by regression and tonic spasms.

Stage 2: tonic flexion of arms and extension of legs, loss of all previously acquired skills, seizures, optic atrophy and blindness.

Stage 3 (before 12 months): immobile, decerebrate and unable to feed.

The LI variant is much less common and begins between 19 months and four years of age [5]. These patients have only moderate mental retardation during the first years, but gradually develop ataxia and spasticity. Peripheral neuropathy is severe. Disease

progression is slower than in EI manifestation, with visual loss, mental regression, seizures and deafness. The prognosis is severe, leading to death 5-7 years after diagnosis.

The late-onset variants are the J (onset at 4 to 19 years) and the AD forms (>20 years). These are characterized by a slowly progressive tetraplegia, sensor-motor demyelinating neuropathy and preserved mental function; survival into the seventh decade is possible [6 7].

1.3 GALC: the gene and the enzyme

The GALC gene was mapped in 1990 by restriction fragment length polymorphism (RFLP) studies: it lies at 14q31 and spans 17 exons over a 60 kb interval [8]. The 5' UTR region, considered as the promoter region, contains 13 GGC sequences and binding sites for SP1, YY1, E2F and AP3 trascription factors [9]. CAAT sequences or TATA box, present in the promoter regions of other lysosomal enzymes, are absent in the GALC promoter. At the 5' end of the first intron, 6 binding sites for Sp1, 1 for AP1 and 8 for AP2, were found. The presence of an inhibitory region, from 800 bp to 300 bp upstream of the start codon, together with a sub optimal transcription start site and the general weakness of the promoter, could explain the low level of the GALC enzyme detected in all tissues examined so far (i.e. fibroblasts, leukocytes). GALC is also expressed at a low level in the nervous system, where the first substrate of GALC, GalCer is present in high concentration [10].

The GALC cDNA, encodes a 669 residue protein of about 80 kDa with a 26 amino acid leader sequence [4]. In the lysosome, this pro-enzyme is further cleaved to a 50 kDa amino terminal and a 30 kDa carboxy terminal subunits. These subunits associate to form the functional enzymatic complex [11].

GALC works within the lysosome at low pH (between 4 and 4.4), together with activators such as Saposine A and C [12]. The main substrates of GALC are GalCer and

Psychosine (Psy): GalCer is hydrolyzed to ceramide (Cer), while Psy is hydrolyzed to Sphingosine (So). Other substrates of GALC are Monogalactosyldiglyceride (MGD) and Lactosylceramide (LacCer) [13] (Figure 1).

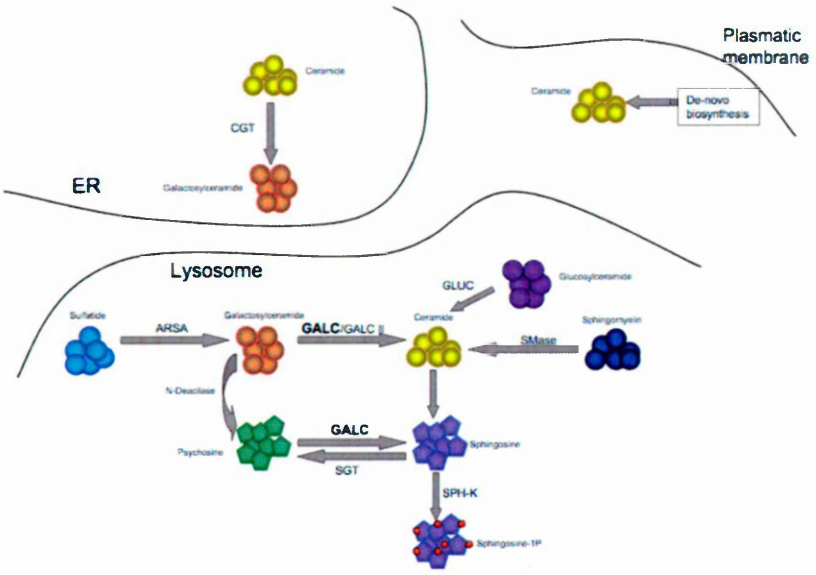

Figure 1. GALC pathway. Galactocerebrosidase (GALC) catalyzes the hydrolysis of Galactosylceramide to Ceramide in the lysosome. Ceramide is also produced at the level of plasmatic membrane (de-novo biosynthesis), while it is converted to Galactosylceramide by Ceramide-galactosyltransferase (CGT) in the endoplasmic reticulum (ER). GLUC: Glucocerebrosidase; SMase: Sphingomyelinase; SPH-K: Sphingosine kinase; ARSA: Arylsufatase A; SGT: Sphingosine-galactosyltransferase; GALC II: Galactocerebrosidase II.

The most relevant of these substrates is GalCer, produced from Cer by Ceramide-Galactosyltransferase (CGT) in the endoplasmic reticulum and from sulfatide by Arylsulfatase A (ARSA) in the lysosome. GalCer and sulfatides represent one third of the whole lipidic myelin mass [14]. Moreover, GalCer is implicated in the transduction of signals for oligodendrocytes differentiation and in axon-glia interaction at paranode level [15] [16]. Although GalCer is the first substrate of GALC, it does not accumulate in GALC deficient tissues, likely due to the activity of a different galactocerebrosidase (see paragraph 1.4). GALC deficiency is actually responsible for Psy accumulation, up to 10-20 times normal levels in human infants and animal models. This toxic storage has been

shown to kill oligodendrocytes by an apoptotic mechanism, resulting in a greatly diminished amount of myelin and astrocytic gliosis and the production of the characteristic globoid cells (for details, see paragraph 1.4).

As shown in figure 1, Cer, the first product of GALC, can be considered to be a metabolic hub since it occupies a central position in sphingolipid biosynthesis and catabolism. Cer and other molecules of this pathway, such as So and Sphingosine-1-Phosphate (S1P), are considered "bioactive sphingolipids": they act as signals regulating a vast number of cellular processes. Cer has been implicated in differentiation, cell cycle arrest and senescence in several cell types, but the most studied function is its role as a pro-apoptotic molecule [17] [18]. An accumulation of Cer has been observed prior to the activation of execution caspases but downstream of initiation caspase [19] [20] [21]. So has also been demonstrated to have a pro-apoptotic activity in a Cer-independent manner, while S1P promotes proliferation, survival and inhibition of apoptosis [22]. In addition to the vast number of processes that sphingolipids are associated with, further levels of complexity arise from the metabolic interconnection of bioactive lipids.

1.4 Pathogenetic mechanism

1.4.1 Accumulation of Psychosine

After GALC was identified as the gene responsible for GLD [23], the lack of accumulation of GalCer in the white matter of GLD patients and the observation of Psy storage was an unexpected finding. It was first hypothesized that this could be due to the early death of accumulating oligodendrocytes [24]. Subsequently, several hypotheses were formulated:

- GalCer might be converted to Psy by N-Deacilase, but the existence of this alternative pathway has never been demonstrated [25] (figure 1).

- Psy is also obtained through galactosylation of sphingosine by UDP-Galactose:sphingosine1-β-Galactosyltransferase [26]. In physiological conditions, GALC converts Psy to sphingosine and hydrolyzes GalCer to Cer; in the absence of GALC, GalCer could be hydrolyzed by Galactosylceramidase II. This enzyme, deficient in GM1 Gangliosidosis, has a low affinity for Psy, which is not metabolized and accumulates in the white matter and, to a lesser extent, in other tissues [27] (Figure 1).

1.4.2 Toxic effects of Psychosine storage

Since sphingolipids and Psy precursors are abundant in myelin, the accumulation of Psy mainly affects myelin forming cells, such as oligodendrocytes and Schwann cells. In affected subjects these cells are rapidly lost; in early onset-forms this loss occurs mainly during the early stages of brain development. Although the toxic effect of Psy storage has been studied in depth, it is still not fully understood. Psy acts mainly in mitochondria, both by a specific inhibition of cytochrome C oxidase and the aspecific alteration of mitochondrial membranes [28]. *In vitro* studies on oligodendrocyte progenitor cells have demonstrated that caspases 8, 9 and 3 are involved in Psy-induced apoptosis [29]. Further studies have shown that Psy-induced cell death also involves the activation of secretory phospholipase A2 (sPLA2), which generates lysophosphatidylcholine and arachidonic acid. sPLA2 activation also leads to oxygen-reactive species (ROS) production and oxidative stress [30]. As well as the activation of oxidative stress and apoptotic oligodendrocyte cell death, Psy down-regulates survival pathways including nuclear factor-kB and PI3K-Akt.

Several studies have reported the expression of pro-inflammatory cytokines and chemokines in cell cultures from GLD patients and twitcher mice, a murine model of GLD (see paragraph 1.6). Moreover, expression of iNOS and glial fibrillary acidic protein (GFAP) in activated astrocytes in the CNS of GLD patients, indicates the

involvement of an inflammatory process in the pathogenesis of GLD. In astrocytes, Psy maintains the production of inflammatory mediators by inducing the nuclear translocation of the transcriptional factor C/EPB, which, in turn, stimulates the production of IL-6, IL-1β and TNF-α [30]. Further studies have shown that Psy mediates the inactivation of AMP-activated protein kinase (MAPK): this results in an alteration of lipids both in astrocytes and oligodendrocytes and in up-regulation of C/EPB [30 31, 32].

Psy also induces alterations at the level of peroxisomes, involved in the biosynthesis of plasmalogens (important constituents of myelin), in β-oxidation of fatty acids and in detoxification from H_2O_2. Indeed, Psy acts by up-regulating sPLA2, which results in the down-regulation of PPAR-α, a factor involved in the transcriptional regulation of peroxisomal proteins [32].

Psy also accumulates into microglia, leading to the formation of globoid cells (GC). GC have mainly been observed in less recent CNS lesions of GLD patients [33]: these cells of the monocytic lineage, are positive to PAS-staining and display microglia-specific markers, such as vimentin and ferritin [34]. In the CNS of GLD patients, the presence of pro-inflammatory cytokines secreted by astrocytes, together with the debris of dead oligodendrocytes, contribute to the generation of a neuroinflammatory environment and the activation of microglia. Activated microglia engulf dead cells and Psy but are unable to metabolize this toxic molecule due to the GALC deficiency. The origin of GC seems to be caused by the effect of Psy on the cell cycle regulation: Psy inhibits cytokinesis without inhibiting cell division [35], leading to the formation of giant GC, filled with non-metabolized material [36] which impairs their scavenger activity. As a direct consequence, the cellular debris cannot be cleared, thus further worsening neuroinflammation [37 38] (Figure 2).

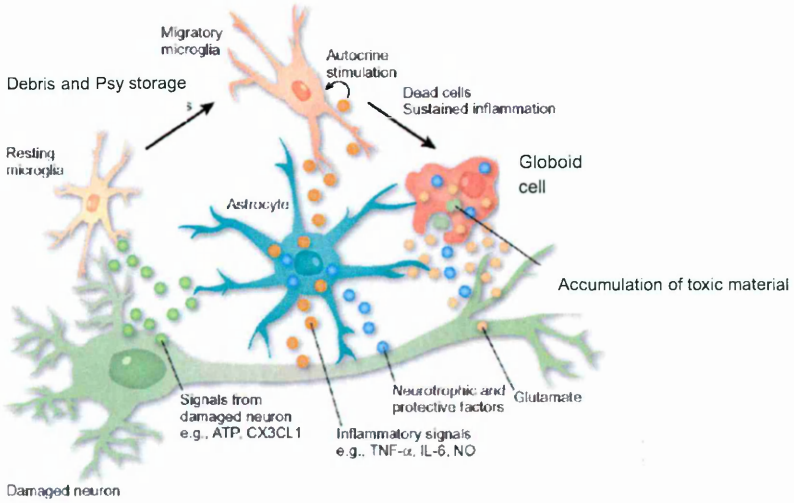

Figure 2. Formation of globoid cells. Inflammatory cytokines secreted by astrocytes and cellular debris activate resting microglia. Activated microglia engulf dead cells and Psy, which is stored in toxic deposits and leads to globoid cell formation.

The role of Psy in the occurrence of inflammation and immune activation of peripheral blood mononuclear cells (PBMC) has recently been demonstrated. PBMC from GLD patients show a basal pro-inflammatory pattern and an increased production of pro-inflammatory cytokines, which seems to be induced and amplified by Psy upon *in vitro* administration [39]. The Psy-induced pro-inflammatory response has been also observed in the liver of twitcher mice. Although the level of Psy accumulation in the liver is lower than that found in the nervous system, the toxic metabolite storage can trigger the induction of an inflammatory response which in turn, increases expression of pro-inflammatory cytokines, such as TNF-α and IL-6. Moreover, although the storage of Psy *per* gram of liver tissue is low, given the large size of the liver itself, this organ may represent an important Psy reservoir [40].

1.5 Diagnosis

1.5.1 Clinical features that suggest an LSD

The diagnosis of a patient with an LSD, initially requires a physician to consider whether the individual's clinical features are suggestive of this possibility. LSDs should

be considered in any individual experiencing developmental delay, loss of learning skills, ataxia, seizures and dementia, in the presence or absence of hepatosplenomegaly and other somatic changes. This is especially true if the individual is regressing after a period of relatively normal development and if the disease seems progressive. It should be remembered that most LSDs are progressive and early diagnosis is of the utmost importance, both for genetic counseling purposes and consideration for treatment. Neurological symptoms, in the absence of additional findings, could signal GLD, metachromatic leukodystrophy (MLD), neuronal ceroid lipofuscinoses or Schindler's disease. Patients with mild to severe neurological symptoms who are also of short stature and have evidence of coarse facial features, hepatosplenomegaly, corneal clouding and /or unusual skin findings, require a larger battery of tests which include analysis for mucopolysaccharidosis (MPS) and Gaucher disease, so as to arrive at a definitive diagnosis (Table 1).

Name of disease	Defective protein	Initial signs and symptoms
Metachromatic leukodystrophy (MLD)	Arylsulfatase A	LI: weakness, hypotonia, developmental delay, genu recurvatum JU: weakness, ataxia, behaviour changes AD: pyramidal or cerebellar signs, psychoses, behaviour changes, dementia
Globoid cell leukodystrophy (GLD)	Galactocerebrosidase	EI-LI: spasticity, irritability, hypotonia, fisting, developmental delay JU-AD: spastic paraparesis, weakness, burning paresthesia, ataxia, vision loss
Mucopolysaccharidosis type I Hurler (MPS I)	α-L-iduronidase	Coarse facial features, developmental delay, dysostosis multiplex, mental retardation, hearing loss, corneal clouding, hernias
Gaucher disease types II and III	Glucocerebrosidase	Hepatosplenomegaly, developmental delay, strabismus, seizures, myoclonus, horizontal supranuclear gaze palsy

Table 1. Examples of LSD with neurological symptoms (MLD and GLD) or with neurological, visceral and skeletal manifestations (MPS I and Gaucher disease).

1.5.2 Diagnostic instrumental evaluation of GLD

A patient suspected of having GLD, according to neurological symptoms, should have a magnetic resonance imaging (MRI) scan to evaluate the white matter: infants with EI and LI GLD have abnormal T1 and T2 intensity, indicating a loss of myelin in the posterior limb of the internal capsule. As the disease progresses, gray matter atrophy and abnormality of cerebellar white matter and pyramidal tracts develop [41 42]. With the progression of GLD, all white matter structures become abnormal, with a high signal in T1-weighted images in the thalamus, suggesting a paramagnetic effect due to the presence of hydrophilic material. At postmortem, these regions show an abundant infiltration of GC and macrophages and severe demyelination. JU and AD GLD can present with relatively mild changes in the posterior corpus callosum and parieto-occipital white matter [43 44 45].

Electrophysiological studies and electroencephalograms (EEG) are helpful in evaluating nerve conduction and monitoring disease progression. The severity of the abnormalities detected by electrophysiological testing (slow nerve conduction), usually correlates with the severity of the abnormalities on MRI scans. EEG is usually normal at the early stages of the disease, but generalized slowing and multifocal epileptic spikes are observed in the later stages [46].

1.5.3 Enzymatic activity and genetic diagnosis

The accurate diagnosis of patients, especially those early in the course of their disease, is a challenge for both the clinician and the laboratory performing diagnostic testing. As clinical features frequently overlap. Between different LSDs as well as other genetic and non-genetic disorders, a wide range of tests may be indicated after examination of a patient. Testing of most LSDs usually entails the measurement of enzymatic activities, using synthetic or natural substrates in easily obtained tissue

samples, detection of an abnormal level of a metabolic product in cells or urine, or identification of a known mutation in certain families or within certain ethnic groups.

1.5.3.1 Enzymatic activity

Most LSDs can be diagnosed by measuring the activity of selected enzymes with commercially available synthetic or radiolabeled natural substrates, using an appropriate sample sent to a laboratory. Typically, the finding of low activity for one lysosomal enzyme and normal values for others, results in a diagnosis. The specific test to confirm the diagnosis of GLD, is the measurement of GALC activity in serum, leukocytes or fibroblasts, using a ^{3}H-GalCer. While normal values range between 0,9-4,4 nmol/h/mg [47], in GLD patients the average of measured GALC activity is 0,07 nmol/h/mg [48]. The reduction of GALC activity can be further confirmed by repeating the same test on cerebrospinal fluid.

1.5.3.2 Molecular analysis

Over 40 different genes are involved in LSDs and most are inherited in an autosomal recessive manner. Many disease causing mutations and polymorphic changes have been identified in these genes and many patients are compound heterozygotes, having two different mutations in the two copies of the same gene. This results in the wide range of clinical features that is characteristic of most LSDs and is responsible for the difficulty in predicting the clinical course of newly diagnosed patients, especially those with J and AD onset. The use of molecular analysis may be beneficial once diagnosis has been made, to aid carrier screening of family members.

Since defects in Saposine A (SapA), the activator of GALC, may also cause GLD [49], genetic testing is the definitive test for GLD diagnosis. In SapA -/- patients, the reduced GALC activity is not due to a defect in the GALC gene, but to the loss of function of Sap A, which is essential for GALC functionality. Seventy-eight variants of the more

common GALC sequence have been identified to date (The Human Gene Mutation Database at the Institute of Medical Genetics in Cardiff – update: December 2007). Among these variants, over 60 mutations affecting GALC are associated with GLD, including base transitions, single amino acidic substitutions and deletions. A 30 kb deletion, from the intron 10 to the 3' end of the gene, is present in 40-50% of cases of EI and LI GLD in Europe [8 50]. This allele frequently carries a polymorphism present in 4% of the population, a C to T transition at position 502. Most of the mutations found in patients with the EI and LI GLD, are located in the region encoding for the 30 kDa subunit of the enzyme, suggesting a critical role of this subunit for the functionality of the enzyme [4]. AD cases are frequently characterized by heterozygosity for a 502/del mutation, but many other mutations, mainly in the region encoding for the 50 kDa subunit, have been found [44 51 45].

When a patient is diagnosed with an LSD, the first question is what clinical course lies ahead for the patient. This is important, in order to select those patients who would benefit most from aggressive therapy. Many authors have analyzed GALC mutations to establish a correlation between genotype and phenotype, but neither the specific mutation nor the residual enzymatic activity are definitively predictive of disease progression. From experiences with patients affected by the late-onset form of GLD, it is clear that there is tremendous variability even between siblings with the same genotype for the GALC gene [13].

1.5.3.3 Prenatal diagnosis and newborn screening for LSDs

Many LSDs are severe, resulting, as in the case of GLD, in early death a few years after diagnosis. However, the success of most treatments, such as hematopoietic stem cell transplantation (HSCT), depends on the accurate diagnosis of patients before symptoms, especially those affecting the nervous system, become overwhelming. The

identification of a patient at birth would result in careful clinical observation and treatment could begin when deemed appropriate (Figure 3). The initial promise of LSD screening using the 'generic' lysosomal storage disease proteins, lysosomal-associated membrane protein (LAMP-1) [52] and saposins, has not been realized in prospective studies. Prenatal diagnosis is extremely accurate using a direct chorionic villus sample, cultured trophoblasts and cultured amniotic fluid cells. There are two different approaches currently used for screening: measurement of lysosomal protein activity [53 54], or of protein amount [55 56]. Both use multiplex assays and usually do 'second-tier' testing on the same initial sample. A third method for newborn screening has recently been developed, based on the quantification of enzyme activity by tandem mass spectrometry on dried blood spots. Previous studies have shown that lysosomal enzymes are active in dried blood spots [55]. Li and colleagues reported that it is possible to incubate rehydrated dried blood spots from newborn-screening cards with buffer containing substrates for five lysosomal enzymes and to use tandem mass spectrometry for the multiplex detection of all five enzymatic products that are relevant to the diagnosis of Fabry, Gaucher, Krabbe, Niemann–Pick and Pompe diseases [57]. While conventional methods of quantifying enzymatic activity rely on the incorporation of a chromophore or fluorophore into the substrate, in this new procedure, substrates are synthetic sphingolipids containing N-linked fatty acyl chains that are shorter than the typical natural substrates. The corresponding products are non-natural ceramides, which are differentiated in the mass spectrometer according to the length of the fatty acyl chains.

In addition to the development of reliable and easy assay for prenatal diagnosis and newborn screening, the development of prevention programs for the detection of heterozygotes of relatively prevalent autosomal recessive diseases, such as LSDs, is a relevant issue for various ethnic groups. A screening prevention program has become available in recent years in Israel. The aim of the program is to determine high-risk couples prior to the birth of affected offspring. This is performed by a population-

screening program which addresses the specific needs and requirements of various population groups in Israel [58].

An experimental newborn screening program for GLD has been active in New York since 2006. In the first stage of screening, GALC activity is measured using tandem mass spectrometry on rehydrated dried blood spots from newborn-screening cards, as described above. Samples with less than 10% of normal activity values are considered positive and DNA analysis for GALC mutations starts. In order to avoid false positive screening, GALC deficiency is confirmed by a second assay performed on blood. When the diagnosis is confirmed, the infant is referred for consideration of a cord blood (CB) transplant. Currently, the transplant center with the most experience of neonatal GLD is Duke University Medical Center (North Carolina).

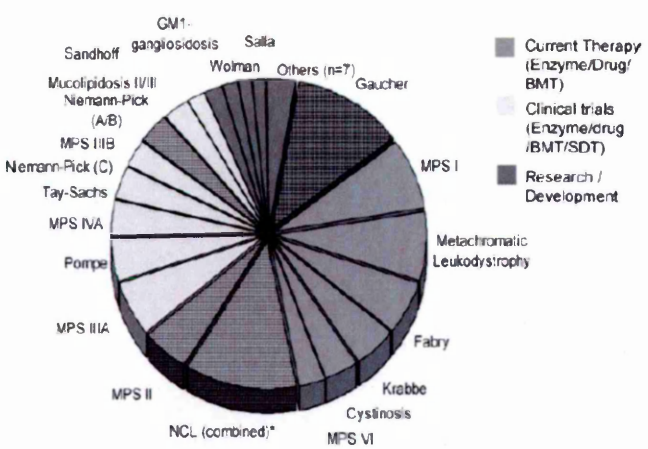

Figure 3. Relative incidence of LSDs based on Australian diagnoses 1981–1996 and of Batten disease diagnoses 1999–2002, modified from Meikle et al.(1999).

1.6 Animal models of GLD

Before the biochemical defect was identified in human patients in 1970, a canine model of GLD was described [59] (Figure 4). Affected Cain and West Highland White terriers present characteristic pathological features of GLD, such as weakness and tremor, a severe deficiency of GALC activity and progressive accumulation of Psy in the

brain. In 1996 the canine cDNA was cloned and the mutation causing GLD in Cain and West Highland White terriers was identified [60].

In 1980, a murine model of GLD, called *twitcher* (twi) was identified at the Jackson Laboratory [61] (Figure 4). These mice of the C57BL/6J strain, present no GALC activity, Psy accumulation in the CNS and PNS and develop clinical signs at approximately 20 days, with twitching and hind leg weakness. Neurological deterioration both in CNS and in PNS is very fast, leading to a progressive hind leg paralysis. They also lose weight as a result of their inability to feed and drink and die by about 40 days of age.

The mapping of the disease to mouse chromosome 12 was very useful in mapping the human disease to human chromosome 14. The miss-sense mutation responsible for the disease in twi mice is a G→A transition at position 1017 of the cDNA, which results in a mutation of a Tryptophan codon to a stop codon.

In 2001 a new transgenic mouse model of GLD was obtained by homologous recombination (trs mouse) [62]. The miss-sense mutation responsible for the disease results in a substitution of a Cysteine with a Histidine. While this mutation in humans decreases GALC activity to only 80% of normal values, in the mouse it results in a more severe reduction of GALC activity (10 to 20% of normal values). Trs mice present a phenotype similar to the one observed in twi mice, but with a delayed onset of about 10 days: twitching and tremors start around day 30 and the life span is about 50 days.

More severe murine models than the twi have been generated, such as the twi IL-6 -/- [63] or the twi mouse with the mixed background C57BL/6-129SvEv [64]. A milder mouse model of GLD was obtained by breeding twi mice with CAST/Ei mice [65]. The synthesis of GALC substrates in these mice, characterized by a low cholesterol and phospholipids turnover, is lower. C57BL/6x CAST/Ei twi mice have an increased life span (about 62 days), a delayed onset of tremor and a delayed decline of walking abilities, compared to C57BL/6 twi mice.

A murine model resembling the phenotype observed in the late-onset forms of GLD, was obtained by Cre/lox knock out of Sap A. SapA-/-mice develop a slowly progressive hind leg paralysis, with clinical onset at about 70 days and survival up to 5 months.

In 1989 the first monkey with pathological signs consistent with a diagnosis of GLD was described [66] (Figure 4). These Rhesus monkeys present a tremor of the head and limbs, deterioration of walking abilities and ataxia. With disease progression, the animals also display a decreased nerve conduction velocity, severe demyelination in both CNS and PNS, accumulation of globoid cells in the white matter and severe gliosis. The life span is around 22 months [67]. In 1997, the GALC cDNA of the rhesus monkey was cloned and a two-base-pair deletion in exon 4 was found in the affected animals. This mutation is responsible for a frameshift that generates a stop codon after 46 nucleotides [10].

Figure 4. Animal models of GLD. (a) Twitcher mouse in C57Bl6/J background. (b) Cain and West Highland White terriers. (c) Rhesus monkey.

1.7 Treatment of LSDs

1.7.1 Cross correction

Currently available treatment options for LSDs are based on cross-correction. This phenomenon was first observed on fibroblasts from patients affected by MPS I and II: the metabolic defect of these cells was corrected by providing "factors" secreted by wild type cells [68]. Furthermore, the "corrective factor" was clarified as being the functional enzyme secreted by wild type cells, up-taken and sorted to the lysosomal compartment of the deficient fibroblasts through the mannose-6-phosphate receptor (M6P-R) pathway [69]. This phenomenon is unique of lysosomal enzymes, as MP6 groups are added exclusively to the N-linked oligosaccharides of these soluble enzymes as they pass through the cis Golgi network. After being modified, the lysosomal enzyme binds the M6P receptor in the trans Golgi network (TGN) and is sorted to the late endosomes to reach the lysosome. About 40% of the enzyme escapes this pathway and is secreted in the extra-cellular space: this enzyme can then bind the M6P-R on the membrane to the producer cell or surrounding cells and can be endocytosed and sorted to the lysosome [70] (Figure 5). Many therapeutic approaches for LSDs are based on cross-correction: in enzyme replacement therapy (ERT), the enzyme, administered through intra-venous

injections, can reach the affected tissues with blood, while in HSCT, the lysosomal enzyme is provided by normal cells of donor origin.

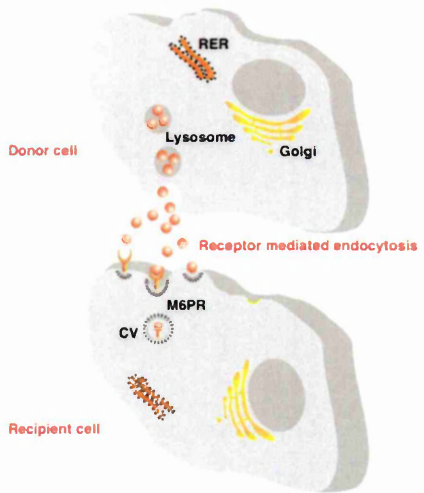

Figure 5. Cross-correction of defective cells by wild type cells. The lysosomal enzyme is released in the extra-cellular space where it is up-taken by defective cells through the M6P-R and sorted to lysosomes.

1.7.2 Enzyme Replacement Therapy

ERT consists of the parenteral administration of the recombinant or purified enzyme and is aimed at reducing the storage of the substrate responsible for the disease. ERT is now available or under investigation for a number of LSDs, including Gaucher disease, Fabry disease, MPS I, II, IVB, VI and VII and Pompe disease [71] [72]. ERT started more than 15 years ago with the large-scale isolation of glucocerebrosidase from human placentas for the treatment of Gaucher disease [72]. The treatment of non-neuronopathic forms of Gaucher disease with this original source of enzyme and the later recombinant form, has been very successful [73]. In particular, the largest experience with ERT is in the treatment of Gaucher disease type I, caused by β-glucocerebrosidase deficiency. In this LSD, the accumulation of lipids within tissue macrophages leads to hepatomegaly, splenomegaly, anemia, thrombocytopenia and bone involvement [74]. ERT significantly alleviates hepatosplenomegaly and hematological manifestations [75].

In order to develop an efficacious ERT for LSDs, the differences between the affected tissues should be taken into consideration. Various cell types express different receptors for the uptake of lysosomal enzymes: the hepatocyte membrane contains galactose receptor, macrophages require mannose residues for uptake, whereas most cells bind exogenous enzymes via the M6P-R. Moreover, diversity in the membrane density of the M6P-R of different cells and tissues has been observed: the highest concentration of receptors was found in the heart and kidneys, the lowest in muscles and the brain [76]. Therefore, since successful ERT requires targeting of multiple cell types, the ideal drug may be one which includes enzymes with various sugar residues and isoforms, so as to take advantage of the many cellular receptors involved in endocytosis.

Recombinant enzymes are currently obtained from cultures of over-expressing Chinese Hamster Ovary (CHO) cells or human fibroblasts [77 78]. The genes for almost all of the lysosomal enzymes have been cloned and theoretically their encoded proteins could be produced in large quantities. Despite this possibility, the small number of patients affected, makes the pharmacological development of ERT likely to be unprofitable to produce and test the protein for most LSDs.

In spite of pressure from concerned families and healthcare providers, significant problems still remain before ERT can be successfully applied to most LSDs. A major limitation of ERT is the inability of the enzyme provided, to efficiently cross the blood-brain barrier (BBB), with a consequent ineffectiveness of this treatment for LSDs with severe CNS involvement [79]. Recent experimental evidence has shown a reduction of substrate storage in the CNS of many animal models of LSD, in the presence of high quantities of enzyme in the plasma [80 81]. The mechanism by which the enzyme could reach the brain is still not fully elucidated, but it was hypothesized that monocytes and macrophages could uptake the circulating enzyme, cross the BBB and release the enzyme in the CNS [80]. Based on these results obtained in animal models, a phase 1 clinical trial of ERT was started recently for the treatment of Metachromatic

Leukodystrophy (MLD), an LSD caused by ARSA deficiency and characterized by a severe CNS involvement, but the effectiveness of the therapy on CNS is still unknown. Similarly, little is known about the possible benefits of ERT in GLD, which has a substantial CNS component. Pre-clinical studies examined the effect of peripheral GALC injections in the twi mouse. Even though immunohistochemical and biochemical analyses have demonstrated GALC uptake in multiple tissues, including the brain and a consequent decrease in Psy accumulation, only a slight increase in the life span of treated animals was observed [82].

Pre-clinical studies are currently directed at promoting transport of the administered enzyme across the BBB. Among the recently explored strategies are the conjugation of the enzyme with molecules recognized by a specific BBB carrier, such as IGF-2, the Fc fragment of antibodies, ApoB, or the TAT protein transduction domain. In one example of these strategies tested for MPS I in Rhesus monkeys, α-L-Iduronidase (IDUA) was fused with a monoclonal antibody directed against the insulin receptor expressed by brain endothelial cells. After intravenous administration, the enzyme was able to reach the CNS. Other approaches being developed to improve the transport across the BBB aim to extend the circulating half-life of the administered enzyme, such as by removing M6P residues and thus inhibiting uptake via M6P receptor by peripheral organs [83].

Another limitation of ERT is the frequent occurrence of immune responses against the injected protein. In LSDs characterized by a complete absence of the enzyme, parenteral administration could result in the recognition of the protein as a non-self antigen, thus triggering a humoral response with IgG production. As a consequence, alteration of the pharmacokinetic, hypersensitivity and very occasionally, neutralization of the administered enzyme, were observed [84 85].

Finally, the high cost of the recombinant enzymes, the need for life-long treatment and the frequency of injections are significant issues for many patients and their families.

1.7.3 Hematopoietic Stem Cell Transplantation

1.7.3.1 Hematopoietic Stem Cells

Hematopoietic Stem Cells (HSC) are somatic stem cells that give rise to all blood cell lineages, including lymphoid (T and B) and myeloid cell lineages. In the adult, HSC mainly reside in the hematopoietic niche of bone marrow (BM). In the niche, HSC are closely associated with stromal cells, which support the maintenance of stem cells and hematopoiesis both by the secretion of factors and by cell-cell interactions. In order to generate mature blood cells, HSC differentiate towards multi-lineage progenitors, which undergo expansion and further commitment steps that restrict their developmental potential. This differentiation process ends up with the generation of terminally differentiated progeny (Figure 6).

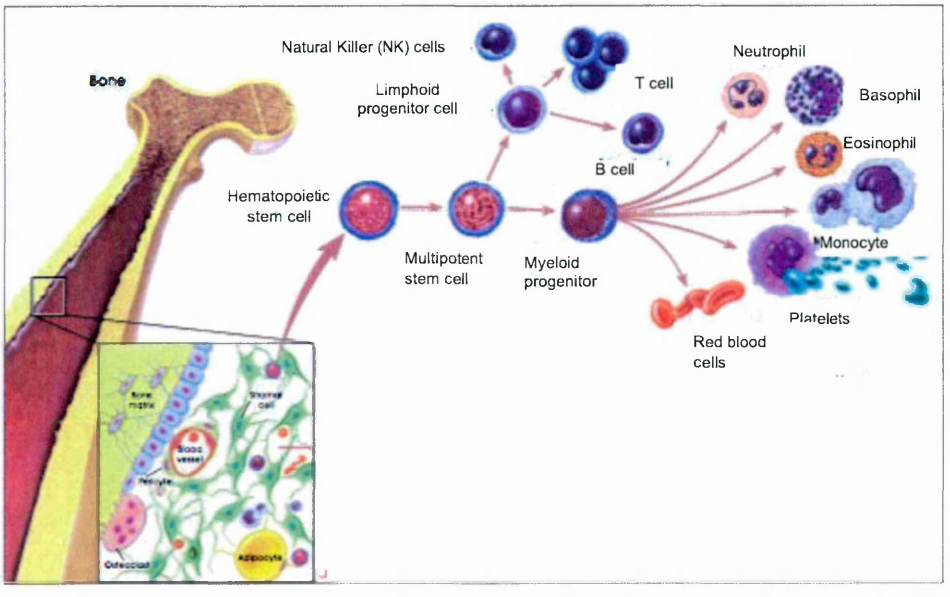

Figure 6. Hematopoietic stem cell differentiation. Hematopoietic stem cells differentiate towards multilineage progenitors, which undergo further differentiation processes to produce lymphocytes, NK cells, monocytes, granulocytes, platelets and red blood cells.

1.7.3.2 Characterization of Hematopoietic Stem Cells

Human HSC can be isolated mechanically from the BM, where they reside, or from peripheral blood upon mobilization. An alternative HSC source is cord blood (CB). The HSC pool is generally identified through the expression of the surface marker CD34 [86] [87], but selection using this marker provides a heterogeneous population containing only a minority of *primitive self-renewing stem cells* (long term – LT-HSC) among a mixture of *multipotent and oligopotent progenitors* (MPP) which have lost their self-renewing ability and acquired differentiation and proliferation capacity [88].

The most accurate definition of HSC is according to their function, measured as their ability to repopulate the hematopoietic system of a myeloablated host. The most primitive human stem/progenitor cells identified so far in experimental models have been called *SCID repopulating cells* (SRC) for their ability to engraft an immunodeficient murine recipient (for detailed description of xenograft models see [89]) while long-term providing differentiated progeny [90]. *Long-term culture-initiating cells* (LTC-IC) have a poorer self-renewal ability than SRC and are identified through a 5-week *in vitro* proliferation assay on a stromal layer [91]. *Colony forming cells* (CFC) are the progenitor fraction already committed toward the lymphoid, myeloid or erythroid lineage and proliferate extensively during a 2-week culture [92]. Unlike SRC, LTC-IC and CFC are unable to efficiently engraft SCID mice.

1.7.3.3 Maintenance of Hematopoietic Stem Cells

The ability of HSC to differentiate without exhausting the pool of HSC, relies on the ability of stem cells to perform both symmetrical and asymmetrical divisions. Symmetrical divisions give rise to two daughter cells with the same potential of the dividing cell, whereas asymmetrical divisions give rise to: I) a cell with the same potential of the dividing cell; II) a progenitor that has a higher degree of commitment, lower self-renewing and proliferative potential and which will generate the differentiated progeny. Thus, symmetrical mitoses are responsible for the maintenance and expansion

of the HSC compartment, while asymmetrical mitoses are responsible for both self-renewal and differentiation. To sustain the hematopoietic system without undergoing exhaustion, HSC must be tightly regulated, both by intrinsic and extrinsic signals. Intrinsic signals converge at the level of gene expression and have been better characterized in the developmental pathways of HSC than in the homeostatic maintenance of HSC in their adult state. On the other hand, extrinsic signals are those provided by the BM microenvironment: in the BM niche. HSC interaction with stromal cells and extracellular matrix through adhesion molecules profoundly influence HSC fate.

1.7.3.4 Hematopoietic Stem Cell Niche and Homing

The hematopoietic niche comprises HSC and their microenvironment, which is defined as the cells adjacent to, or surrounding, the stem cells (Figure 7). The microenvironment of the BM is fundamental for HSC maintenance, self-renewal and differentiation [93]. Stem cells represent a very small fraction of the niche in which they are contained, as most niche cells are non-hematopoietic and most niche-associated hematopoietic cells are committed progenitors or differentiated cells. The microenvironment is composed of endosteal osteoblasts and progenitor cells [94 95], mesenchymal stem cells (MSC), fibroblasts and the peri- and endothelial cells of bone marrow capillaries. Moreover, the niche contains extracellular factors produced by these cells, such as Stromal cell Derived Factor 1 (SDF-1), osteopontin, fibronectin, collagen, vitronectin and tenascin [96]. The generation of mature blood cells requires a close interaction between HSC and their niche and pathological conditions responsible for alteration of the niche microenvironment could result in hematopoietic defects. In particular, the sympathetic nervous system seems to play an important role in maintaining the trophism of the endosteal niche. Katayama and colleagues have recently

reported that aberrant nerve conduction is responsible for a dysregulation of HSC attraction to their niche, leading to a severe lymphopenia in CGT knok- out mice [97].

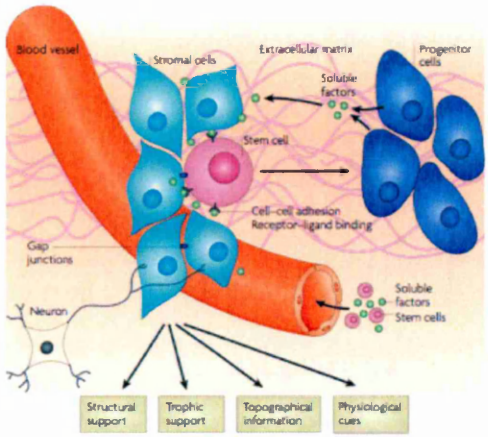

Figure 7. The stem cell niche. The hematopoietic niche comprises HSC and their microenvironment, including mesenchymal stem cells and stromal cells such as osteoblasts, fibroblasts and adipocytes.

Since in physiological conditions, HSC reside in the BM niche, in an HSC transplantation setting (HSCT), transplanted HSC must migrate through the blood, cross the vasculature and seed in the niche. This migration requires an active process called *homing*. Like other HSC features, homing is regulated by factors expressed in the niche microenvironment, such as adhesion molecules and hematopoietic cytokines. The interaction between SDF-1, expressed by endo-osteal osteoblasts, stromal and endothelial cells and CXC chemokine receptor 4 (CXCR4), expressed by HSC, has been proposed as a fundamental axis regulating retention, migration and mobilization of HSC during homeostasis and stress [98 99]. Adhesion molecules, such as integrins and selectins, mediate rolling and adhesion of homing cells before extra-vasation. Very late antigen 4 (VLA-4) and VLA-5 integrins have been found to participate in HSC homing [99].

1.7.3.5 Hematopoietic Stem Cell Transplantation in LSDs

An increasing number of patients with LSDs are undergoing HSC transplantation (HSCT) in an attempt to slow the course of the disease, prevent the onset of clinical symptoms and improve some pathological findings. The most promising results are obtained when HSCT is performed in pre-symptomatic patients, identified in the uterus or at birth because of family history.

The rationale for the use of HSCT to treat LSDs is the reconstitution of recipient's macrophage and microglia populations by functional cells of donor origin (Figure 8). Animal studies have shown that donor-derived cells of the monocytic lineage infiltrate different tissues including the CNS of the recipient, replacing the local macrophage population. These cells are not only the major effectors contributing to the clearance of the stored material throughout the tisses, but also act as mini-pumps synthesizing and secreting a portion of their lysosomal enzymes which can be taken up by neighboring cells [100] [101]. Those lysosomal enzymes, endocytosed by the M6P-R-mediated pathway, localize in the lysosomes and hydrolyze the stored substrate.

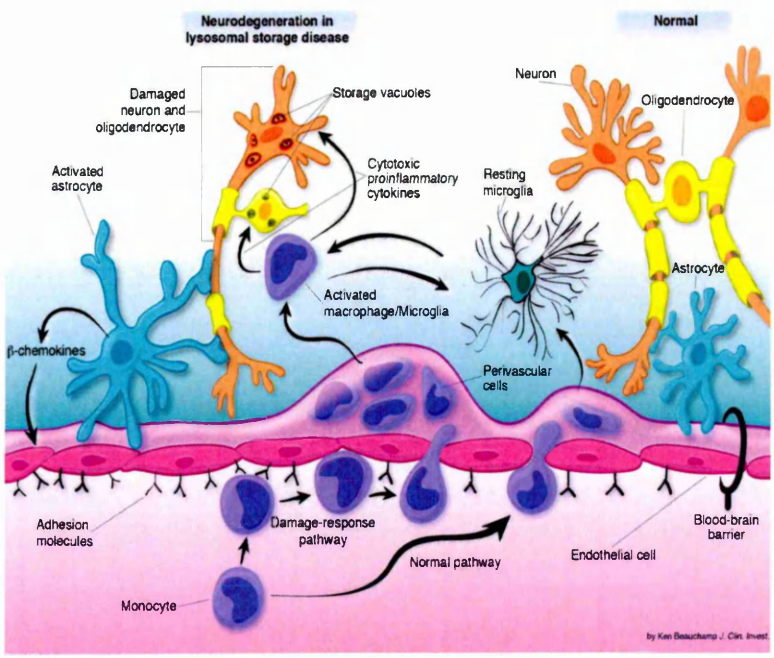

Figure 8. Microglia reconstituton upon HSCT. Upon HSCT, cells of donor origin differentiate and reconstitute microglia in the host CNS.

While the reconstitution of visceral organ macrophages by donor-derived cells has been clearly demonstrated, a substantial debate exists on the occurrence of CNS microglia replacement by the progeny of the transplanted donor HSC. In particular, factors affecting microglia replacement following HSCT have been identified in pre-clinical models. The replacement of brain microglia by donor-derived macrophages is favored in LSDs characterized by neuroinflammation or neurodegeneration [102 103 104 105, 106]. In fact, microglia recruitment could be enhanced by both pro-inflammatory cytokines and an increased BBB permeability [107]. For this reason, the myeloablative conditioning regimen applied before HSCT, might also play a fundamental role in the timing and extent of reconstitution. Irradiation promotes microglia reconstitution by increasing the permeability of the BBB; however, when myeloablation is obtained by administering chemotherapic agents such as busulphan, the replacement of host microglia with cells of donor origin might be enhanced by the production of pro-inflammatory cytokines triggered by the neurotoxic effect of the drug [108-110 111]. Recent studies demonstrated that the reconstitution of brain microglia upon HSCT may also be influenced by the characteristics of the transplanted HSC. In particular, the mechanical flushing of femurs and tibiae used in pre-clinical studies to collect HSC, could damage the BM niche, thus allowing microglial progenitors to enter in circulation and possibly cross the BBB. In physiological conditions, these cells should not be able to leave the bone marrow and enter into circulation [110 108]. In any case, microglia replacement following HSCT might take many months or even years to accomplish in humans [112]. Therefore HSCT may not be beneficial for rapidly progressing LSDs or for symptomatic patients.

HSCT is associated with a fairly high morbidity and mortality which limits its use to conditions that are themselves essentially life-threatening. Major causes of morbidity

and mortality are engraftment failure, regimen-related toxicity, graft-versus-host disease (GvHD) and sepsis.

Engraftment failure is the inability of the transplanted HSC to engraft and repopulate the recipient. This inability might be related to HSC or to the recipient. Several studies analyzed the risk factors related to engraftment failure and of particular interest is a study performed on a cohort of MPS I-Hurler patients transplanted between 1994 and 2004 [113]. This study observed that the percentage of engrafted patients after one HSCT was only 56% going up to 81%, after one to three transplantations [113]. Among the factors analyzed, T cell depletion was found to increase the risk of graft failure. HLA disparity was found to be a risk factor in 1994-1998 but not after, probably thanks to improvements in supportive care. Moreover, an HLA mismatch exerts a different effect depending on the source of HSC. In fact, a less mixed chimerism was observed in patients transplanted with CB HSC, in comparison to patients receiving cells from BM or PBMC. These differing outcomes might be due to the higher HLA mismatch of CB cells which could exert a stronger graft-versus-marrow (GvM) effect [114]. The GvM is associated with a subclinical GvHD, likely since CB cells have a more naïve phenotype. This might make the marrow more sensitive to GvM in comparison to the known target organs of GvHD. Another explanation for the higher engraftment of CB cells could be the increased pluripotential capability and the higher proliferative potential of these cells in comparison to BM HSC [115].

The application of a myeloablative regimen is necessary prior to HSCT to allow engraftment of HSC. Unfortunately, the myeloablative action of the chemotherapic regimen is often accompanied by a toxic effect on different tissues. As mentioned above, while the neurotoxic effect of busulphan might enhance microglia reconstitution on the one hand, it could result in seizures and other neurological symptoms following conditioning, on the other.

GvHD is an inflammatory disease, unique to allogeneic transplantation. It is an attack of the donor's immune cells against the recipient's tissues. This can occur even when the donor and the recipient are HLA-identical, because the immune system still recognizes other differences between their tissues. Acute GvHD typically occurs in the first three months after transplantation and may involve the skin, intestine, or the liver. Chronic GvHD is the major source of late complications.

After myeloablation and prior to engraftment, patients may go for several weeks without appreciable numbers of white blood cells to help fight infection. This puts a patient at risk of infections, sepsis and septic shock, despite prophylactic antibiotics. The immunosuppressive agents employed in allogeneic transplants for the prevention or treatment of GvHD further increase the risk of opportunistic infection.

In order to optimize transplant procedures, recent HSCT protocols use CB as a source of HSC. Banked CB is prospectively HLA typed, screened for infections and other risk factors and readily available for transplantation. In a disease where the time from diagnosis to definitive treatment represents a crucial period for the prevention of further disease progression, a readily available source of HSC is extremely desirable. The incidence of acute GvHD is usually lower in HSCT from CB compared to when HSC are derived from BM, and the hematopoietic reconstitution is faster [116 117]. The use of CB HSC greatly has influenced the outcome of HSCT in LSDs. When allogeneic HSCT is performed using BM HSC, the donor is usually a sibling and often he/she is a carrier of LSD. On the one hand, this means that the time to find a suitable donor is reduced, but, on the other, that the amount of enzyme provided by donor cells is lower than normal levels, thus compromising the positive outcome of the treatment. Transplantation of CB-derived HSC, increases the number of available donors since a lower standard of histocompatibility between donor and recipient, is acceptable. In addition, HSC would not come from LSD carriers but from healthy donors and thus supply a normal level of therapeutic enzyme.

HSCT was initially considered as a therapeutic option for those LSDs involving BM and hematopoiesis and was then applied to those LSDs also involving CNS. The results obtained following successful engraftment in transplanted MPS I-Hurler patients, have been gratifying. Treated subjects showed a restored enzymatic activity and resolution of cardiac pathology [117] [118]. Allogeneic HSCT has also proved to be effective for patients affected by the cerebral form of Adrenoleukodystrophy (ALD) [119, 120]. The data to date clearly shows that the degree of disease correction is dependent on the symptomatic stage at the time of treatment: the cerebral outcomes are superior following engraftment at an earlier stage of the disease compared to later stages. This could be explained by the ratio between disease progression and the rate of microglia reconstitution from donor-derived cells, which changes according to the time when treatment is applied.

Despite the promising results obtained in the above-mentioned LSD, HSCT showed a poor outcome when applied to MLD patients. Failure to obtain an improved, or even stabilized quality of life and to halt disease progression was reported. The majority of treated patients displayed a continuous decline in their neurological performance, despite full donor engraftment and restoration of enzymatic activity to normal in peripheral blood mononuclear cells [121].

In order to increase the effectiveness of HSCT in LSDs, transplantation has been associated with ERT in recent phase I clinical trials for MPS I Hurler. The enzyme Laronidase® was administered 11-14 weeks before HSCT and 8 weeks after HSCT, by parenteral infusion. All patients engrafted with more than 90% donor hematopoiesis, thus demonstrating that ERT does not affect the engraftment of donor cells and could be used to stabilize patients while waiting for HSCT [122].

1.7.3.6 Hematopoietic Stem Cell Transplantation in GLD

HSCT was initially tested on twi mice. Transplanted mice displayed a sustained increase of GALC activity in the CNS, a stabilization of Psy storage and a reduction in both the number of globoid cells and demyelination [123] [124] [125] [126] [101]. Preliminary evidence has shown that HSCT could be effective for patients affected by the infantile form of GLD, if applied within the first months of life. When the disease is diagnosed early and when an HSC donor is available, HSCT can delay the onset of GLD and halt its progression. Pre-symptomatic and symptomatic children with the infantile form of GLD have been successfully transplanted with HSC from unrelated CB [127]. Preliminary results have shown a positive effect if patients have been transplanted very early in life before the onset of symptoms. In such patients, the progression of the disease has been slowed and their phenotype seems milder compared to untreated controls. However, in patients transplanted at a symptomatic stage, disease progression has been shown to be as fast as in non transplanted children. Good results were also obtained when HSCT was performed in patients affected by the late-onset form (J and Ad) of GLD [128] [129]. Transplanted patients showed an improvement in CNS functions as well as an increase in nerve conduction velocity, thus confirming the therapeutic potential of HSCT for the treatment of GLD [121].

1.7.4 Substrate reduction therapy

In cases wherein mutant cells express residual enzyme activity, metabolic homeostasis may be restored or maintained in diseased cells by limiting the amount of intra-lysosomal substrate build-up, by inhibiting the number of precursors synthesized [130]. This approach, called substrate reduction therapy (SRT), seeks to strike a balance between the amount of substrate that ultimately needs to be degraded and the mutant cells intrinsically low enzyme activity. This could be accomplished by compounds such as L-cycloserine, which inhibit a very early step in the synthesis of sphingolipids. Pre-

clinical studies demonstrated that administration of L-cycloserine to twi mice, from both C57BL/6 and B6; CAST/Ei background, resulted in a longer life span and a delayed onset of clinical manifestations [131] [132]. SRT could also be combined with HSCT to enhance its efficacy, thus increasing the number of patients who could benefit from the treatment. Studies on twi mice demonstrated that SRT combined with HSCT resulted in a greater benefit than either treatment alone [65].

There were legitimate concerns that treatments based on the use of substrate synthesis inhibitors might influence the presence and distribution of sphingolipids which play a number of important functions in cellular metabolism, including signal transduction, cell adhesiveness and nerve impulse transmission [133] thus adversely influencing cell growth and differentiation. To some extent these concerns were mitigated by the availability of authentic animal models and pre-clinical studies performed in twi, Sandhoff and Niemann-Pick type C (NPC) mice, which revealed that SRT delayed the onset of symptoms, improved behavior and prolonged survival [134] [135]. The lack of any significant deleterious effects in the mice exposed to the drug, may reflect the fact that the inhibition of substrate synthesis is a partial, rather than a full or complete block. However, the "genetic" substrate reduction in CGT-/- twi-/- double ko mice led to unexpected findings [136]. In this mice GC are not present at any age, while a progressive neuronal pathology was observed in the brainstem and spinal cord after 45 days. This new disease phenotype, different both from the twi and the CGT single ko phenotype, is similar to the one observer by Suzuki in twi mice that had received bone marrow transplantation treatment (unpublished data). This finding might suggest that either some unknown substrates of GALC are synthesized in the absence of CGT or some of the usual CGT products can be synthesized by other enzymatic mechanism.

SRT has been successfully applied to patients affected by type I Gaucher disease. Oral administration of a glucosylceramide synthesis (N-butyldeoxynojirimycin) inhibitor, proved to be effective in reversing clinical symptoms in these patients, with

mild to moderate disease manifestations [137]. Clinical trials that should reveal the value of substrate reduction for the treatment of neuronopathic variants of Gaucher disease, NPC, late-onset Tay-Sachs disease and Sandhoff disease, are under way.

2. Gene Therapy

Gene therapy is the delivery of genetic material into an individual's cells and tissues with the aim of curing a disease or at least improving the clinical status of a patient. It could be used to treat both inherited or acquired diseases, or for prophylactic purposes [138].

Depending on the target of gene transfer, gene therapy may be classified into the following types:

I. *Germ line gene therapy*: germ cells, i.e., sperm or eggs, are modified by the introduction of functional genes, which are ordinarily integrated into their genomes. Therefore, the change due to therapy would be heritable and would be passed on to later generations. Theoretically, this new approach should be highly effective in counteracting genetic disorders. However, this option is prohibited for application in human beings, at least for the present, for a variety of technical and ethical reasons.

II. *Somatic cell gene therapy*: the gene is introduced only into somatic cells, especially for those tissues where expression of the gene concerned, is critical for health. Expression of the introduced gene can relieve/eliminate symptoms of the disorder, but this effect is not heritable as it does not involve the germ line. At present, somatic cell therapy is the only feasible option and clinical trials addressing a variety of conditions have already begun.

Referring to the aim and the genetic material used, gene therapy could be defined as follows:

Replacement therapy: a functional gene is provided or inserted into the genome to replace the function of an endogenous defective one. The most common method is the

insertion of the functional gene into a non-specified location within the genome. An alternative method is to "correct" the mutant gene through homologous recombination.

Addictive: a DNA or RNA portion is transferred into the patient's cells, in order to provide a supplementary biological function (i.e. resistance to viral infection).

Ablative: patient's cells are provided with genetic material which can down-regulate or suppress the expression of a target gene (i.e. miRNA, siRNA and antisense oligonucleotides could be used to interfere with mRNA maturation and translation).

Gene transfer can be obtained using an *in vivo* or *ex vivo* procedure. The *in vivo* method inserts genetic material directly into the patient's target tissues. This procedure is, in theory, easier and once optimized, could be applied to a great number of patients. However, it is an invasive procedure which might lead to inadvertent gene transfer into tissues and cell types that are not the proper target (Figure 9).

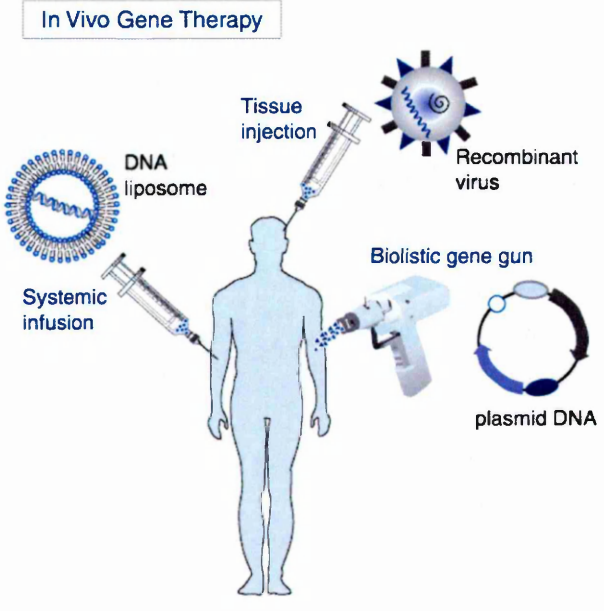

Figure 9. In vivo Gene Therapy. Genetic material (DNA liposomes, viral vectors or plasmids) is inserted directly into the patient.

In the *ex vivo* method, tissue is removed from the patient, target cells are isolated and genetically modified before returning them to the patient. This procedure is less invasive and the time in which the target cells are exposed to the vector used for gene transfer, is limited. However, *in vitro* manipulation could modify the treated cells,

possibly impairing their functionality or engraftment potential. Moreover, some tissues are difficult to remove for *ex vivo* manipulation (Figure 10).

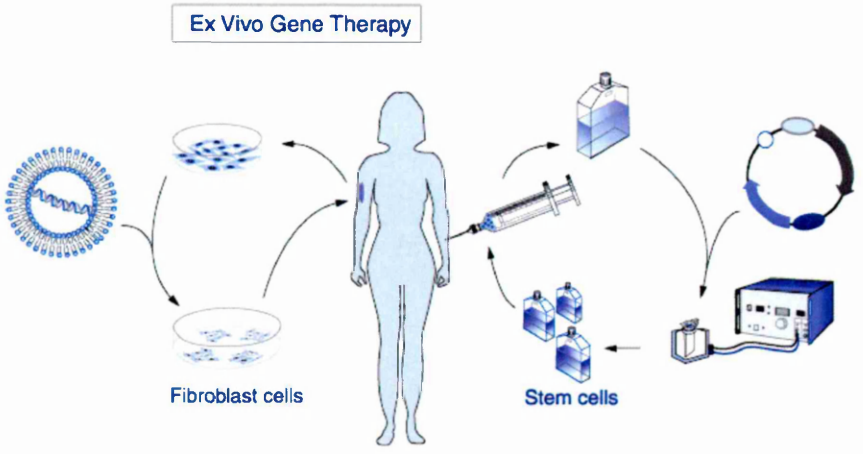

Figure 10. Ex vivo Gene Therapy. Target cells are isolated and genetically modified before returning them to the patient.

2.1 Non-viral vectors

Several gene transfer methods have been developed. Non-viral approaches take advantage of physical delivery methods (i.e. direct DNA injection, electroporation, nucleofection, gene guns) and chemical approaches (i.e. liposomes) to transfer the genetic material into target cells or tissues [115 139 140 141]. The efficiency of gene transfer by non-viral approaches is generally low, particularly in non-dividing cells, due to the inability of liposomes, gene gun complexes or nude DNA to enter the nuclear membrane when it is not disrupted, such as during cell division. Moreover, upon *in vivo* administration, non-viral vectors bind negatively-charged plasmatic proteins, thus greatly decreasing the amount of vector available for target cells [142]. A new non-viral approach based on a transposon system (i.e. sleeping beauty transposon) has recently been developed; although it should ensure integration of the genetic material into the target cell chromatin, the efficiency and safety of this system still need to be evaluated (for a review see [143]). The application of gene transfer by non-viral approaches, has been limited by its poor efficiency, mostly to pre-clinical studies, with some phase I clinical trials [144 145].

2.2 Viral vectors

The basic concept of viral vectors is to harness the innate ability of viruses to deliver genetic material into the infected cell. A virus (from the Latin *virus* meaning "toxin" or "poison"), is a sub-microscopic infectious agent that is unable to grow or reproduce outside a host cell. In general, the major occupation of viruses is to replicate and produce copious amounts of progeny. Many viral infections lead to deleterious effects on the host, accompanied by destruction of infected host cells. Damaging effects can be caused by induction of genes whose products are hazardous to the host. The basic principle of turning these pathogens into delivery systems, relies on the ability to separate the *cis-acting* sequences of the viral genome that act on the same sequence during the infection cycle from the *trans-acting* sequences that encode for viral structural and non-structural proteins. Next, dispensable genes are deleted from the viral genome to reduce replication and pathogenicity, as well as expression of immunogenic viral antigens. This procedure generates enough space into the viral genome to insert the *expression cassette*, made up of a transgene and transcriptional regulatory elements sequences. The recombinant virus is generated by supplying *in trans* the gene products required for virion production [146]. Since viral methods are usually more efficient than non-viral methods, they have been widely studied as tool for gene transfer. Moreover, some viral vectors allow for stable integration into the cell chromatin. Nevertheless, concerns about the safety of the viral sequences contained within the gene transfer vector, the risk of insertional mutagenesis and the potential immunogenicity of the vector particles, have been raised.

The more widely used viral approaches are based on Adenovirus, Adeno-Associated virus, Herpes Simplex virus and Retrovirus [147]. In particular, Retrovirus-based vectors (RV) are highly relevant for gene therapy, given their ability to efficiently transduce a

wide spectrum of target cells, including hematopoietic cells and to integrate their genome into the host chromatin. Retroviruses are RNA viruses, whose replication strategy is based on an intermediate DNA form (provirus), which stably integrates into the infected cell chromatin. Retroviruses possess two copies of RNA genome, a proteic core (capsid) and a lipidic envelope derived from the infected cell, into which the viral glycoproteins are inserted (Figure 11).

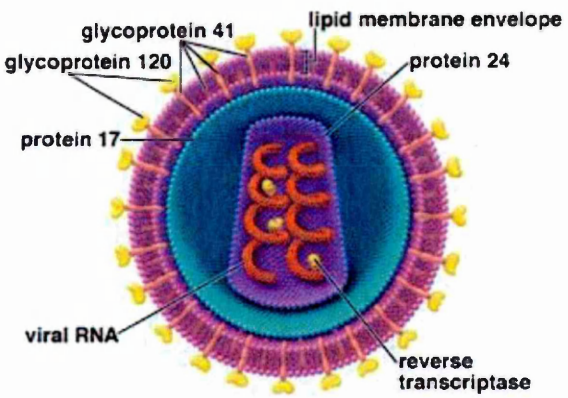

Figure 11. Structure of a Retrovirus. Retroviruses are made up of a lipidic envelope, containing the viral glycoproteins gp 41 and gp 120, a proteic capsid and a proteic core containing copies of RNA.

The viral RNA contains three essential genes, *gag*, *pol* and *env and* is flanked by long terminal repeats (LTR). The *gag* gene encodes for the core proteins capsid, matrix and nucleocapsid, which are generated by proteolytic cleavage of the *gag* precursor protein. The *pol* gene encodes for the viral enzymes protease, reverse transcriptase and integrase, which are usually derived from the *gag-pol* precursor. The *env* gene encodes for the envelope glycoproteins, which are inserted into the lipidic envelope, involved in the virus entry.

This family of viruses has been divided into three subfamilies: **Gamma retroviruses (or Oncoviruses), Lentiviruses and Spumaviruses**. Oncoretroviruses are simple viruses encoding only the structural genes: *gag*, *pol* and *env*, whereas lentiviruses

and spumaviruses have a more complex genome organization and encode for additional viral proteins.

The production of all RV relies on the supply of all the structural proteins by separate plasmid(s) [138]. This strategy can be based on either co-transfection procedures or transfection of the transfer vector into packaging cell lines stably producing the viral proteins. In both cases, the structural proteins needed for vector production are expressed only in the producer cells. In fact, in the vector transduced cells, the sequences encoding for viral proteins will be absent, because they lack the signals for encapsidation and thus replication of the vector will be inhibited, unless recombination events occur between the vector genome and the viral genes to reconstitute a functional viral genome. Since the tropism of the RV is dictated by the envelope glycoproteins, the choice of the suitable envelope should be performed according to the target cells. The process of exchanging the wild type envelope proteins of RV with other envelope proteins, thus modifying the tropism of the vector, is known as *pseudotyping* [148 149 150 151]. According to the envelope selected, different procedures of vector production and concentration are applied.

2.2.1 Oncoretroviruses and derived vectors.

The vast majority of RV is based on the Moloney murine leukemia virus (MLV), a member of the oncoretroviruses family. MLV-derived vectors (MoRV) can package up to 10 kb of foreign genetic material [138]. *In vivo* transplantation studies established MoRV's ability to transduce HSC, an important target for gene therapy [152 153]. Given this ability, many phase I-II clinical gene therapy trials for several genetic diseases, such as Adenosine Deaminase Severe Combined Immunodeficiency (ADA SCID), X-linked

Severe Combined Immunodeficiency (X-linked SCID) and Chronic Granulomatous Disease (CGD), have been performed or are currently ongoing [154 155 156].

The limitations of MoRV are mainly related to their inability to transduce quiescent cells, since they require nuclear membrane disruption and thus mitosis, to gain access to the chromatin [157]. Given that HSC are mostly non-proliferating cells, all protocols developed for retroviral vector-mediated HSC gene transfer, involve prolonged *in vitro* manipulation and/or cell cycle entry induction [90 158 159 160], thus increasing the risk of compromising HSC's long-term repopulating ability.

Another limitation of utilizing MoRV in gene therapy is related to the risk of vector integration, since insertional mutagenesis leading to leukemia, has occurred in recent clinical trials [161 162 163] (see paragraph 2.2.4).

2.2.2 Spumaviruses and derived vectors.

The Spumavirus genome encodes for structural proteins common to all retroviruses and for a set of regulatory and accessory proteins. Despite the name of the Spumavirus prototype, Human Foamy Virus (HFV), spumaviruses are not endemic in human populations [164]. This, coupled with their non-pathogenicity in natural hosts (non-human primates), has supported the development of HFV-derived vectors (FVV) for gene therapy. In addition to safety considerations, the broad host and tissue tropism of spumaviruses [165] and the ability of FVV to package up to 9.2 kb of foreign genetic material [166], have made FVV promising gene transfer tools. Recently, it has been shown that FVV ultimately require mitosis for transgene expression, but the transduction intermediate is stable and persists in non-dividing cells for some days [167]. Investigation continues as to whether these vectors can permit transgene expression in quiescent cells such as more primitive HSC, which are possibly non-proliferating during transduction and will not divide soon after.

2.2.3 Lentiviruses and derived vectors

Lentiviruses are the most complex family among retroviruses. In addition to *gag*, *pol* and *env*, lentiviruses encode for three to six additional viral proteins, which contribute to virus replication and persistence of infection [168] (Figure 12). The most studied lentivirus is the human immunodeficiency virus 1 (HIV-1).

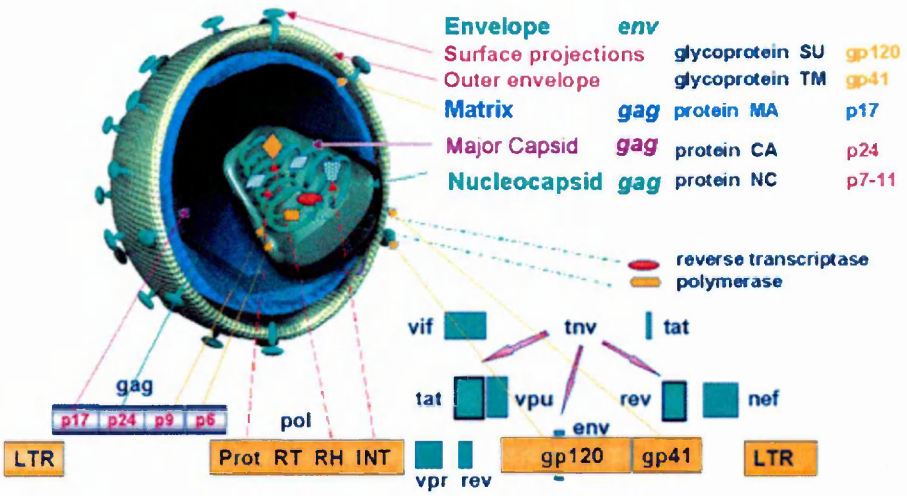

Figure 12. Structure and genome of a lentivirus (HIV-1). The RNA viral genome is flanked by LTR sequences (made up of U3-R-U5) generated during retro-trascription. R region: terminally redundant sequence; U5: unique 5' sequence; U3: unique 3' sequence. Vif, vpu, vpr, nef, tat, rev: regulatory genes. RT: retrotrascriptase; INT: integrase.

HIV regulatory proteins are Tat and Rev. Tat is a potent *trans*-activator of transcription which, through binding to the TAR sequence in the U3 LTR region, activates the transcription of the HIV genome. Alternative splicing of the full-length transcript generates the array of mRNAs required for expression of all viral genes. The full-length transcript itself also serves as a translational template, as well as being a source of new viral genomes. Thus, the un-spliced genome, which constitutes the genome of new virions, must be transported from the nucleus to the cytoplasm, an event that ordinarily does not occur in the cell. This problem is overcome by Rev, which binds the RRE sequence of the transcribed genome and allows nuclear export of the un-spliced RNA. Since Tat induces a number of potentially detrimental cellular responses [169], it has been deleted from the design of the latest generation lentiviral vectors (LV). This is

possible if the U3 region of the 5' LTR in the transfer vector construct, is replaced by constitutively active promoter sequences, thus rendering Tat dispensable. REV is the only regulatory/accessory protein that has been maintained in the design of the latest generation LV. In fact, its activity is required to express the transfer vector RNA.

HIV accessory proteins are Vif, Vpr, Nef and Vpu. Vif is incorporated in the virion and is required for replication in "nonpermissive" cells, which include the natural targets of HIV-1 (lymphocytes, monocytes, dendritic cells and brain microglia). In "permissive" cells (most HIV-1-infectable cell lines), Vif is completely dispensable. In "nonpermissive" cells, Vif-defective HIV is unable to complete reverse transcription [170]. Vpr is present in the viral particle and increases virus production by delaying infected cells at the G2 phase of the cell cycle [171]. Nef helps the budding of the virus from infected cells and protects infected cells from being recognized and killed by cytotoxic T lymphocytes [172]. Furthermore, Nef enhances virion infectivity, likely because it is involved in the uncoating and reverse transcription processes [173] [174]. Vpu mainly facilitates virus release. It down-regulates CD4 expression in the ER to prevent interaction with HIV-1 envelope proteins during virus budding and stimulates the release of virions, possibly by acting as an ion channel [175]. All the HIV accessory proteins have been deleted in the latest generation of LV designs.

2.2.3.1 Lentivirus life cycle

A major difference between lentiviruses and oncoretroviruses is the ability of the former to cross the intact nuclear membrane and integrate into the chromatin of non-proliferating cells [176] [177]. To better understand the reason for this important difference, it is necessary to look at the lentiviral life cycle.

The main stages of lentivirus life cycle are: entry, uncoating, reverse transcription, nuclear import, integration, transcription and production of viral proteins, assembly of

new viruses and release of viruses (Figure 13). After retrotranscription, the dsDNA proviral genome, flanked by the LTR regions, and together with other molecules, forms a pre-integration complex (PIC). The composition of PIC is still not fully understood, mainly because of technical limitations in the isolation of the particles. However, the complexes isolated by most protocols retained the *pol* encoded proteins [178]. To reach the nuclear membrane, PIC must travel through the cytoplasm exploiting the cellular cytoskeleton [179]. After reaching the nuclear envelope, HIV PIC is translocated through the nuclear pore, most likely by relying on the cellular nuclear import machinery. Although there is no agreement about the viral components needed for nuclear translocation, it is likely to be mediated by the importin/karyopherin cellular machinery [180]. After entering the nuclear membrane, the viral DNA integrates into the host genome. This process is carried out by the viral integrase protein. For a long time, the integration of lentiviruses and more generally all retroviruses, was believed to occur randomly into the host chromatin. Nevertheless, recent reports indicated specific biases for integration into transcriptionally active genes [181] [182], (see paragraph 2.2.4).

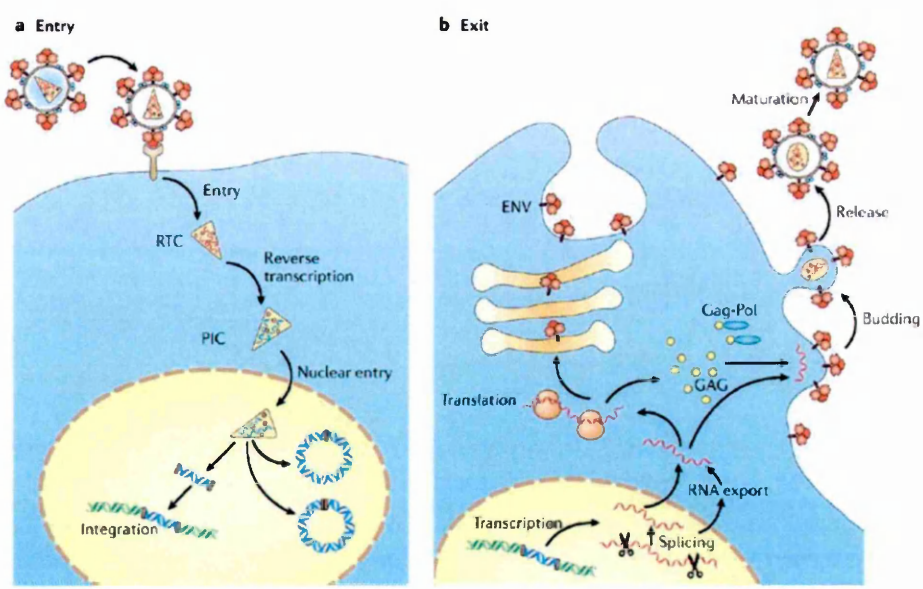

Figure 13. Lentivirus life cycle *Entry:* the envelope glycoproteins bind to specific receptors on the cell membrane and the virus enters the cell through membrane fusion. The initial binding is between the viral glycoprotein gp120 and CD4; then gp120 binds to a co-receptor

(CCR5 or CXCR4) [183] to allow the fusion between virus and cell membrane. *Uncoating:* the viral core is released into the target cell cytoplasm and undergoes a progressive disassembly. The RNA viral genome is released in the cytoplasm. *Retrotranscription:* the viral RNA genome is retrotranscribed into double stranded DNA by the viral reverse transcriptase. Two LTR sequences are generated. *Nuclear import:* double stranded viral DNA forms a pre-integration complex (PIC #168) with cellular proteins and enters the nuclear membrane. *Integration:* HIV integrates into the host chromatin. *Transcription and production of viral proteins:* RNA polymerase II transcribes the integrated provirus. Once in the cytoplasm, transcribed RNA is translated to new viral proteins or is inserted into new viral particles [184]. *Assembly of new viruses:* the viral proteins MA (for the matrix), CA (capside) and NC (nucleocapside) are required. *Virus release:* new virions budding from cell membrane. During this process the envelope is acquired.

2.2.3.2 Lentiviral vectors

The first LV was developed from HIV-1 [185]. Starting with initial constructs, which contained all HIV-1 sequences, several studies were performed to limit viral sequences/proteins without losing transduction efficiency. The state of the art HIV-1 derived vectors are made of a packaging system consisting of at least four plasmids, in which all the accessory proteins have been deleted, and a Self-Inactivating (SIN) transfer vector (Figure 14) [186 187].

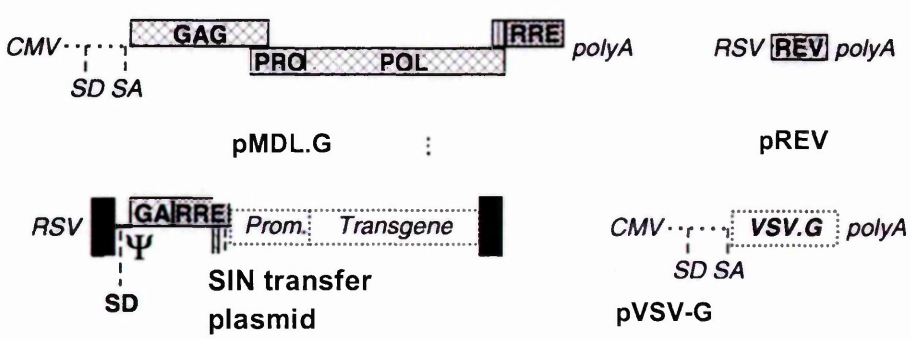

Figure 14. Third generation plasmids. (Adapted from (Dull, et al. 1998). pMDL.G: packaging plasmid encoding for viral enzymes and structural proteins. pREV: plasmid used in third generation LV, codifying for *rev*. pVSV-G: plasmid encoding for viral glycoproteins. PRRL-SIN: transfer plasmid, containing the expression cassette (transgene and internal promoter).

The first construct (pMDL.G) is the packaging plasmid, containing *gag* and *pol,* which encode for viral enzymes and structural proteins. The second plasmid (pVSV-G) expresses the glycoprotein of the envelope, which determines the tropism of the virus; in order to broaden the host range of lentiviral vector, they can be pseudotyped with the vesicular stomatitis virus glycoprotein (VSV-G) *env* [188]. Other viral glycoproteins have also been used to pseudotype lentiviral vectors and provide alternative cell tropism [189] [190]. The third plasmid (pREV), used in third generation vectors, expresses the Rev protein. The fourth construct is the transfer plasmid: it contains the expression cassette for the transgene and the essential *cis-acting* sequences, such as ψ to allow the encapsidation of the virion. The four plasmids are co-transfected into 293T cells, where they are transcribed. As a result, viral particles containing RNA sequence encoding for the transgene instead of the viral genome, are released into the medium by producer cells. These LV are harvested from the supernatant and those pseudotyped with VSV-G can be concentrated by ultracentrifugation to produce high-titer preps. Particle titer can be determined using assays which measure the amount or activity of proteins incorporated in the vector particles, such as the p24gag ELISA assay (see method section) [146].

In this design, the dispensable viral genes and the sequence homologies between the different plasmids are greatly reduced, making recombination and production of replication-competent lentiviruses very unlikely to occur [191]. The first generation packaging vectors, contain all the viral proteins except *env,* which is provided *in trans* by another plasmid [192] [193]. In this plasmid the encapsidation signal is deleted, the 5'LTR is replaced by an heterologous promoter and the 3'LTR is replaced by an heterologous polyadenilation signal of the SV40 virus [194]. In the second generation packaging vectors, *vif, vpu* and *vpr* genes are deleted, while in third generation vectors, two constructs are

used: the first is a second generation plasmid, in which *tat* and *rev* genes have been deleted; the second plasmid provides the *rev* gene [186 195].

In order to increase the safety and the efficiency of LV, transfer vectors have also been improved. In the first transfer constructs, a sequence spanning from *gag* to *env* is deleted, thus removing all the regions encoding for viral genes [185]. The SIN design of the transfer vector, where the enhancer/promoter sequence (U3) of HIV-1 has been deleted, has greatly improved safety. In fact, the SIN-Long Terminal Repeat (SIN-LTR) cannot initiate transcription of the vector genome and, thus, should not permit mobilization of the vector, for instance following superinfection by HIV. Finally, the SIN design has improved vector performance, allowing for the use of internal promoters, which can be selected according to the application.

In addition, more elements such as cPPT (central poly-purine tract) were added into the transfer vector, which, together with CTS (central termination site), increase the efficiency of the vector by promoting the provirus entry into the nucleus. The level of transgene expression was also improved by the WPRE (woodchuck hepatitis post-transcriptional regulatory element) [196 197] (Figure 15).

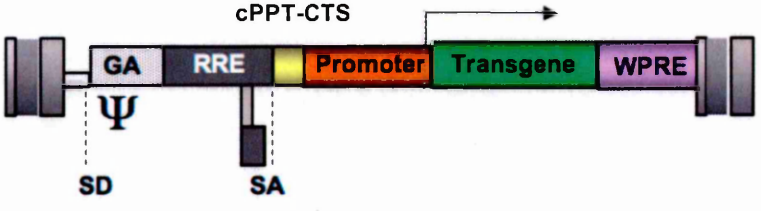

Figure 15. Scheme of last generation transfer plasmid. SD: Splicing Donor site; SA: Splicing Acceptor site; cPPT: central poly-purine tract; CTS: central termination site; WPRE; woodchuck hepatitis post-transcriptional regulatory element.

2.3 Gene transfer into hematopoietic stem cells

HSC are attractive targets for gene therapy in a variety of inherited and acquired genetic diseases, including immunodeficiencies and metabolic disorders. These disorders have been treated for some time by allogeneic bone marrow transplantation. However, the development of GvHD in transplanted patients is a frequent and life-threatening complication so the higher than normal levels of expression of the functional gene in autologous HSC and their progeny, might improve the therapeutic potential/outcome of HSC transplantation. For this reason, the transplantation of gene corrected, autologous HSC has been proposed as an alternative therapy. HSC can be supplied with the therapeutic gene by *ex vivo* transduction and then be re-infused into the donor. If gene transfer occurs in primitive HSC and the genetic material is inserted into the target cell chromatin in order to be maintained during HSC proliferation and differentiation processes, transplanted HSC will self-renew and generate large numbers of gene corrected, differentiated progeny, theoretically for the lifespan of the host. Moreover, the use of vectors capable of higher than normal levels of expression of the functional gene in HSC and their progeny, might improve the therapeutic benefit of HSCT.

When a protocol for *in vitro* culture and transduction of HSC has to be defined, critical issues are related to the maintenance of HSC stemness and homing capacity. The development of protocols that maintain HSC in culture without affecting their biological properties, is closely linked to the knowledge of extrinsic signals regulating HSC *in vivo*. Since the majority of these stimuli still need to be elucidated, the specific combination of the most suitable factors for *in vitro* culture and gene transfer, has yet to be determined. Moreover, the use of different vectors for HSC gene transfer poses diverse requirements for cell stimulation. Since MoRV have been the most exploited vectors for HSC gene transfer, the majority of designed protocols include several days of cell stimulation, to induce cell proliferation. The main issue is to induce HSC

proliferation without impairing their clonogenic potential, keeping *ex vivo* manipulation time to a minimum. Several studies have addressed this issue with the most studied factors for HSC stimulation being IL-6, IL-3, SCF, Flt3L and TPO which have been shown to preserve function, allow moderate expansion and aid in transduction of HSC [198 199 200].

Since supporting niche cells act on HSC through specific molecular interactions, promoting either their quiescence or expansion according to physiological needs, an alternative approach could be to mimic these interactions in vitro. The strategy that was first exploited to recreate the natural condition of HSC, was to grow them on a layer of BM stromal cells, which would provide physiological amounts of cytokines and trophic factors to cultured cells [201]. Nevertheless, this procedure presents technical limitations. Firstly, it is very difficult to standardize this kind of culture. Furthermore, its clinical application is challenging given the need to either harvest autologous stromal cells weeks before the HSC harvest [159], or to introduce foreign human or animal antigens, when using heterologous stromal cells. In order to provide support for HSC in culture and overcome the limitations of stromal cells, fibronectin (FN) has been widely used to coat culture dishes or bags. FN is abundantly expressed in the BM microenvironment, where it plays an important role in cell-cell and cell-matrix interaction. It has been proved that cells cultured on FN, show an increased survival and better maintenance of clonogenic capacity during *ex vivo* culture compared to those grown on a stromal layer or in suspension [159]. Moreover, by allowing co-localization of RV and target cells, FN increases the HSC transduction rate [202 203].

Beyond the choice of which are the best factors for maintaining HSC, another issue that has been investigated in the gene transfer field is the period of cell culture. Since MoRV have been the most exploited vectors for HSC gene transfer, most designed protocols included several days of cell stimulation, to induce cell proliferation [204 205]. Some of these trials have already given encouraging results in terms of efficacy, but

only long-term analysis of the patients' graft will determine whether transduced cells were short-term or long-term progenitor HSC. Additional studies are currently ongoing in an attempt to further increase transduction efficiency and evaluate the safety and repopulation potential of transduced HSC. Xenotransplant studies performed in NOD/SCID models, showed that 4 days in culture greatly reduced HSC engraftment ability in a competitive setting [206], supporting the idea that minimal HSC manipulation should be preferred.

Even in the best cases reported, SRC transduction with MoRV never reached sustained levels, likely due to the need for cycling cells. This issue has been markedly improved using LV, which efficiently transduce HSC without extensive manipulation. Nevertheless, in apparent contrast with the lack of LV requirement for target cell proliferation, a significant enhancement in gene transfer in the presence of a combination of early-acting cytokines was found [150 207].

The therapeutic potential of LV-mediated *ex vivo* gene transfer has been demonstrated in murine models of MLD [208], β-thalassemia [209], sickle cell anemia [210], Wiskott-Aldrich syndrome [211] and Chronic Granulomatous Disease [212]. Clinical trials on β-Thalassemia and X-linked ALD are currently ongoing [213].

2.4 Safety of integrating vectors

Integration of a transgene into the cell chromatin may ensure stable expression of the gene product in the target cell and its progeny. For this reason, integrating vectors, such as retrovirus-based vectors, have been the preferred choice for gene delivery into HSC. On the other hand, vector integration may significantly affect the expression of cellular genes consequently altering cell growth control and eventually triggering cell transformation.

2.4.1 Adverse events in gene therapy

Given their ability to achieve high expression levels in the hematopoietic system, MoRV carrying wild type LTRs have been largely and in some cases, successfully used in gene therapy for blood disorders since 1991. These vectors were considered relatively safe, since integration was thought to be randomly distributed in the genome and the chance of accidentally disrupting or activating a gene was considered remote. This assumption was reconsidered when a lymphoproliferative disorder was reported in one patient treated for X-SCID with MoRV-transduced HSC [162]. Mapping of MoRV integrations in the predominant T-cell clone revealed a single proviral insertion within the LMO-2 locus, associated with up-regulation of transcript and protein levels. A similar complication was reported in three more patients enrolled in the same clinical study [163] and in another patient recruited in an independent X-SCID trial [161]. These five adverse events have remarkable features in common: all but one malignant clone hosted at least one MoRV insertion near to the proto-oncogene LMO2, resulting in LMO2 protein over-expression and leukemia developed 2 to 5 years after gene therapy treatment. This observation led the scientific community to reconsider both the assumption of random distribution of retroviral integration in the genome and the risks associated with retroviral gene transfer in human beings.

2.4.2 Insertional mutagenesis

Upon integration upstream from a gene in a tandem orientation, the proviral LTR can generate transcripts that read through and form chimeric transcripts including all, or part of the coding sequences of the downstream gene. Such read-through transcription occurs because the polyadenylation sites within the R region of the LTR are relatively weak and inefficient. If the vector genome contains an active splice donor (SD) site, aberrant splicing can lead to a truncated transcript that is missing a portion of the 5' mRNA sequences. As a result, such a read-through transcription can increase the amount

of the normal gene product or, alternatively, lead to the generation of a truncated protein, which may have adverse effects (Figure 16). Alternatively, the proviral genome could integrate in any orientation upstream, within, or downstream of a gene, interacting with its cellular promoter. The activity of viral LTR enhancers on the cellular promoters might increase the expression level of genes found within a genomic region of up to 300 kb flanking the vector integration site. A third possibility is intragenic integration. Proviral integration might interrupt gene expression, either by inducing premature polyadenylation at a site within the vector genome or by triggering aberrant splicing which eliminates or alters the gene product. This mechanism becomes relevant for somatic genes only if the insufficient haploid state is associated with a potentially deleterious effect.

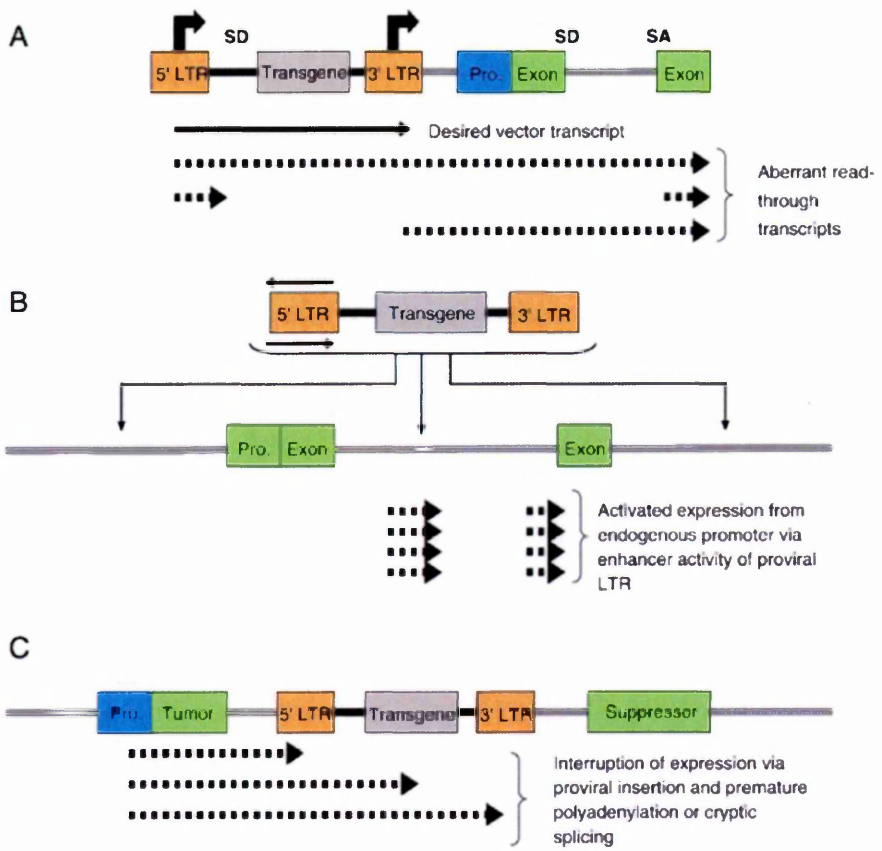

Figure 16. Insertional mutagenesis. Potential mechanisms of insertional mutagenesis following retroviral integration. (A) Read-through transcription of a downstream gene. Upon integration upstream from the gene in a tandem orientation, the proviral LTR can generate transcripts that read through and form chimeric transcripts. (B) Promoter activation by an LTR enhancer. As illustrated in this diagram, a proviral genome integrated in any orientation may increase the level of expression of a gene by virtue of interactions between an enhancer in one of

the LTR and the cellular promoter. (C) Decreased gene expression secondary to intragenic insertion of a proviral genome. The potential mechanism whereby proviral integration may interrupt gene expression is illustrated.

2.4.3 Pattern of integration

Recent reports have also challenged the notion that retroviral integration occurs randomly in the target cell chromatin and have indicated specific biases for integration into transcriptionally active genes, for both MoRV and HIV [182 214 181]. These recent findings have prompted the scientific community to study and compare integration site selection among different integrating vectors in greater depth, in order to evaluate the risk-benefit ratio in gene therapy applications and to develop safer vectors. In our lab, the use of a tumour-prone mouse model, allowed us to demonstrate a dose-dependent acceleration of leukemia/lymphoma onset triggered by MoRV upon HSC gene transfer and tranplantation. By contrast, tumorigenesis was unaffected by SIN-LV [215]. The different integration site selection patterns of the two vectors and the lack of transcriptionally active LTRs in the LV design were recently shown to contribute to the low genotoxicity of LV observed in this model (Montini et al, JCI, in press). Recent studies confirmed the different integration pattern of LV, which unlike MoRV, rarely integrate in proximity to expressed genes [182].

3. Gene therapy for LSDs

LSDs are excellent candidates for gene therapy. Firstly, they represent generally well-characterized, single gene disorders and secondly, a partial reconstitution of enzyme activity is usually sufficient for clinical efficacy [216].

3.1 *In vivo* gene therapy for LSDs

3.1.1 Systemic vector administration

In vivo gene therapy in LSDs is usually designed to establish a sustained source of therapeutic enzyme within the body for metabolic correction. Intravenous delivery of viral vectors may represent an effective strategy to target gene transfer to tissues, which are readily accessible from the bloodstream and may thus become efficient sources of systemic enzyme distribution. It has been shown that intravenous administration of Adenoviral vectors (AdV) [217], Adeno-associated vectors (AAV) [218 219 220], RV [221 222 223] and LV [194 224] leads to efficient liver cell transduction. By using these different approaches, the liver can produce large amounts of therapeutic enzyme, thus becoming a depot organ. The efficacy of this strategy has been evaluated in several LSD animal models. Neonatal intravenous MoRV gene therapy has been evaluated in mice and dogs. Newborn mice affected by MPS I, caused by IDUA deficiency, were intravenously injected with MoRV expressing canine IDUA. Treated animals achieved stable expression of IDUA in serum, a reduction of storage material in tissues and a reduction of some major clinical manifestations. Interestingly, these results were not observed in mice treated with a lower dose of vector, suggesting that a high expression of the transgene is required for gene therapy to be effective [222]. Similar results were obtained in dogs affected by MPS VII and injected with MoRV expressing the canine b-

glucuronidase (GUSB). Treated animals displayed stable levels of GUSB in serum, at or above the heterozygous levels, an absence of major clinical signs of the disease such as cardiac abnormalities and a marked amelioration of the skeletal, cartilage and synovial disease [222] [223]. AAV were also successfully used for systemic gene delivery in LSDs. Mice affected by MPS II caused by iduronate 2 sulfatase (IDS 2), were injected intravenously with AAV2/8 expressing IDS 2. Treatment resulted in the full clearance of storage substrate and restoration of IDS 2 activity in plasma and tissues [225].

Despite encouraging pre-clinical data, this approach reveals some relevant limitations when considering clinical translation: i) the occurrence of immune responses directed towards the vector or the novel therapeutic protein can lead to clearance of the transduced cells and/or loss of enzyme activity [226]; ii) poor therapeutic potential in LSDs with CNS involvement, since the secreted enzyme is unable to cross the BBB, thus limiting the benefit to peripheral organs, without correcting nervous system manifestations; iii) the safety and toxicity of parenteral vector administration and the possible risk of inadvertent gene transfer to the gonads and germ-line transmission of the vector will have to be established.

The development of immune responses may be reduced by the use of liver-specific promoters capable of restricting transgene expression to parenchymal cells of the liver, thereby reducing the expression within antigen-presenting cells [227]. Moreover, the residual off-target expression of the transgene has been recently prevented by using microRNA regulation: Brown et al. demonstrated that transgene expression could be inhibited in antigen presenting cells by microRNA-regulated LV and allow establishing stable long-term therapeutic gene transfer in the liver [228]. These novel approaches are currently being tested in vivo, for therapeutic efficacy in LSD models.

3.1.2 Direct CNS gene delivery

To overcome the issue of poor BBB permeability for lysosomal enzymes, delivery systems have been developed for direct *in vivo* gene transfer into the CNS. Efficient transduction of the neurons of adult rodent brains was observed with all generations of LV [229] [230] [187] [231] and effective gene transfer was also observed in the neurons of non-human primates [232]. The main cellular target of LV in the CNS are neurons (over 90% of transgene-expressing cells after administration of VSV-pseudotyped LV), while glial cells are transduced *in vivo* to a lower efficiency. Pre-clinical studies have been performed on animal models for several LSDs. LV encoding the lysosomal ARSA enzyme were stereotactically injected into the brains of mice affected by MLD. Treated animals displayed a significant improvement of disease-associated neurological and behavioral symptoms [233]. Similar results were obtained by injecting AAV coding for α-iduronidase into the brains of murine and canine MPS I models: the procedure prevented the accumulation of gangliosides and allowed for clearance of the storage material present at the time of treatment [234] [235]. Stereotactical injections of AAV were also performed on small and large animal models with late infantile neuronal ceroid lipofuscinosis (LINCL), an LSD caused by tripeptidyl peptidase 1 (TPP1) deficiency. LINCL mice that received intracranial injection of AAV2 and AAV5, showed a marked reduction in stored material and neurological abnormalities, but motor neuron function was preserved only when gene therapy was performed in a pre-symptomatic stage [236]. In a related study, this group demonstrated a reduction of storage material, but significant recovery did not occur when the treatment was applied after the onset of symptoms [237]. Given these encouraging results, a clinical protocol for CNS-directed gene therapy has been approved for LINCL patients', where an AAV2 encoding for TPP1 is administered directly into the brain [238]. Preliminary data showed a modest diffusion of the enzyme in the CNS and disease progression was reported to be slowed. Unfortunately, serious adverse events were also observed: one patient died after developing epileptic seizures,

while another showed a humoral response against the transgene [239]. A clinical protocol of CNS-directed gene therapy has also been approved for Canavan disease [240]. In this LSD the deficiency of the lysosomal enzyme aspartoacylase (ASPA) is responsible for toxic accumulation of substrates in the CNS, leading to myelination impairment and spongiform degeneration of the brain. Patients treated with intracranial infusions of recombinant AAV2 expressing ASPA showed minimal systemic signs of inflammation. Three out of 10 patients developed a low level of neutralizing antibodies. This data suggested that intraparenchymal administration of AAV2 is relatively safe, while the efficacy of this treatment will be evaluated in phase II/III trials.

In summary, *in vivo* gene therapy approaches for LSDs have demonstrated up to date satisfactory safety and efficacy. The effective correction of disease manifestations throughout large sectors of the brain despite the focal vector administration has been shown to be due to the transduction of neurons, which, through their projections, could distribute the enzyme into the CNS [241] [236]. Nevertheless, the invasiveness of the gene transfer procedure and the adverse events described in the LINCL clinical trial caution for further development of this approach. Ongoing pre-clinical studies in primates and upcoming clinical trials will clarify the tolerability and therapeutic potential of direct CNS gene transfer by different vectors.

3.2 *Ex vivo* gene therapy for LSDs

3.2.1 HSC-based *ex vivo* gene therapy

Based on the positive clinical experiences with HSCT in some LSDs, HSC-mediated gene therapy has been considered as an attractive alternative for the treatment of LSDs. Importantly for LSDs characterized by a severe involvement of the nervous system (see paragraph 1.6.3), HSC progeny might contribute significantly to the turnover of CNS microglia [102] [242], which play a major role in the pathogenesis of CNS involvement in

many LSDs, including GLD [243] [244]. Gene transfer strategies aimed at correcting the genetic defect in HSC may have significant advantages when compared with conventional allogeneic HSCT protocols. Because autologous cells are used, transplant-related mortality and morbidity are reduced. Moreover, genetically modified cells may express higher levels of the therapeutic enzyme, thus becoming more effective than wild type cells.

Several pre-clinical studies have been performed on murine models of LSDs. In the case of MLD, LV-mediated transduction of HSC allowed a supra-physiological expression of the lysosomal enzyme ARSA. Major disease manifestations were prevented in mice transplanted with ARSA-transduced HSC when treated in a pre-symptomatic stage and pre- established neurophysiological and neuropathological damage was corrected when transplanted in a symptomatic stage [208] [102]. The efficacy of HSC gene therapy has also been demonstrated in MPS I mice. Transplantation of MoRV-transduced HSC allowed for the reduction of stored toxic material in the liver, spleen, kidney, choroid plexus and thalamus [245]. This result was likely due to the reconstitution of peripheral macrophages by cells of donor origin, over-expressing the therapeutic enzyme. The level of enzyme over-expression required to achieve therapeutic efficacy could vary for different diseases. LSDs characterized by CNS involvement or by bone alterations might require a higher enzyme expression, compared to those characterized by visceral manifestations. In order to achieve high enzyme activity and therapeutic efficacy, a high level of transgene expression by HSC and their progeny may be required. High transgene expression relies on multiple vector integration into HSC, a condition that might increase the risk of integration-dependent adverse events (see paragraph 2.4).

In HSC gene therapy, as in the case of allogeneic HSCT, CNS inflammation might enhance the efficacy of the treatment by accelerating the rate of microglial reconstitution. This phenomenon has been observed in the murine model of

gangliosidosis GM-1: upon transplantation of HSC transduced with MoRV coding for lysosomal β-Galactosidase, animals showed correction of disease phenotype [107]. These results highlighted the concept that therapeutic HSCT actually corrects a nervous system damage-response pathway which is defective in LSDs. Vector-mediated over-expression of the therapeutic enzyme in macrophages/microglia may serve to enhance the corrective potential of this pathway.

3.2.2 Neural stem cells-based *ex vivo* gene therapy

In 1992, Reynolds and Weiss were the first to isolate neural progenitor and stem cells from the striatal tissue, including the subventricular zone – one of the neurogenic areas - of adult mice brain tissue. Neural stem cells (NSC) are the self-renewing, multipotent cells that, *in vitro,* generate the main phenotypes of the nervous system: neurons, astrocytes and oligodendrocytes. Since then, neural progenitor and stem cells have been isolated from various areas of the adult brain, including non-neurogenic areas, such as the spinal cord and from various species including humans [246].

NSC-based *ex vivo* gene therapy exploits the engraftment potential and the multipotency of NSC. The identification and mapping of persistent NSC and progenitor cells in the CNS highlight the potential of neuroplasticity in adulthood [247] [248] and emphasized the possible role of NSC and progenitors in the treatment of LSDs. In many metabolic myelin disorders, such as GLD, oligodendrocytes are killed by toxic metabolites; the engraftment of glial progenitor cells is associated with astrocytic and oligodendrocytic production, while undifferentiated NSC can migrate widely throughout the CNS and can, to some extent, differentiate and integrate in a regionally appropriate fashion. As such, both glial progenitors and NSC seem to be promising vehicles for the distribution of enzyme-producing cells throughout the brain parenchyma. Lacorazza and colleagues reported the expression of β-Hexosaminidase upon engraftment of transduced NSC into recipient mice [249]. Similar results have been obtained in a murine

model of MPS VII: upon implantation of MoRV or LV-tranduced NSC into the CNS, high levels of therapeutic enzyme and correction of brain disease manifestations have been observed [250] [251].

3.3 Gene therapy for GLD

The first gene transfer studies on GLD were performed on fibroblasts. Gama Sosa and colleagues demonstrated that retroviral-mediated gene transfer of human GALC cDNA into twi fibroblasts and primary human fibroblasts from a patient with juvenile-onset GLD, was able to correct the GALC-deficient phenotype of the disease, reaching a supra-physiological level of GALC activity [252]. Furthermore, the cross-correction mechanism was demonstrated in fibroblasts and oligodendrocytes cultured in conditioned medium from transduced cells [253] [254]. Rafi and colleagues transduced primary cultures of fibroblasts, obtained from a GLD patient, with a MoRV containing the human GALC cDNA. Transduction permitted over-expression of GALC up to 100 times the normal value. Moreover, untransduced GLD fibroblasts cultured in the conditioned medium of transduced cells, displayed a reconstitution of enzymatic activity, thus confirming that GALC could be secreted and internalized by neighboring cells. Further analysis confirmed that GALC was correctly sorted to lysosomes of cross-corrected fibroblasts [254]. Although fibroblasts could be useful for basic studies, they do not have abnormalities related to sphingolipid accumulation. Therefore, enzyme reconstitution following transduction and cross-correction was evaluated in oligodendrocytes. Luddi and colleagues transduced twi oligodendrocytes with a MoRV expressing GALC. In transduced cells GALC activity was increased to heterozygous levels and correction of morphology was observed. In this study, GALC expression following transduction was lower in respect to that observed in transduced fibroblasts. A possible explanation could be the poor transduction efficiency of MoRV on slowly dividing cells, such as oligodendrocytic precursors. Further experiments demonstrated

that transduced oligodendrocytes are able to secrete GALC into the culture medium and untransduced oligodendrocytes are able to uptake the enzyme as well [253].

These results have been the background for further pre-clinical studies. Most strategies that have been developed and that involve AdV, AAV, MoRV or LV, are *in vivo* gene therapy approaches. In 2001, the first case of gene delivery directly to the CNS in GLD models, was reported. AdV coding for the human GALC was intra-ventricularly injected into 0 day-old or 15 day-old twi mice. The treatment, when performed at birth, resulted in increased GALC activity and partial correction of the pathology in the brain, but without a significant improvement of the phenotype. Moreover, pathology correction was not observed when twi mice were treated at 15 days, suggesting that the timing of intervention should be precocious [255]. Similar studies further demonstrated that *in vivo* approaches targeting the CNS only, are not able to correct the disease. Intraventricular injection of AAV1 in twi and in trs mice (see paragraph 1.6) achieved a prolonged lifespan and a correction of pathologic signs of disease, but treated animals died with the same disease manifestation as controls [256]. Comparable results were obtained with intracranial injections of AAV2 or AAV2/5 expressing murine GALC, performed on twi mice [257] at 3 days of age. In general, intracranial injection of viral vectors expressing GALC, resulted in high levels of enzyme activity in the brain. However, this supraphysiological level of GALC activity resulted only in a slowing of disease progression, with minimal improvement of phenotype and lifespan. Moreover these results were obtained only when treatment was performed at a pre-symptomatic stage. The major limitation of this approach is the lack of efficacy at the level of the PNS. For this reason, the combination with a systemic approach, such as ERT or HSCT, which could provide the enzyme to the PNS, might give better results. Lin and colleagues combined CNS gene delivery with HSCT [258]. Twi mice were injected with AAV vector expressing GALC in the CNS and underwent HSCT from wild type donors. Treated animals showed a significant reduction in

demyelination, astrocytosis and macrophage infiltration. Their survival was longer, not only in respect to untreated controls, but also compared to that obtained with either single treatment, thus suggesting a synergy between the two therapies. Interestingly, the increase of GALC activity in the tissues of mice that received the combination treatment, was higher compared to either therapy alone and even higher than the sum of the activity from the individual treatments. This finding enforced the hypothesis of a synergistic effect of AAV injection in the CNS and HSCT.

Besides direct CNS gene delivery, cell-based gene therapy strategies have also been tested. Pellegatta and colleagues engrafted twitcher mice with cultured LV-transduced NSC [259]. Although the engrafted GALC-over-expressing cells did not survive well in the highly inflammatory twitcher brain, they migrated appropriately to active sites of demyelination, in a manner similar to the one observed in adult mice by [260] [261]. The therapeutic effect of the treatment was modest, due to the clearance of transduced cells, likely due to the activated microglia. The hypothesis that the CNS of twi mice could be a non-permissive environment for transplanted cells was also investigated by Snyder's group. The inflammatory milieu of twi CNS was not found to be a limiting factor for NSC engraftment, but, rather, it appeared to serve as a tropic factor, drawing transplanted NSC towards damaged areas. Moreover, they investigated the sensitivity of NSC to the toxic storage of Psy, present in the CNS of two mice. NSC showed an increased resistance to the detrimental effect of Psy, if compared to more differentiated cells, such as oligodendrocytic progenitors [262]. Therefore, in order to develop an effective cell gene therapy strategy for the treatment of GLD, the sensitivity of transplanted cells to the toxic environment where they are transplanted, should be considered. This issue could also be relevant for developing HSCT-based gene therapy strategies. Previous studies demonstrated that Insuline-Like Growth Factor 1 (IGF1) is involved in survival pathways of different cell types and could rescue oligodendrocytes from apoptosis induced by the toxic effect of Psy accumulation [29]. The usefulness of

IGF1 in helping to improve HSCT has recently been tested. *In vitro* stimulation with IGF1, before transplantation, resulted in an increased engraftment of HSC and prolonged survival of transplanted mice [263]. Overall, these findings suggest that gene therapy for a complex disease like GLD should consider different aspects, including the level of enzyme expression required, the characteristics of transplanted cells and the permissiveness of the environment where cells are transplanted or where viral vectors are injected.

AIM OF THE WORK

First aim of this work was to develop a gene therapy approach for the treatment of GLD, based on HSPC and LV. From the experience with MLD, we learned that for HSC gene therapy to be efficacious in LSD, effective gene transfer and enzyme over-expression in HSPC must be obtained. First, we tested the feasibility of GALC over-expression in HSPC upon GALC.LV transduction. Then, we set up a transplantation protocol in twitcher mice. Unfortunately, our work showed that transduction with GALC encoding LV affects the functionality of HSPC, which become unable to repopulate lethally conditioned twitcher mice, For this reason, we then attempted to evaluate the safety of GALC over-expression in HSPC. We studied the maintenance of the functional properties of HSPC upon GALC over-expression both *in vitro*, evaluating their clonogenic potential by CFC assay, and *in vivo*, evaluating their repopulation potential by HSCT in mice. Moreover, we verified whether transduction affected HSPC survival, by monitoring the occurrence of apoptosis by TUNEL assay and annexin V staining at different time points after gene transfer. Indeed, we demonstrated that GALC expressing HSPC undergo a rapid and massive apoptosis, associated to a functional impairment both *in vitro* and *in vivo*. The mechanism responsible for this overt toxicity observed in HSPC upon GALC *de novo* expression was further investigated. We performed a sphingolipid profile of GALC.LV transduced HSPC, and demonstrated that ceramide and sphingosine1P accumulation is likely to be responsible for the observed acute apoptosis.

Third aim of the work was to overcome the limitation of GALC *de novo* expression toxicity in HSPC in order to develop HSC gene therapy for GLD. First, we evaluated the sensitivity to GALC toxicity of differentiated hematopoietic cells and in cells of other lineages. Since microglia and macrophages, the effector cells of HSC gene therapy, were not affected by GALC de novo expression, we tested two new strategies to restrict

transgene expression to differentiated hematopoietic cells. The first strategy was based on myeloid-specific promoters (transcriptional regulation), in order to allow GALC expression only in microglia and macrophages, the effector cells of HSC gene therapy. The second strategy exploited microRNA-based post-transcriptional regulation to repress transgene expression only in HSC and not in differentiated cells. Although these two approaches proved to be very promising in protecting HSPC from enzyme toxicity both *in vitro* and *in vivo* in heterozygous GLD mice, gene-corrected HSPC failed to repopulate lethally irradiated homozygous GLD mice. This poor result might be explained by the existence of a niche defect in homozygous GLD mice, which might hamper the engraftment of HSPC.

METHODS

1. Reagents and suppliers

1.1 Chemicals

All chemicals were obtained from FLUKA or Sigma-Aldrich. Other chemicals used during the study were obtained from the following sources:

Lymphoprep:	Axis-Shield PoC AS
CH296 (retronectin):	Takara BIO
Metaphor agarose:	BMA
Fluorsave Reagent:	Calbiochem
Papain:	Worthington
EDTA:	ProLabo

1.2 Enzymes and buffers

All DNA modification enzymes and buffers were obtained from Roche. All restriction enzymes and buffers were obtained from either Roche or New England Biolabs.

GoTaq polimerase enzyme was supplied by Promega.

1.3 Bacterial strains

The Top10 bacterial strain was supplied by Invitrogen (code number 44-0301).

1.4 Cell culture

Cells were incubated at 37°C in a 5% CO incubator. All tissue culture plastic ware (tissue culture plates and tubes) was obtained form BD Falcon.

Trypsin-EDTA solution: Phosphate Buffered Saline 0,05% trypsin, 4mM EDTA pH 7.3.

Media, sera and supplements:

IMDM:	Sigma-Aldrich
RPMI:	1640 Euroclone
DMEM:	Euroclone
StemSpan SFEM:	Stem Cell Technologies
Cell Gro:	Cell Genics
MethoCult H4434:	Stem Cell Technologies
MethoCult M3434:	Stem Cell Technologies
Foetal Bovine Serum (FBS)	BioSera
Trypsin:	Invitrogen
L-Glutamine:	Invitrogen
Penicillin/Streptomycin:	Invitrogen
Polybrene:	Sigma-Aldrich
Cytokines:	Peprotech
PBS:	Sigma-Aldrich
Matrigel:	Beckton Dickinson

2. Plasmids

LV were produced by co-transfection of 4 plasmids: transfer construct, packaging construct, Rev-encoding construct and envelope construct. All the plasmids contain the gene encoding for Ampicillin resistance.

Transfer constructs:

pCCLsin.PPT.hPGK.eGFP.pre [186 264 187]

pCCLsin.PPT.hPGK.eGFP.142mirTag.pre

pRRLsin.PPT.hPGK.GALC.pre

pRRLsin.PPT.hPGK.GALC.HA.pre

pRRLsin.PPT.hPGK.GALC.142mirTag.pre

pRRLsin.PPT.CD11b.GALC.pre

pCCLsin.PPT.hPGK.ARSA.pre [102]

pCCLsin.PPT.hPGK.IDUA.pre

pCCLsin.PPT.hPGK.DNGFR.pre

Packaging constructs:

pCMVΔR8.74 [186] was used in the production of second generation vectors.

pMDLg/pRRE [186] was used to package third generation vectors.

Rev-encoding construct: pRSV-REV [186]

Envelope constructs: pMD2.VSV-G [186]

3. Transformation of competent bacteria and plasmid preparation

Plasmid DNA (0.5-10ng) to be transformed was mixed with 50μl of chemically competent Top10 cells prepared specifically for the heat shock mediated transformation method. The mix was incubated on ice for 30 minutes, then 1 minute at 42°C, and then returned to ice for a further 5 minutes. The mix was then plated onto Luria Bertani (LB) agar plates, containing 100μg/ml ampicillin and placed overnight in a 37oC bacterial incubator. The following day, colonies were picked and placed into 2 ml of Terrific Broth (TB) media for GALC-plasmids, or LB media for all other plasmids containing

carbenicillin (ampicillin homologue), and grown over day with agitation at 37°C. 10 µl of the over day culture were placed in 200ml of TB or LB media containing carbenicillin, and grown overnight shaking at 37°C. The following day, cell suspension was measured by spectrophotometer analysis (λ=600nm) to check for optimal cell density (about 1-1.5 O.D.) and subjected to large-scale plasmid DNA preparation. Plasmid DNA preparation was performed using High Purity Plasmid Purification Systems (Marligen Biosciences). This system is based on alkaline lysis, followed by DNA purification on an anion exchange resin. After elution, plasmid DNA was then desalted and concentrated by alcohol precipitation washed in 70% ethanol and resuspended in TE buffer (10mM Tris-HCl pH 8.0, 0.1 mM EDTA).

4. Vector production

4.1 Transfection

Reagents:

2X HBS: 281mM NaCl, 100mM HEPES, 1.5mM Na_2HPO_4, pH 7.12, 0.22µM filtered, stored at –20°C or –80°C.

2.5M $CaCl_2$: tissue culture grade, 0.22µM filtered, stored at –20°C.

0.1X TE buffer: 10mM Tris (pH 8.0), 1mM EDTA (pH 8.0) diluted 1:10 with dH_2O, 0,22µM filtered, stored at 4°C.

dH_2O: endotoxin-free, tissue culture grade (Sigma-Aldrich).

Vector stocks were prepared by calcium phosphate transfection and concentrated by ultracentrifugation. Vectors were produced by transfection of human embryonic kidney 293T cell line (containing the mutant gene of SV40 Large T Antigen, see paragraph 5. Cell lines), because these cells are optimal DNA recipients in transfection procedures and the backbones of the vector construct contain SV40 origin of replication. $9x10^6$

293T cells *per* dish were seeded and incubated in 15 cm dishes, 24 hours before transfection in IMDM, 10%FBS, Penicillin (25U/ml), Streptomycin (25U/ml). Two hours before transfection medium was replaced. To produce LV, plasmid DNA mix was prepared by mixing (*per* dish):

9µg pMD2-VSV-G

16,25µg pCMVΔR8.74 or 12,5µg pMDLg/pRRE

6,25µg pRSV-REV

32µg transfer construct

The plasmid solution was made up to a final volume of 1125µl with 0.1XTE/dH_2O (2:1) in a 15 ml polypropylene tube. Finally 125µl of 2.5M $CaCl_2$ were added. The precipitate was formed by drop wise addition of 1250µl 2X HBS solution to the 1250µl DNA-TE-$CaCl_2$ mixture while vortexing at full speed. The precipitate was added to 293T cells immediately following addition of the 2X HBS and cells were incubated at 37°C. 14-16 hours after transfection, medium was replaced. 30 hours after medium changing, supernatant was collected, filtered through 0.22µm pore nitrocellulose filter and ultracentrifugated at 19,500 rpm in SW32Ti rotor (Optima L-60 preparative Ultracentrifuge; Beckman) 2 hours at room temperature. Pellets containing the vector were resuspended in a volume of sterile PBS representing 1/500 of the starting medium volume, pooled and rotate on a wheel at room temperature for 1 hour. The concentrated vector preparation was then divided into small aliquots (20-50µl) and stored at –80°C.

4.2 Vector particle amount determination

Vector particle amount was determined by immunoenzymatic assay, using the Alliance HIV-1 p24 antigen ELISA kit (PerkinElmer), following manufacturer's instructions. Serial dilutions of the vector stock (see below vector titer determination) were plated in triplicate in microplate wells, which are coated with a highly specific

mouse monoclonal antibody to the HIV-1 capsid protein p24, and vector particle envelope was lysed by 5% Triton X-100. The captured antigen was then complexed with biotinylated polyclonal antibody to HIV-1 p24, followed by a streptavidin-HRP (horseradish peroxidase) conjugate. The resulting complex was detected by incubation with ortho-phenylenediamine-HCl (OPD), which produces a yellow colour that is directly proportional to the amount of HIV-1 p24 captured. The absorbance of each microplate well was determined using a microplate reader (Versa Max, Molecular Devices) (λ 490nm) and quantity of p24 protein was calculated using an HIV-1 p24 antigen standard curve.

4.3 End-point titration

End-point titration is performed by transducing a permissive target cell line with serial dilutions of the vector preparation. 10^5 HeLa cells were plated per well in 3.5cm wells in 1 ml of IMDM 10% FBS; 6 hours later, a vector aliquot was thawn and to prepare serial ten-fold dilutions of 2X viral stock (from 10^{-3} to 10^{-8}) in IMDM 10% FBS. Medium of cells was replaced with 500µl of medium 16µg/ml polybrene (2X final polybrene concentration) plus 500µl of serial dilutions (one dilution *per* well). Cells were cultured in a 5% CO2 incubator at 37°C. 16 hours later the medium was replaced. After 7-10 days cells were harvested for expression titer (FACS analysis) or for integration titer (Real-time Quantitative-Polimerase Chain Reaction (Q-PCR) analysis). The titer is defined as number of transducing units per milliliter (TU/ml) of vector preparation. Expression titer is based on the assumption that a single vector copy integrated in the host genome will give a positive cell. Assuming that all the cells are equally susceptible to transduction, following Poisson distribution for random independent events, a single transduction event, and not more, has occurred in most positive cells, when the percentage of positive cells in the total population is below 25%. It follows that expression titer must be calculated from a sample corresponding to a

vector dilution where positivity of cells ranges between 1% (to ensure an acceptable signal over the instrument noise) to 25%, in order not to underestimate the titer when multiple transduction events per cell have occurred. Integration titer must be calculated from a sample corresponding to a vector dilution where vector copies *per* cells rages between 0.01 and 0.25. Proof of linearity must be obtained showing that different dilutions in the optimal testing range yield linear increase in transduction frequency.

The equation to calculate expression titer is:

Titer (TU/ml) = (number of cells at the time of vector addition) X (% transgene+ cells/100) X (dilution factor)

The equation to calculate integration titer is:

Titer (TU/ml) = (number of cells at the time of vector addition) X (vector copies per cell) X (dilution factor)

For FACS and Q-PCR analyses see relative paragraphs below. Titers of vectors used in this project ranged between 10^9 and 10^{10} TU/ml (vector stock concentrated 500x).

4.4 Infectivity of the vector stocks

Infectivity is a reliable parameter to evaluate the quality of the vector stock and can be defined as the transducing activity *per* unit of physical particle, where the first parameter is expressed as TU/ml, as obtained by end-point titration and the second as ng p24/ml, as determined by immunoenzymatic assay. Since one ng of p24 could theoretically contain 1.2 X 10^7 particles, if all the particles in the vector stock were infectious, a titer of 10^8 TU/ml would correspond to a p24 concentration of about 10 ng/ml. Indeed, a concentration in the range of 500-1000 ng p24/ml is more reasonably expected. This is due to two major reasons. The first reason is that end-point titer fails to estimate the real content of infectious particles in a vector preparation, because vector particles move by Brownian motion in the medium and only a fraction of them has the

chance to get in contact with a cell in the monolayer and transduce it in the time window of the assay. The second reason instead is crucially linked to the quality of the vector batch tested. In fact, the efficiency of packaging of infectious particles is lower than what is predicted by theoretical calculations, and a good fraction of the total p24 protein is not assembled into infectious virions. Vector infectivity can be calculated by the following equation:

Infectivity = (TU/ml)/(ng p24/ml) = TU/ng p24

Infectivities were 10^3-10^5 TU/ng p24 for all vector types.

5. Cell lines

HeLa (ATCC Number CCL-2), 293T (originally called 293tsA1609ne, and derived from 293 cells, a continuous human embryonic kidney cell line transformed by sheared Type 5 Adenovirus DNA, by transfection with the tsA 1609 mutant gene of SV40 Large T Antigen and the Neor gene of E. Coli - ATCC Number CRL-1573; cells were maintained in Iscove's Modified Dulbecco's Medium (IMDM) and U-937 (ATCC Number CRL-1593.2) in RPMI-1640, both supplemented with 10% foetal bovine serum (FBS), 100 IU/ml penicillin, 100 μg/ml streptomycin, and 2mM L-glutamine. To detach adherent cells PBS 0.05% trypsin, 4mM EDTA (pH 7.3) was used.

6. Mice studies

Twitcher (twi) mice were obtained from Jackson laboratories. Congenic FVB/N.B6Galc-(*twi/twi)* (FVB/twi) mice were generated in our animal research facility by breeding Twi heterozygous (+/-) C57BL6 mice with wild type (+/+) FVB mice. Mice were screened as indicated in paragraph 6.1 and heterozygous offspring were intercrossed to obtain an inbred strain.

Rag2-/-γchain -/- mice (Rag2γc) were obtained from Charles River laboratories.

Procedures were performed according to protocols approved by the Animal Care and Use Committee of the Fondazione San Raffaele del Monte Tabor (IACUC #325) and communicated to the Ministry of Health and local authorities according to Italian law.

6.1 Genotyping of FVB/twi mice

Genotyping of FVB/twi mice was performed on DNA from tail biopsies. The sequence of GALC containing the mutation was amplified by PCR and the product of amplification was digested by EcoRV endonuclease enzyme.

6.1.1 DNA extraction

Tail tissue was lysed by Proteinase K (PK)(Roche) at the concentration of 1 mg/ml for 2 hours at 56 °C. The buffer used for PK lysis was TRIS 10 mM pH 7.2, EDTA 25 mM, NaCl 10 mM, SDS 10%. After complete digestion, DNA was extracted through a salting-out method. The sample was spinned 5 minutes at 13200 rpm in a standard tabletop centrifuge to remove residues of bones or fur. One volume of fenol/chloroform/isoamilic alcohol 25:24:1 was added to the sample, vortexed and spinned at 13200 rpm for 7 minutes. The upper phase was harvested and 10% volume of Sodium Acetate 3M pH 7.3 and 2 volumes of ethanol 100% were added. Sample was gently mixed and DNA flocculate was pellet by centrifugation at 12000 rpm for 5 minutes. Pellet was washed with ethanol 70 % and resuspended in 100-200 µl of sterile water.

6.1.2 Amplification of GALC sequence by PCR

Amplification of GALC sequence was performed as described [265]. The forward was designed on an intronic sequence 230 bp upstream the mutation site (TwF: 5'-CACTTATTTTCTCCAGTCAT). The reverse primer was designed on an esonic sequence immediately after the mutation site (TwR: 5'-TAGATGGCCCACTGTCTTCAGGTGATA). The amplification generates in the mutant DNA a target sequence for the restriction enzyme EcoRV. Details of PCR reaction are reported:

Buffer 5x (Promega)	5µl	step 1:	95°C 10'	1 cycle
Primer F 10µM (Primm)	0.5µl	step2:	95°C 30"	38 cycles
Primer R 10µM (Primm)	0.5µl		54°C 30"	
dNTPs 10µM (Roche)	0.6µl		72°C 30"	
Go Taq (Promega)	0.25µl	step 3:	72°C 10'	1 cycle
H2O	14,65µl			
DNA	200ng			

6.1.3 EcoRV restriction analysis

The 260 bp PCR product was digested by EcoRV in a final volume of 25 µl. Digestion of one half of PCR volume is enough to visualize the bands on gel. Details of reaction are reported:

Buffer B (Roche)	2.5 µl
EcoRV (Roche)	0.7 µl
H_2O	11.8 µl
DNA (from PCR)	10 µl

Fragments obtained from EcoRV digestion were visualized on Metaphor 4% (BMA) agarose gel. EcoRV digestion of wild type DNA results in the generation of a band of 260 bp; heterozygous restriction pattern shows 2 bands: one of 260 bp (wild type allele), another of 234 bp (mutant allele); homozygous restriction pattern shows only a band of 234 bp.

7. Haematopoietic stem/progenitor cell (HSPC) enrichment

7.1 Human HSPC (hHSPC)

Cells from human subjects were obtained with informed consent according to the Declaration of Helsinki, and to a protocol approved by the San Raffaele Scientific Institute Bioethical Committee. Mononuclear cells were obtained from human either CB or BM scheduled for discard by density separation, and CD34+ cells were isolated by positive selection. CB or BM were diluted 1:2 in PBS, stratified on half a volume of Lymphoprep and spinned at 1500 rpm in Heraeus Megafuge 1.0 (Kendro Laboratory products) 30 minutes at room temperature, without brake. Plasma upper layer containing platelets was removed and the interphase between plasma and lymphoprep, containing PBMC, was transferred in a new tube and washed with PBS. Cells were then resuspend in 20ml MACS buffer (PBS pH 7,2, 0.5 % Bovine Serum Albumin – BSA, Sigma-Aldrich - and 2mM EDTA). PBMC were then subjected to CD34 positive selection, by using the MACS Indirect CD34 Progenitor Cell Isolation Kit. The magnetically labelled cells were enriched on LS separation columns in the magnetic field of the MidiMACS magnet (all Miltenyi Biotech), following manufacturer's instructions. Cells were centrifuged at 1000 rpm 10 minutes at 4°C, resuspended in 300µl MACS buffer *per* 10^8 cells and incubated with 100 µl Fc receptors blocking reagent (to block aspecific binding

of the antibody) together with 100 µl apten-conjugated anti- CD34 antibody *per* 10^8 cells 20 min at 4°C. Cells were then washed with 20ml MACS buffer as above, resuspended in 400µl MACS buffer *per* 10^8 cells and incubated with a secondary magnetic beads-conjugated anti-apten antibody 20 min at 4°C. Cells were washed again, resuspended in 1ml MACS buffer *per* 10^8 counted cells and subjected to two rounds of separation on LS columns. Flow through was discarded. CD34+ cells, recovered by removing the column from the magnetic field and by using the plunger, were then counted and either frozen in 90% FBS, 10% Dimethyl Sulfoxide (DMSO) or used fresh.

7.2 Murine HSPC (mHSPC)

BM cells were harvested from FVBtwi mice of 4-8 weeks and were subjected to negative selection by using the StemSep Mouse Hematopoietic Progenitor Cell Enrichment kit and the StemSep Magnet with StemSep 0.3" Negative Selection Gravity Columns (all Stem Cell Technologies), following manufacturer's instruction. BM cells were harvested by flushing from femurs and tibias with PBS 2% FBS and counted in a Burker chamber. After spinning at 1500 rpm 5 min at room temperature, and cells were resuspended at a concentration of $5x10^7$cells/ml in PBS 2% FBS, 5% rat serum and incubated 15 min at 4°C to block aspecific binding of antibodies. Cells were then incubated with 35µl/ml StemSep Enrichment Cocktail, which contains a combination of rat biotinilated monoclonal antibodies anti-mouse lineage specific markers (CD5, CD11b, CD45R/B220, Gr-1, Neutrophils (7-4) and TER119) 15 min at 4°C. After washing with PBS 2% FBS, cells were resuspended at $5x10^7$cells/ml in PBS 2% FBS, incubated with 100µl/ml Anti-Biotin tetrameric antibody complexes 15 minutes at 4°C and then with 60µl/ml magnetic colloid 15 min at 4°C. Cells were then loaded on a primed and equilibrated column in the magnetic field. Flow though, which contains lineage negative (Lin-) cells, was harvested and cells were washed, resuspended in StemSpan medium and counted. mHSPC were used fresh for HSCT, for CFC assay or

were kept in culture in RPMI medium, 10% FBS, penicillin 100U/ml and streptomycin 100 μg/ml, L-glutamine 2 mM and cytokines (mSCF 50ng/ml, mFlt3L 10ng/ml, mIL3 10ng/ml, mIL6 20ng/ml).

7.3 Isolation of Sca1- murine hematopoietic progenitors

BM cells were harvested from FVBtwi mice of 4-8 weeks and were subjected to Sca1 positive cells depletion by using MACS Sca1+ Progenitor Cell Isolation Kit (Miltenyi), following manufacturer's instructions. BM Cells were centrifuged at 1000 rpm 10 minutes, resuspended in 800 μl MACS buffer (see chapter 7.1) and incubated with 200 μl/ 10^8 cells of anti-Sca1 magnetic beads-conjugated antibody. After 20 minutes at 4°C, cells were washed with 20ml MACS buffer, resuspended in 1ml MACS buffer *per* 10^8 counted cells, and subjected to one rounds of separation on LS columns. Sca1+ cells were retained in the column, while Sca1- progenitors were collected in the flow through.

8. Isolation of human lymphocytes

8.1 T lymphocytes

T lymphocytes were obtained from PBMC, isolated from buffy coat as described for CD34+ cell selection from CB. PBMC were cultured for 3 days at the concentration of $1x10^6$ cells/ml in IMDM 5% human serum and PHA 1μg/ml in order to stimulate T lymphocyte proliferation. Cells were then cultured in IMDM 5% human serum and IL-2 300U/ml for at maximum two weeks.

8.2 B lymphocytes

B lymphocytes were obtained from PBMC, isolated from buffy coat as described for CD34+ cell selection from CB as described for CD34+ cell selection. PBMC were infected with Epstein-Barr virus (EBV) supernatant from B95.8 cells for 3 hours [266]. After infection, cells were washed with PBS and cultured at the concentration of $2x10^6$ cells/ml in IMDM 20% FBS, 100 IU/ml penicillin, 100 μg/ml streptomycin, and 2mM L-glutamine and PHA 2 μg/ml for 2 days. Medium was replaced twice a week (IMDM 20% FBS, 100 IU/ml penicillin, 100 μg/ml streptomycin, and 2mM L-glutamine). B-lymphocytes were either frozen in 90% FBS, 10% DMSO or used fresh.

9. Primary cultures

9.1 Isolation of human monocytes

Monocytes were obtained from PBMC, isolated from buffy coat as described for CD34+ cell selection from CB. PBMC were washed with PBS and counted. PBMC were then subjected to CD14 positive selection, by using the MACS CD14 Isolation Kit. The magnetically labelled cells were enriched on LS separation columns in the magnetic field of the MidiMACS magnet, following manufacturer's instructions. Flow though was discarded. CD14+ cells, recovered by removing the column from the magnetic field and by using the plunger, were then counted and plated on matrigel-coated cover-slips (for TUNEL assay) in RPMI supplemented with 10% FBS, 100 IU/ml penicillin, 100 μg/ml streptomycin 2mM L-glutamine and with GM-CSF 100 ng/ml, at the concentration of $5x10^5$ cells/ml. Alternatively, $2.5x10^6$ CD14+ cells were seeded in a 3.5 cm dish (for GALC activity assay). One half of medium was replaced every 2 days.

9.2 Isolation of murine peritoneal macrophages

Primary culture of murine macrophages were obtained through peritoneal wash with DMEM (8-10 ml/mouse). Cells were centrifuged at 1200 rpm 10 minutes and pellet was resuspended in DMEM supplemented with 10% FBS, 100 IU/ml penicillin, 100 μg/ml streptomycin 2mM L-glutamine. Cells were then counted and seeded at the concentration of $4x10^6$/ml in a 3.5 cm dish and cultured in incubator for 2 hours. After this time, medium containing non-adherent cells was removed and adherent cells were washed with PBS. The adherent fraction was cultured in DMEM 10% FBS, 100 IU/ml penicillin, 100 μg/ml streptomycin 2mM L-glutamine supplemented with GM-CSF 50 ng/ml. One half of medium was replaced every 2 days.

9.3 Isolation of murine microglia

Primary cultures of microglia were established from 2-day-old mice [267]. Mice were sacrificed with a tribromoethanol injection and brains were removed and put in cold PBS for 15 minutes. Cortex was then dissected and disaggregated by incubation at 37°C 20 minutes in EBSS with Papain 0.7 mg/ml, EDTA 0.2 mg/ml, L-Cysteine 0.2 mg/ml, DNAseI 10 μg/ml. After disgregation, cells were washed 3 times with DMEM and centrifuged at 1000 rcf 10 minutes. Each time supernatant was removed and pellet was resuspended by carefully pipetting. Cells were then resuspended in DMEM 10% FBS 100 IU/ml penicillin, 100 μg/ml streptomycin 2mM L-glutamine, using a final volume of 12 ml of medium to resuspend cells from 2 brains. After 7-10 days of culture, microglia was separated from the mixed culture through one hour of agitation at 195 rpm at 37°C. Detached microglia was harvested, washed and counted. Cells were then plated on matrigel-coated coverslips ($5x10^4$ cells/ml) in DMEM 10% FBS 100 IU/ml penicillin, 100 μg/ml streptomycin 2mM L-glutamine.

9.4 Isolation of murine oligodendrocytes

Primary cultures of oligodendrocytes were established from 2-day-old mice, as described for primary cultures of microglia. After one week of culture, microglia was separated from the mixed culture through one hour of agitation at 195 rpm at 37°C, and was removed. Oligodendrocytes were detached through over-night agitation at 195 rpm at 37°C. Oligodendrocytes were then plated on matrigel-coated coverslips ($5x10^4$ cells/ml) in chemically defined DMEM:F-12 1:1 medium [268] with FBS 2% and thyroid hormone T3 400 ng/ml.

10. Transduction

10.1 Human HSPC

10.1.1 CD34+ cells from CB

CD34+ cells from CB were incubated over-night at a concentration of $1x10^6$ cells/ml in Stem Span serum-free medium with 20 ng/ml recombinant human-Interleukin 6 (rh-IL6), 100 ng/ml rh-Stem Cell Factor (rh-SCF), 100 ng/ml rh-fms-like tyrosine kinase 3 Ligand (rh-FLT3L), and 20 ng/ml rh-thrombopoietin (rh-TPO). Transduction was carried out for 8 hours with 10^8 TU/ml (MOI 100) in the same medium [269]. After the transduction period CD34+ cells were washed twice with PBS and maintained in IMDM medium 10% FBS containing 20 ng/ml rh-IL6, 100 ng/ml rh-SCF, and 20 ng/ml rh-Interleukin 3 (rh-IL3) for suspension culture and/or plated for Colony Forming Cell Assay (see below).

10.1.2 CD34+ cells from BM

CD34+ cells from BM were incubated in retronectin-coated plates at a concentration of $1x10^6$ cells/ml in Cell Gro (Cell Genics) with IL-3 60ng/μl, TPO 100ng/μl, SCF 300ng/μl, Flt3-L 300ng/μl) for 24 hours. After pre-stimulation, cells were transduced at MOI 100 for 12 hours. After transduction, cells were washed twice with PBS and maintained in IMDM medium 10% FBS containing IL-3 60ng/μl, IL-6 60ng/μl, SCF 300ng/μl for suspension culture and/or plated for Colony Forming Cell Assay (see below).

10.2 Murine HSPC

Lin- cells were incubated at a concentration of $1x10^6$ cells/ml in Stem Span serum-free medium in presence of mSCF 50ng/ml, mFlt3L 10ng/ml, mIL3 10ng/ml, mIL6 20ng/ml (all from Peprotech) and transduced for 16 hours with 10^8 TU/ml of LV (MOI 100). After the transduction period cells were washed twice with PBS and maintained in RPMI medium 10% FBS containing mSCF 50ng/ml, mFlt3L 10ng/ml, mIL3 10ng/ml, mIL6 20ng/ml for suspension culture and/or plated for Colony Forming Cell Assay (see below).

10.3 Sca1- murine hematopoitic progenitors

Sca1- murine hematopoitic progenitors were incubated at a concentration of $1x10^6$ cells/ml in Stem Span serum-free medium in presence of mSCF 50ng/ml, mFlt3L 10ng/ml, mIL3 10ng/ml, mIL6 20ng/ml (all from Peprotech) and transduced for 16 hours with $5x10^7$ TU/ml of LV (MOI 50). After the transduction period, cells were washed twice with PBS and transplanted into mice.

10.4 U-937

U-937 cells were transduced in RPMI medium 10% FBS 100 IU/ml penicillin, 100 μg/ml streptomycin 2mM L-glutamine at the concentration of $6x10^5$ cell/ml. Transduction was performed at MOI 50 and 100 for 12 hours.

10.5 T lymphocytes

T lymphocytes were seeded in IMDM 5% human serum and IL-2 300U/ml at the concentration of 10^6 cell/ml. Transduction was performed at MOI 200 for 12 hours. After the transduction cells were washed twice with PBS and maintained in IMDM 5% human serum and IL-2 300U/ml.

10.6 B lymphocytes

B lymphocytes were seeded in IMDM 10% FBS 100 IU/ml penicillin, 100 μg/ml streptomycin 2mM L-glutamine at the concentration of $1x10^6$ cell/ml. Cells were transduced with two hits of 12 hours at MOI 100. After the first hit of transduction, B lymphocytes were washed with PBS and maintained in IMDM 10% FBS 100 IU/ml penicillin, 100 μg/ml streptomycin 2mM L-glutamine for 12 hours.

10.7 Microglia

Microglia was transduced after 2 days of culture in DMEM 10% FBS 100 IU/ml penicillin, 100 μg/ml streptomycin 2mM L-glutamine at MOI 25 and 50 for 12 hours. After transduction, cells were washed with PBS and maintained in culture for not more than 5 days.

10.8 Oligodendrocytes

Oligodendrocytes were transduced after 2 days of culture in DMEM:F-12 1:1 medium [268] with FBS 2% and thyroid hormone T3 400 ng/ml at MOI 25 and 50 for 12 hours. After transduction, cells were washed with PBS and maintained in culture for not more than 5 days.

10.9 Monocytes

After one week of culture in RPMI 10% FBS, 100 IU/ml penicillin, 100 µg/ml streptomycin 2mM L-glutamine and with GM-CSF 100 ng/ml at the concentration of $5x10^5$ cells/ml, human monocytes were transduced at MOI 200 for 16 hours. After transduction, cells were washed with PBS and maintained in culture for not more than 5 days.

10.10 Macrophages

Murine macrophages obtained from peritoneal wash were transduced 2-3 days after establishment of the culture. Transduction was performed at MOI 50, over-night, in DMEM 10% FBS, 100 IU/ml penicillin, 100 µg/ml streptomycin 2mM L-glutamine supplemented with GM-CSF 50 ng/ml.

11. Colony Forming Cell (CFC) Assay

CFC assay was used to assess clonogenic potential of HSPC. After transduction, m- and hHSPC were washed, counted and seeded at a density of 1000 cells/ml fpr hHSPC or 5000 cells/ml for mHSPC in semisolid medium (MethoCult). Cells were mixed with a syringe and 1,1ml of cell suspension were plated in a 3.5cm dish. Each sample was

plated in duplicate and dishes were put in a humid chamber in order to avoid drying of the semisolid medium. Cells were incubated for 10-14 days and then scored by light microscopy for number or plucked for quantitative PCR analysis.

12. HSCT in mice

12.1 HSCT in murine models of GLD

8-days old FVB/Twi mice were lethally irradiated (850 rad) (Rad Gil EN 60601-1, Gilardoni) 4 hours before transplant. mHSPC were washed and resuspended in PBS at a density of 1x107cells/ml approximately and were intra-peritoneally injected into recipient mice (10^6 cells/mouse).

12.2 HSCT in Rag2γc mice

Rag2γc mice at postnatal day (pnd) 2 were sub-lethally irradiated (550 rad splitted in 2 doses) 24 hours before transplantation. hHSPC were washed and resuspended in PBS at a density of $2.5x10^7$cells/ml approximately and were injected into the temporal vein of recipient mice ($2.5x10^5$ cells/mouse). In the 2 weeks after HSCT Gentalin (Shering-Plough) was added to 200 ml of drinking water for prophylactic purpose.

13. Anti-apoptotic treatment

Incubation with Insulin-like Growth Factor 1 (IGF1) was performed after transduction. mHSPC, washed after LV transduction, were treated in vitro with IGF1 50 ng/ml in RPMI without serum at room temperature for 40 minutes. After incubation, mHSPC were washed twice with PBS and seeded for CFC assay or transplanted into recipient mice.

14. GALC activity

GALC activity was determined using two alternative protocols:

14.1 GALC activity assay, method A

Cells were centrifuged and pellet was resuspended in Sodium Acetate 0.5 M pH=5 at 4°C. After 2 hours, cells were sonicated, centrifuged and supernatant wash harvested for GALC activity quantification. N-lyssamine-rhodamine-galactosyl-sphingosine was used as substrate; products of enzymatic reaction were loaded on a thin layer chromatography. Fluorescent Ceramide spots were visualized by using a UV lamp, scraped and quantified by using a spettrofluorimeter [270].

14.2 GALC activity assay, method B

Cell pellets were lysed in sodium phosphate buffer 10mM pH6 0.1% (v/v) Nonidet NP40, sonicated, centrifuged and the supernatant was collected for GALC activity and protein quantification. 4-MU-b-D-galactoside 1.5mM, dissolved in citrate phosphate buffer pH4, in the presence of AgNO3 11mM (to inhibit b-Galactosidase activity), was used. Enzymatic reactions were performed using 2mg of proteins (in 50µl) incubated with 100µl of substrate at 37°C and stopped by Glycine/NaOH 0.2M pH10.6. Fluorescence of 4-methylumbelliferone was measured on a Perkin Elmer LS3 spectro-fluorimeter (excitation: 360nm, emission: 446nm)(Tiribuzi et al., submitted for publication).

15. Analysis of sphingolipids on cell extracts

15.1 Internal Standards for Mass Spectrometry

Internal standards for the mass spectrometric analyses were obtained from Avanti Polar Lipids (Alabaster, AL); these were: C17-sphingosine (d17:1), C17-sphinganine (d17:0), C17-sphingosine1-phosphate, and C17-sphinganine-1-phosphate, C12-ceramide (N-dodecanoyl-sphingosine, d18:1/12:0), C12-Ceramide 1-phosphate, C12-glucosylceramide, C12-lactosylceramide and C12-sphingomyelin. The internal standards were prepared as 1 mM stocks in ethanol that were mixed to produce a cocktail that contained each compound at 50 μM.

15.2 Experimental Procedures

The sphingolipids were extracted and analysed as described [271] as described below:

Extraction of cells

To prepare the cells for extraction, the medium was removed, the dishes were washed twice with ice cold PBS to remove excess medium, then the cells were scraped from the dish in a minimum volume of PBS and transferred into 13 x 100 mm borosilicate screw cap test tubes with Teflon caps. To the cells was added 0.5 ml of methanol and the internal standards (in 10 μl). The cells were dispersed using a bath type sonicator (Bronson 1510 ultrasonicator) at room temperature for 30 s, 0.25 ml of chloroform added, and the capped tubes incubated at 48°C overnight in a heating block. After cooling, 75 μl of 1 M KOH in CH_3OH were added, mixed briefly by sonication, incubated in a heating block for 2 h at 37°C, and centrifuged to clarify. For analysis of sphingoid bases and related compounds, 0.4 ml was removed and transferred to a new test tube, the solvent was removed under vacuum at room temperature (in a Savant Speedvac), then the lipids redissolved in the LC mobile phase for reverse phase

chromatography with sonication, centrifuged to clarify and transferred to autoinjector vials. The remainder of the extract was neutralized with 3 µl of glacial acetic acid, and 1 ml of $CHCl_3$ and 2 ml of H_2O were added. The samples were mixed and then centrifuged, the lower layer was removed with care to recover the interface, transferred to a new test tube, and the solvent was removed under vacuum at room temperature (in a Savant Speedvac), then the lipids were redissolved in the LC mobile phase for normal phase chromatography with sonication, centrifuged to clarify and transferred to autoinjector vials.

Liquid Chromatography Electrospray Tandem Mass Spectrometry

Sphingoid bases and 1-phosphates (including ceramide 1-phosphate) were separated by reverse-phase HPLC using a binary system (Perkin Elmer Series 200 MicroPump) and a Supelco 2.1 mm i.d. x 5 cm Discovery C18 column and a flow rate of 1 ml/min. Mobile phase A consisted of CH_3OH:H_2O:HCOOH (58:41:1) (all mobile phase solvents are given in v:v); mobile phase B consisted of CH_3OH:HCOOH (99:1); both also contained 5 mM ammonium formate. For each analysis, the column was equilibrated with 60:40 (A:B) for 0.4 min, the sample was injected (50 µL by a Perkin Elmer Series 200 Autosampler) and 60:40 (A:B) was continued for 0.5 min., followed by a 1.8-min linear gradient to 100% B, which was held for 5.3 min, then the column was re-equilibrated at initial conditions for 0.5 min.

Complex sphingolipids (Cer, SM,) were separated by normal phase chromatography using a Supelco 2.1 mm i.d. x 5 cm LC-NH_2 column and a flow rate of 1.0 ml/min. Mobile phase A consisted of CH_3CN:CH_3OH:CH_3COOH (97:2:1); mobile phase B consisted of CH_3OH:H_2O:$CH_3(CH_2)_3OH$:CH_3COOH (64:15:20:1); both also contained 5 mM ammonium acetate. For each analysis, the column was equilibrated with 98:2 (A:B) for 0.5 min, the sample was injected, and 98:2 (A:B) was continued for 1.1 min, followed by a 0.2 min. linear gradient to 82% A. This state is held for 0.4 min, followed

by a 0.8 min linear gradient to 100% B, and re-equilibration of the column at initial conditions for 0.5 min.

The mass spectrometry data was collected using a PE Sciex API 3000 triple quadrupole mass spectrometer equipped with a turbo ion-spray source. Dry N_2 was used as the nebulizing gas at a flow rate of 6 L/min. The ionspray needle was held at 5500 V, and the orifice and ring voltages were kept low (30-40 V and 180-220 V, respectively) to minimize collisional decomposition of molecular ions prior to entry into the first quadrupole, and the N_2 drying gas temperature was set to 500 °C. N_2 was used to collisionally induce dissociations in Q2, which was offset from Q1 by 30-40 V. Q3 was then set to pass molecularly distinctive product ions. The fatty acyl chain length variation was examined by product ion scans for *m/z* 264.4 through the ceramide and HexCer range and by precursor ion scans of *m/z* 184.4 for SM subspecies.

16. Detection of apoptosis

16.2 Annexin V staining

To detect early apoptotic cells the "Annexin V-PE apoptosis detection kit" (Beckton Dickinson) was used. Annexin V is a Ca2+-dependent phospholipids-binding protein that has high affinity for phosphatidylserine, which is translocated from the inner to the outer leaflet of the plasma membrane during the earliest stage of apoptosis. Cell were washed twice with PBS and resuspended in Binding Buffer at the concentration of 10^6 cells/ml and labelled following manufacturing protocol. Apoptotic Annexin V positive controls were obtained by an incubation with Camptothecin 5 μM 5 hours in the medium. Sample were analysed by flow cytometry (FACS CANTO, Beckton Dickinson) within 1 hour. 10,000-20,000 events were scored and results were analyzed by FlowJo 8.3 software.

16.2 TUNEL assay

TUNEL (Terminal deoxynucleotidyl Transferase Biotin-dUTP Nick End Labeling) assay allows in situ identification of apoptotic cells through the deossinucleotidiltransferase (TdT) –mediated transfer of biotinilated dUTP to 3'-OH of DNA double strand fragments which are generated in late stages of apoptosis. Biotinilated dUTP are then recognised by TMR-red conjugated avidine. TUNEL assay was performed by using In situ Cell Death Detection Kit, TMR red (Roche) following manufacturer's instructions for adherent cells or for cell suspensions.

Adherent cells: Cover-slip were coated with Matrigel (BD Matrigel Matrix Growth Factor Reduced, BD Bioscences) 1:50 in IMDM 1 hour at 37°C, in order to increase adherence of cells and to minimize cell loss during the assay. Matrigel was removed and cells were seeded on cover-slip in their medium. Before performing the assay, cells were fixed with freshly prepared Paraformaldehyde 4% 1 hour at RT. Cells were then washed twice with PBS and labelled following the protocol for adherent cells. TUNEL positive cells were detected by confocal microscopy.

Cell suspensions: cells were resuspended in freshly prepared Paraformaldehyde 2% and incubated 1 hour at RT. Cells were then washed twice with PBS and labelled following the protocol for cell suspensions. TUNEL positive cells were detected by cytofluorimetry. Alternatively, cells were forced to adhere to a glass slide by a centrifugation at 800 rpm 5 minutes with a Cytospin (Cytospin3, Shandon). Cell spots were then air-dried, fixed with Paraformaldehyde 4% 1 hour at RT and labelled following the protocol for adherent cells. TUNEL positive cells were detected by confocal microscopy.

Apoptotic TUNEL positive controls were obtained by incubation with Camptothecin 5 μM 5 hours in the medium. When samples were analyzed by microscopy, cells were also incubated 5 minutes at RT with ToProIII (Molecular Probes) diluted 1:1000 in PBS,

in order to label nuclei. Samples were analyzed by confocal microscopy (Radiance 2100; Bio-Rad) (λexcitation = 488, 586, 660). Fluorescent signal was processed by Lasersharp 2000 software and analyzed by Adobe Photoshop CS 8.0 software.

17. Genomic DNA extraction and Real-time Quantitative-PCR (Q- PCR) analysis

In order to evaluate vector copy number *per* cell, Q-PCR was performed on genomic DNA extracted from transduced cells either grown in culture, from CFC or from mouse bone marrow. Cells in culture were grown for 10 days before analysis to exclude non-integrated vector forms from the analysis.

17.1 Genomic DNA extraction

Genomic DNA extraction from BM or CFC samples was performed by using the Blood and Cell Culture DNA kit (Mini kit; Qiagen). This system is based on cell lysis, followed by DNA purification on an anion exchange resin.

Genomic DNA extraction from HeLa cells was performed by using DNA automatic extractor (Maxweel 16, Promega). Cultured cells were detached by trypsin-EDTA solution (for adherent cells) and washed with ice-cold PBS by spinning at 1000 rpm in Heraeus Megafuge 1.0 R (Kendro Laboratory products) 10 min at 4°C. Cell pellet was resuspended in 300 µl of PBS for a confluent 10 cm-dish and sample was loaded on Tissue DNA Extraction Cartridge. Genomic DNA was finally quantified by spectrophotometer analysis and run on a 0.8% agarose gel to check for possible RNA contaminations and degradation of the sample. DNA was then stored at –20°C.

17.2 Real-time Q-PCR

Q-PCR was performed in Optical 96-well Fast Thermal Cycling Plates (Applied Biosystem) on ABI PRISM 7900 Sequence Detector System (Applied Biosystem), using the following thermal cycling conditions: one cycle at 50°C for 2 min, one cycle at 95°C for 10 min, 40 cycles at 95°C for 15 seconds and 60°C for 1 min. For each sample, the Sequence Detector System 2.3 software provided an amplification curve constructed by relating the fluorescence signal intensity (Rn) to the cycle number. Cycle threshold (Ct) was defined as the cycle number at which the fluorescence signal was more than 10 SD of the mean background noise collected from the 3rd to the 15th cycle. Vector copy number was determined by using as standard curve serial dilutions (200ng, 100ng, 50ng, 25ng and 12,5 ng for murine DNA; 200 ng, 40 ng, 8 ng, 1,6 ng for human DNA) of genomic DNA extracted from a transgenic mouse or from a human cell line clone stably containing a known number of LV integrations (copy number of the standard curve was previously defined by Southern Blot analysis). To determine vector copy number per cell, LV copy numbers were normalized to human DNA content, which was assessed by Q-PCR. Each sample was run in triplicate in a total volume of 25µl/reaction, containing 12,5µl TaqMan Universal Master Mix (4304437; Applied Biosystem), 100ng of sample DNA and one of the following amplification systems at the following concentrations.

Human samples:

- hTERT (human Telomerase Reverse Transcriptase) forward primer: 5'-GGT GAA CCT CGT AAG TTT ATG CAA-3' final concentration 300 nmol
- hTERT reverse primer: 5'-GGC ACA CGT GGC TTT TCG-3' final concentration 300 nmol
- hTERT probe: 5'-(VIC)-TCA GGA CGT CGA GTG GAC ACG GTG-(TAMRA)-3' final concentration 200 nmol

- HIV forward primer: 5'- TCT CGA CGC AGG ACT CG-3' final concentration 300 nmol
- HIV reverse primer: 5'-TAC TGA CGC TCT CGC ACC-3' final concentration 300 nmol
- HIV probe: 5'-(FAM)- ATC TCT CTC CTT CTA GCC TC-(MGB)-3' final concentration 200 nmol

VCN was determined by using the following formula:

absolute number of copies HIV/ absolute number of copies hTERT x ploidy (*)

(*) Ploidy of HeLa cells is 4.

Murine samples:

- β-actin forward primer: 5'-AGA GGG AAA TCG TGC GTG AC-3' final concentration 300 nmol
- β-actin reverse primer: 5'-CAA TAG TGA TGA CCT GGC CGT-3'final concentration 300 nmol
- β-actin probe: 5'- (VIC) –AGC TCT CTC GAC GCA GGA CTC GGC-(MGB)-3'final concentration 200 nmol

- PSI HIV forward primer: 5'-TAC TGA CGC TCT CGC ACC-3' final concentration 300 nmol
- PSI HIV reverse primer: 5'- TCT CGA CGC AGG ACT CG-3' final concentration 300 nmol
- PSI HIV probe: 5'-(FAM)- ATC TCT CTC CTT CTA GCC TC-(MGB)-3' final concentration 200 nmol

VCN was determined by using the following formula:

ng DNA HIV/ng DNA β-actin x standard VCN(*)

(*) Standard VCN is 5.

18. Flow Cytometry

18.1 Expression titer

To determine expression titer, HeLa cells were detached by trypsin- EDTA solution, washed with PBS, fixed with PBS, 1% paraformaldehyde, 2% FBS (400µl/sample) and analysed by flow cytometry (FACS CANTO, Beckton Dickinson) for GFP expression. To assess transduction efficiency cells were grown for at least 5 days after transduction to reach steady state GFP expression and to rule out pseudotransduction (detection of GFP protein associated with the virus particles during vector production and transferred to the target cells during infection). Adherent cells were detached by trypsin-EDTA solution, washed with PBS and resuspended in PBS, 1% paraformaldehyde, 2% FBS. Untransduced cells were used as negative control to set parameters and gates. 10,000-20,000 events were scored. Results were analyzed by FlowJo 8.5.3 software.

18.2 Analysis of Rag2γc mice receiving HSCT

The engraftment of hHSC in Rag2γc mice was evaluated by flow cytometry.

Tissue processing: BM cells were harvested by flushing femurs and tibias with PBS 2% FBS and counted in a Burker chamber. Splenocytes were obtained by mechanic disgregation of spleen in RPMI 10% FBS, 100 IU/ml penicillin, 100 µg/ml streptomycin 2mM L-glutamine supplemented with 2-mercaptoethanol 28.4 mM. Thymocytes were obtained by mechanic disgregation of thymus in IMDM 20% FBS, 100 IU/ml penicillin, 100 µg/ml streptomycin 2mM L-glutamine. After spinning at 1500 rpm 5 minutes at

room temperature, 2.5x103 cells were resuspended in 50 µl of blocking solution (PBS 1%BSA, 5%FBS).

Labelling procedure:

- Blocking: 20 minutes at 4°C in the dark
- Antibodies diluted 1:100 in blocking solution, 20 minutes at 4°C in the dark. All the anibodies were from BD.
    - CD45 APC
    - CD34 RPE
    - CD13 RPE
    - CD19 TC
    - CD3 TC
    - CD4 RPE
    - CD8 TC
    - CD11b RPE

Cells were then washed with PBS and centrifuged at 1500 rpm 5 minutes, resuspended in 300 µl of PBS, 1% paraformaldehyde, 2% FBS and analyzed by FACS CANTO. 10,000-20,000 events were scored. Results were analyzed by FlowJo 8.5.3 software.

19. Immunofluorescence

Cells were seeded on Matrigel-coated coverslip and fixed with PBS 4% paraformaldehyde 20 minutes at RT. Cells were then washed twice with PBS and blocked with PBS 1% BSA, 5% goat serum 1 hour at RT. After blocking, cells wren incubated with the primary antibody diluted in PBS 10% goat serum, 0.3% triton 2 hours at RT or over-night at 4°C (for dilutions, see the list below). Samples were washed three times with PBS and were incubated 1 hour at RT with the secondary antibody

conjugated with the fluorochrome (see the list below), diluted 1:500 in PBS 0.1% triton. Samples were washed three times with PBS, in the dark, and nuclei were labelled by incubation with ToProIII as described for TUNEL staining. Samples were mounted with Fluorsave Reagent (Calbiochem). Samples were analyzed by confocal microscopy (Radiance 2100; Bio-Rad) (λexcitation = 488, 586, 660). Fluorescent signal was processed by Lasersharp 2000 software and analyzed by Adobe Photoshop CS 8.0 software.

Primary antibodies:

- Ceramide (Alexis Biochemicals), 1:50
- Lamp1 (abcam), 1:300
- NG2 (Chemicon, AB5320), 1:300
- Gal-Cer (Chemicon, MAB342), 1:200
- anti-HA High Affinity, rat monoclonal antibody (clone 3, Roche), 1:100
- F4/80 (MCAP497, Serotec), 1:200

Secondary antibodies:

- Goat IgG anti-Rabbit Alexa Fluor 488 (green), Molecular Probes, A11008, 1:500
- Goat IgG anti-mouse Alexa Fluor 633 (blue), Molecular Probes, A21050, 1:500
- Goat IgG anti-Rat Alexa Fluor 546 (red), Molecular Probes, A11081, 1:500

20. Western Blot

15μg of total cell protein/60μg of total medium protein were re-suspended in sample buffer, heated for 5 minutes at 95°C and separated via SDS-PAGE under reducing conditions. Western blotting was performed as previously described [272] using the following primary antibodies: polyclonals raised against either precursor or mature protein forms of Cathepsin D (*=Santa-Cruz Biotechnology, USA) or anti-Caspase-9 and anti-Caspase-3 (Cell Signaling Technology, MA-UK) or anti-PAR4 (*) and b-actin (*). Immunostaining was performed using the ECL kit from GE-Healthcare (UK). Quantification was assessed based on a protein standard included in each test.

RESULTS

1. Forced GALC expression in HSPC

In order to assess the feasibility of GALC over-expression in mHSPC, we isolated Lin- cells from FVB/twi (GALC -/-) mice. mHSPC were transduced at MOI 100 with GALC.LV in the presence of an optimized cytokine combination [102]. After transduction, cells were cultured 10-14 days in vitro to assess enzymatic activity and the vector copy number (VCN) by Q-PCR. We compared the expression level of GALC with the over-expression of other lysosomal enzymes, Arylsulfatase A (ARSA) and α-Iduronidase (IDUA), obtained by transducing mHSPC with the control vectors ARSA.LV and IDUA.LV. All vectors expressed the transgene from the same expression cassette containing the human PGK promoter. Since our aim was to compare the enzyme over-expression in transduced -/-HSPC with respect to physiological enzyme levels in wild type HSPC, mHSPC obtained from ARSA KO mice and from IDUA KO mice were used for ARSA.LV and IDUA.LV transduction, respectively. Transduction of mHSPC reconstituted lysosomal enzyme activity in -/- cells and led to enzyme over-expression with respect to wild type levels in the cultured progeny of transduced -/- mHSPC (Figure 17A). However, the increase in GALC expression (2 fold above wild type) was significantly lower as compared to the increase in IDUA and ARSA obtained by IDUA.LV and ARSA.LV controls (320 and 5.6 fold over wild type, respectively), despite similar VCN.

A similar experiment was performed on human HSPC (hHSPC), isolated through CD34+ selection from CB obtained from normal donors (n.d.). hHSPC were transduced at MOI 100 with GALC.LV, ARSA.LV and IDUA.LV, using previously optimized transduction protocols [269]. Similarly to mHSPC, we evaluated enzyme activity reconstitution and VCN upon in vitro culture of the transduced cells. GALC.LV transduction of HSPC from n.d. CB (n = 4) led to limited over-expression of the enzyme

in the cultured cell progeny as compared to IDUA.LV (n = 3) and ARSA.LV (n = 6) controls (Figure 17B).

2. Impaired in vitro function of GALC expressing HSPC upon LV-mediated GALC expression

2.1 Impaired in vitro function of murine HSPC

The effects of transduction and enzyme expression on mHSPC clonogenic potential were assessed by CFC assay. Equal number of GALC/GFP/ARSA.LV transduced mHSPC were seeded for colony assay. ARSA was chosen as control lysosomal enzyme since it was previously shown to not affect HSPC function [269]. In 12 independent experiments GALC.LV transduced -/- and +/+ mHSPC gave rise to a significantly reduced number of colonies as compared to GFP.LV and ARSA.LV transduced cells (Figure 18A for GALC -/- cells). Colonies from GALC.LV transduced mHSPC were of markedly reduced size as compared to controls (Figure 24B). These results suggested that GALC over-expression upon LV transduction impaired mHSPC clonogenic potential. The relative proportion of erythroid and myeloid colonies upon GALC.LV transduction was similar to controls (not shown), suggesting that enzyme expression impaired the different hematopoietic lineages to the same extent.

The reduced clonogenic potential of GALC.LV transduced mHSPC could result from the death of highly transduced GALC over-expressing hematopoietic progenitors. In order to investigate the possible occurrence of an *in vitro* negative selection of highly transduced mHSPC, we quantified the VCN of colonies by Q-PCR. Q-PCR was performed on DNA extracted from each pool of 4 colonies (pools were made in order to have a sufficient amount of material for the analysis). Colonies obtained from GALC.LV transduced mHSPC showed a significantly lower vector content when

compared to controls (Figure 18A), suggesting the occurrence of negative selection of highly transduced progenitors.

According to these data, we could not discriminate whether functional impairment and in vitro selection were due to a toxic effect of transduction *per se* or to the presence of contaminants released by vector-producer cells and co-purified with the vector. It must be mentioned that, during GALC.LV production, 293T cells detach from plates, suggesting that GALC expression is toxic also to these cells. For this reason, the incorporation of toxic molecules deriving from dead 293T cells into the vector preparation could not be excluded. To address this issue, we generated a control vector regulated by an hematopoietic-specific microRNA, GALCmir142T.LV [228]. Four target sequences for the microRNA 142 incorporated downstream the transgene allow to suppress expression in mHSPC and in their progeny without impairing GALC expression in non-hematopoietic cells, such as 293T LV-producing cells. This technology is based on microRNA post-transcriptional regulation: microRNA 142, expressed only by hematopoietic cells, recognizes its target sequence downstream the transgene and inhibits the translation of the transcript and expression of the transgene. As expected, transduction of mHSPC with GALCmir142T.LV was not associated to an increase of GALC activity (Figure 18B). Moreover, mHSPC transduced with GALCmir142T.LV (n = 6) showed unaffected clonogenic potential and similar vector content as compared to controls, thus confirming the previously observed impairment being dependent on *de novo* GALC expression (Figure 18A).

2.2 Impaired in vitro function of human HSPC

We investigated the effect of GALC over-expression also on human HSPC. hHSPC were isolated from n.d. CB and BM and from the collected BM of a GLD patient that was scheduled to be discarded. An equal number of hHSPC were transduced with GALC.LV or ARSA.LV or GFP.LV control vectors were seeded for CFC assay, in order to assess the clonogenic potential of transduced hHSPC. As in the case of murine

cells, GALC.LV transduced n.d. and GLD hHSPC showed an impaired clonogenic potential (Figure 19A). Colonies from GALC.LV transduced hHSPC showed a significantly lower vector content, when compared to controls, a reduced size and conserved erythroid-myeloid proportion, again suggesting negative selection of the highly transduced progenitors (Figure 19A). Also in this case, the control vector GALCmir142T.LV was used to rule out an aspecific toxic effect of transduction. As in the case of murine cells, GALCmir142T.LV transduced hHSPC (n = 4) showed GALC activity and clonogenic potential similar to those observed in control cells (Figure 19A and B).

Overall these data indicate that forced GALC *de novo* expression upon LV transduction exerts a detrimental effect both on murine and human HSPC, leading to negative selection of GALC over-expressing cells and to functional impairment.

3. Impaired in vivo function of HSPC upon LV-mediated GALC expression

We performed *in vivo* experiments with the aim of assessing the repopulation potential of m- and hHSPC upon GALC.LV transduction and GALC *de novo* expression. *In vivo* studies were performed on twi and FVB/twi mice for mHSPC, and on Rag2γc mice for hHSPC.

3.1 Engraftment failure of GALC.LV transduced cells in twi mice

Our initial experiments were performed on twi mice, a severe model of GLD, as described in the Methods section. A first set of experiments was devoted to set the condition for HSCT in twi mice. Total BM transplantation from wild type donors was performed in these mice, resulting in a significant increase of their lifespan up to 100 days, as previously reported by [111]. These preliminary experiments allowed defining the optimal irradiation dose. The use of donor HSC carrying the CD45.1 allele allowed evaluating donor cell engraftment, since twi mice carry the CD45.2 allele. Because our goal was to transduce twi HSC., we tried to set up transplantation of Lineage marker negative (Lin-) hematopoietic stem and progenitor cells (HSPC), in order to reduce the number of cells to be transduced and transplanted as compared to the use of total BM cells. HSPC from wild type (+/+) mice were transduced at MOI 100 with PGK_GFP.LV (GFP.LV), in the presence of an optimized cytokine combination [102] (Figure 20A). After transduction, cells were transplanted into lethally irradiated 8 day-old twi mice or +/- controls. Control groups included also twi mice transplanted with wild type BM or Lin- cells. Surprisingly, and differently from control animals, HSPC-transplanted -/- twi mice

did not survive after lethal conditioning, thus suggesting that Lin- cells alone could not repopulate twi mice (Figure 20B).

We thus decided to support GFP.LV transduced HSPC engraftment by co-transplantation of untransduced BM-derived hematopoietic committed progenitors, depleted of HSC. These cells were obtained by magnetic depletion of Sca1+ cells from total BM of +/+ mice. Interestingly, twi mice transplanted with GFP.LV transduced +/+ Lin- cells and untransduced +/+ Sca1- cells reached a survival similar to the one obtained with +/+ total BM transplantation (Figure 20B). The engraftment of GFP.LV transduced HSPC was evaluated by flow cytometry on peripheral blood. Five-six weeks after transplantation, cytofluorimetric analysis revealed a high engraftment of GFP+ HSPC-derived cells (Figure 20C). Thus, co-transplantation of +/+ Sca1- progenitors rescued the defective engraftment of purified HSPC and allowed prolongation of lifespan and amelioration of phenotype of twi mice similar to those obtained with total +/+ BM transplantation [111 273].

Once the transplantation procedures had been optimized with +/+ HSPC and GFP.LV, twi mice were transplanted with GALC.LV transduced -/- HSPC and with either +/+ or GALC.LV transduced -/- Sca1- cells. Twi mice that received GALC.LV transduced -/- HSPC and +/+ untransduced cells survived significantly longer than mice transplanted with +/+ total BM or with +/+ HSPC and Sca1- progenitors, and showed amelioration of their phenotype and slower disease progression (Figure 20B). This data suggested that GALC over-expressing HSPC transplantation provides a unique therapeutic benefit as compared to conventional HSCT. However, when we evaluated the presence of GALC.LV transduced cells in the BM of these mice by Q-PCR, we found a low Vector Copy Number (VCN), between 0.8 and 1, thus suggesting that only GALC.LV transduced cells with low VCN had been able to engraft.

Nevertheless, twi mice that received -/- Lin- and Sca1- cells, both transduced with GALC.LV, died after lethal conditioning or had a lifespan similar to untreated mice.

These results suggested that GALC.LV transduced progenitors failed to support HSPC engraftment, resulting in engraftment failure and autologous reconstitution of hematopoiesis.

3.2 Engraftment failure in milder murine models

We decided to use FVB/twi mice instead of the usual twi model of GLD to take advantage from the slightly less severe model: previous experiments showed us that the successful transplantation of Lin- cells without the need of Sca1- supporting cells was possible in this model. Moreover, FVB/twi mice have larger litters, thus allowing us to have a larger number of -/- mice to isolate mHSPC. Transduced mHSPC were transplanted into lethally irradiated 8 day-old FVB/twi -/- and heterozygous (+/-) recipients (Figure 21). In order to reduce biological variability, we transplanted -/- and +/- littermates. Mice of the control group were transplanted with GFP.LV transduced +/+ cells. For this control group, the transduction efficiency was evaluated by cytofluorimetry 7 days after transduction on the in vitro culture, while the engraftment of transduced cells was evaluated by cytofluorimetry on peripheral blood 6 weeks after HSCT. The transduction efficiency was very high, ranging between 75% and 93% of GFP+ cells. All the GFP-transplanted animals showed a high engraftment of transplanted cells (between 63% and 85%), and all the irradiation controls (lethally irradiated mice that did not received HSCT) died within 3 weeks after conditioning, thus confirming the correct setup of HSCT conditions. -/- mice receiving GFP.LV transduced +/+ mHSPC achieved prolonged survival after lethal conditioning (up to 150 days), as compared to un-transplanted control mice. The survival of the untreated and GFP-transplanted FVB/twi mice was longer with respect to that observed in the respective groups of twi mice, thus confirming the influence of the genetic background on the severity of the phenotype. The engraftment of transduced mHSPC was also evaluated by Q-PCR on DNA extracted from BM transplanted mice at sacrifice. A significant

engraftment of GFP.LV transduced mHSPC, measured as VCN *per* genome, was observed (Table 2). Strikingly, both -/- and +/- mice transplanted with GALC.LV transduced -/- or +/+ mHSPC did not survive to lethal irradiation (death within 21 days, similar to that of irradiation controls) (Figure 21 and data not shown). Q-PCR revealed very low to undetectable VCN in their BM (Table 2). These results indicated a functional impairment of GALC-transduced mHSPC, which became unable to repopulate a lethally conditioned host.

3.2 GALC.LV transduced hHSPC repopulate Rag2γc mice

The long-term repopulation potential of GALC.LV transduced hHSPC was tested in Rag2-/-γc-/- mice. CB-derived hHSPC were prestimulated with a combination of cytokines and transduced at MOI 100 with GALC.LV or with the control vector ARSA.LV. We previously demonstrated that ARSA over-expression does not impair the viability and the function of hHSPC [269]. After transduction, cells were transplanted into sub-lethally irradiated neonate Rag2-/-γc-/-mice or seeded for CFC assay to confirm the results obtained in previous *in vitro* experiments. Five mice were transplanted with GALC.LV transduced hHSPC and four mice were transplanted with ARSA.LV transduced hHSPC. Mice were euthanized ten weeks after HSCT and BM, spleen and thymus were analyzed for human cell engraftment by flow cytometry (Figure 22). CD45 positive human cells were present in all the hematopoietic tissues from both GALC and ARSA transplanted mice, except for one mouse transplanted with ARSA.LV transduced hHSPC, in which transplanted cells did not engraft. As expected, thymus was the organ with the highest engraftment (average of CD45+cells in GALC group = 92.7%±6.1%); (average of CD45+cells in ARSA group = 87.6%±8.1%), (Figure 22B). Engraftment of human cells in spleen was 7.8%±1.5% and 5%±1.9% for GALC and ARSA respectively (Figure 22C); engraftment of human cells in BM was 32%±3.9% and 29.7%±6.4% for GALC and ARSA respectively (Figure 22A). The differentiation potential of the

transduced hHSPC was evaluated by flow cytometry using specific human lineage markers. All the tissues analyzed showed multilineage differentiation of transplanted hHSPC (Figure 21D-F), thus suggesting that GALC.LV transduction does not impair the differentiation potential of hHSPC. Also in the thymus, human lymphocytes showed a normal differentiation pattern (Figure 22G) Finally, the long-term persistence of transduced hHSPC was evaluated on thymus, spleen and BM by Q-PCR, using the hTert-HIV system (see method section). Thanks to the specificity of this system for the human Telomerase Reverse Transcriptase, the number of vector copies integrated into the genome was normalized to the content of human DNA and not to the murine one. The average VCN was similar in the two experimental groups (VCN in thymus = 1±0.9 for GALC and 2.5±2 for ARSA; VCN in spleen = 1.2±1.1 for GALC and 1.1±0.4 for ARSA; VCN in BM = 1.4±1 for GALC and 1.3±0.6 for ARSA), (Figure 22H). The results obtained with CFC assay were similar to the previous experiments, both in term of VCN and number of colonies (data not shown). Overall, these results demonstrate that, despite the clonogenic impairment and the negative selection observed *in vitro* upon GALC.LV transduction, GALC expressing CB-derived hHSPC are capable of long-term engraftment and multilineage differentiation when transplanted in Rag2-/-γc-/- mice. However, the VCN measured in thymus, spleen and BM was similar to what we found in the BM of FVB/twi mice transplanted with GALC.LV transduced -/- HSPC and +/+ progenitors.

4. Apoptosis of GALC expressing murine and human HSPC

Having detected a functional impairment of GALC.LV transduced HSPC, we evaluated whether this could be due to apoptosis of the transduced cells mediated by *de novo* GALC expression. The occurrence of apoptosis was evaluated at two different time points, 2 and 5 days after transduction, when transgene expression presumably reaches steady state (see GFP expression in Figure 23B) by Annexin V staining and TUNEL assay. The first technique labels early apoptotic cells, and the second one late apoptotic cells. m- and hHSPC were transduced with GALC.LV and control GFP/ARSA.LV. After transduction and washing, cells were plated on matrigel-coated coverslips for TUNEL assay or cultured in usual plates and stained for Annexin V and TUNEL. At confocal microscopy, the large majority of GALC.LV transduced mHSPC were TUNEL positive and exhibited enlarged nuclei with condensed chromatin, demonstrating the widespread occurrence of apoptosis at both time points (Figure 23A-B). On the contrary, ARSA/GFP.LV transduced cells were mostly TUNEL negative. Annexin V staining confirmed the occurrence of apoptosis, showing a higher fraction of apoptotic cells among GALC-transduced m- and hHSPC, as compared to controls (Figure 23C).

5. IGF1 rescues GALC expressing HSPC from apoptosis and functional impairment

The experiments presented above indicated that GALC *de novo* expression upon LV transduction triggered apoptotic cell death in cultured HSPC and likely explain the functional impairments observed in the biological assays. In order to further confirm the occurrence of apoptosis and support this causal relationship, and to develop a strategy aimed at overcoming this limitation, we tested *in vitro* and *in vivo* the anti-apoptotic activity of Insulin-Like Growth Factor 1 (IGF1). Several studies have implicated IGF1 in preventing cell death due to the activation of the phosphatidylinositol-3 kinase (PI3K)/Akt signaling pathway [274]. This pathway appears to be required for the survival of a number of cell types [275], including hematopoietic cells [263] and oligodendrocytes [29]. Cer, the first product of GALC, acts on this pathway by inhibiting the phosphorylation of Akt and Erk1/Erk2 (Erk1/2) [276] [277]. After transduction with either GALC.LV or GFP/ARSA.LV, mHSPC were washed and briefly (40 minutes) stimulated in vitro in the presence of IGF1. Similarly to the previous experiments, HSPC clonogenic potential was assessed by CFC assay, vector content was measured by Q-PCR on colonies, and apoptosis was evaluated by TUNEL. IGF1 treatment rescued GALC.LV transduced mHSPC from toxicity: a significant increase in the number of colonies and in the VCN were observed, up to the values obtained on GFP/ARSA.LV transduced cells (Figure 24A). The colonies grown from GALC.LV transduced, IGF1-treated mHSPC showed an increase in size (Figure 24B), whereas the proportion of myeloid and erythroid colonies was similar in all conditions (not shown). The rescue of the clonogenic potential by IGF1 was associated to the protection of GALC over-expressing cells from apoptosis (Figure 24C). This data further confirmed the occurrence of apoptosis upon GALC.LV transduction of HSPC and the HSPC functional impairment being due to apoptotic cell

death. Surprisingly, this rescue from apoptosis was not associated to an increase of GALC expression levels in IGF1-treated GALC.LV transduced cells (Figure 24D). Once we had tested the anti-apoptotic activity of IGF1 treatment *in vitro,* GALC.LV transduced IGF1-treated mHSPC were transplanted into irradiated +/- and -/- FVB/twi mice. The aim of this experiment was on the one hand to confirm that the impairment of the repopulation potential of GALC over-expressing HSPC was due to their apoptosis, and on the other hand, to develop a feasible HSCT gene therapy approach for GLD. Indeed, IGF1-treated GALC.LV transduced mHSPC were able to prevent recipient animals from early death. Transduced cells were detected in BM 20 days after the transplant at comparable levels (by VCN measurement) to those detected in mice transplanted with GFP.LV HSPC (Figure 25 and Table 3), thus confirming that apoptotic cell death of GALC over-expressing HSPC was responsible for the observed in vivo functional impairment, and could be rescued by in vitro IGF1 treatment. In the long-term however, transduced cells were no longer detectable in -/- recipients, which consequently died due to GLD manifestations. It seems likely that the effect of the brief in vitro treatment with IGF1 had been exhausted and was thus unable to protect the transduced HSPC from GALC *de novo* expression toxicity long-term (Figure 25 and Table 3). Indeed, +/- recipients survived long-term but showed absence of transduced cell engraftment, indicating successful reconstitution of hematopoiesis only by either donor non transduced or autologous cells (Figure 25 and Table 3).

6. Investigating the mechanism of GALC *de novo* expression toxicity

6.1 Apoptosis of GALC expressing HSPC is associated to accumulation of bioactive GALC product

We then aimed at better understanding how GALC *de novo* expression could induce cell death in HSPC. Upon evaluation of the GALC metabolic pathway, we hypothesised that the apoptosis observed upon GALC.LV transduction could be due to a modification of the sphingolipid content of the cell. Indeed, Cer, the first product of GALC, plays a central role in sphingolipid metabolism (see introduction). Sphingomyelin (SM), Cer, So, S1P and Psy are all involved in apoptosis, cell differentiation and survival, and a modification of the balance between these molecules might explain the apoptotic death we observed. An intracellular sphingolipid profile was performed on control vector and GALC.LV transduced mHSPC at different intervals of culture from gene transfer. SM, Cer, So, S1P and Psy could be detected by gas chromatography and tandem mass spectrometry in the culture progeny of both +/+ and -/- mHSPC (Figure 26A). At the beginning of the in vitro culture (12h), the intracellular content of SM, Cer and So was significantly higher in +/+ mHSPC than in mHSPC isolated from GLD mice (Figure 26A), suggesting that GALC-dependent metabolism may represent one of the pathways regulating intracellular levels of these sphingolipids in HSPC. The C:16 fractions of SM and Cer were shown to be those most represented among the measured isoforms. Intracellular SM levels were substantially higher than those of the other sphingolipids tested. Psy intracellular levels in mHSPC from GLD mice appeared to be slightly, but not significantly, increased as compared to cells from +/+ animals (Figure 26A).

Importantly, after 2 and 7 days of in vitro culture following GALC.LV transduction, we detected significant accumulation of Cer both in -/- and +/+ HSPC, as compared to GFP.LV transduced controls (Figure 26B and data not shown). Moreover, a similar

significant increase in the intracellular levels of Cer downstream products So and S1P was observed (Figure 26C). No significant changes were detected in the intracellular content of the other sphingolipids, although Psy content in GALC.LV transduced -/- mHSPC showed a tendency to decrease (data not shown).

In order to further confirm the presence of Cer in mHSPC, we performed immunofluorescence stainings on GALC.LV transduced cells. We used commercial antibodies against Cer and against Lamp1 (a well characterized lysosomal marker) to verify the intracellular localization of Cer. For this experiment, PGK_DNGFR LV was used as control, in order to avoid a GFP direct fluorescence that would be deleterious for double immunofluorescent staining. At the same time, commercial antibodies for Delta-NGF Receptor (DNGFR) allowed us to verify by cytofluorimetry the frequency of transduction (data not shown). Cer signal co-localized more abundantly with the lysosomal marker Lamp1, as compared to HSPC transduced with a control vector (Figure 26D), suggesting that the intracellular Cer increase might be due to an increase of lysosomally generated Cer.

6.2 Cathepsin D and PAR-4 are not involved in apoptosis of the transduced HSPC

The protease Cathepsin D has been proposed as a specific target for lysosomally generated Cer, and may couple the action of lysosomal acid sphingomyelinase to the mitochondrial pathway of apoptosis [278]. We thus evaluated by western blot whether the apoptosis observed in GALC.LV transduced HSPC was due to the activation of the Cathepsin D cascade. The monocytic cell line U937 was used as control, since it was not affected by *de novo* GALC expression (see section 7). Western blot analysis revealed a different basal content of activated Cathepsin D in mHSPC: precursor and mature forms of Cathepsin D were almost undetectable in mHSPC at the beginning of the in vitro culture (GFP 12h) (Figure 27). No increase in the mature form of Cathepsin D was observed after GALC gene transfer in mHSPC and their culture progeny (Figure 27).

The precursor of Cathepsin D accumulated in GFP-transduced cells after 7 days of culture (GFP.LV 7 days), while its accumulation was less pronounced in the presence of GALC (GALC 5 days), culminating with disappearance of both the precursor and mature forms after 7 days (Figure 27). Moreover, no secretion of Cathepsin D was observed in the culture medium of GFP.LV and GALC.LV transduced HSPC (not shown). We also evaluated the activation of caspases-9 and -3. Neither the inactive precursor form nor the active mature form of caspase-9 were detected in mHSPC in all conditions tested, nor accumulation of active caspase-3 was observed in the GALC.LV transduced HSPC (data not shown). Overall these findings confirmed that Cathepsin D pathway was not detectably involved in the apoptosis of GALC.LV transduced HSPC.

The prostate apoptosis response protein 4 (PAR4) is another key element among signaling pathways known to participate in ceramide-induced cell death in hematopoietic cells [279] [280]. We thus evaluated the expression of PAR4 upon GALC.LV transduction. PAR4 was undetectable in both GFP and GALC.LV transduced mHSPC both in basal conditions, ie. before the occurrence of transgene expression, as well as 5 and 7 days after transduction, when apoptosis and sphingolipids accumulation occur (data not shown).

7. Sensitivity to GALC expression toxicity is dependent on differentiation and cell lineage

Macrophages and microglia represent the HSPC effector progeny reconstituting enzyme activity in affected tissues, including the nervous system, in HSPC gene therapy approaches for LSD (see peragraph 1.7.3 of the Introduction). We evaluated whether a prototypical monocytic cell line (U937), primary human monocytes, primary murine macrophages and microglia could experience GALC expression toxicity upon LV mediated gene transfer. Moreover, for further dissecting the specificity of GALC-induced apoptosis along hematopoietic differentiation, we tested T and B lymphocytes. Eventually, we examined oligodendrocytes, which are the most relevant GALC recipient cells in the CNS, not derived from HSPC. To permit immunodetection of GALC and estimate transduction efficiency, in some experiments we used a C-terminally tagged transgene, in which the gene is fused in frame with the sequence encoding the HA peptide from the hemagglutinin protein of the human influenza virus [208]. The HA-tagged enzyme had a specific activity comparable with that of the un-modified enzyme, and was properly sorted to the lysosomal compartment (data not shown). After transduction, we evaluated at different time points the occurrence of apoptosis by TUNEL assay and GALC activity. As expected, all the cell types analyzed showed a different level of basal GALC activity (Figure 28).

7.1 Monocytes, macrophages and microglia are not sensitive to GALC expression toxicity

Murine macrophages were obtained as the adherent fraction of peritoneal cell collection. Primary cultures of microglia were isolated from the brain of +/+ and -/- FVB/twi mice by established protocols [267] [268]. Further, we tested both primary

monocytes and U937 monocytic cell line. Human monocytes were isolated from PBMC by positive selection for the CD14 monocytic marker. Transduction conditions were set up using GFP.LV and analyzing the transduction efficiency by cytofluorimetry (when possible) or by confocal microscopy. Once the transduction protocol had been optimized, microglia and macrophages were efficiently transduced with GALC.LV/GALC-HA.LV and control vectors at MOI 50 and 200, respectively, and expressed GALC above basal levels (Figure 29). Even when high expression levels (up to 40 fold to wt level) were achieved, TUNEL assay demonstrated low frequency or no apoptosis following GALC.LV transduction and GALC over-expression in all tested cells (Figure 29). No difference was observed between +/+ and -/- microglia (Figure 29 and other data not shown). These results demonstrate that HSC gene therapy effector cells are not sensitive to GALC toxicity, thus suggesting that, in order to develop a HSC gene therapy strategy for GLD, GALC expression should be avoided in HSPC, whereas it should be promoted in differentiated hematopoieic myeloid cells, capable of targeting the enzyme to affected tissues.

7.2 Human T and B lymphocytes are not sensitive to GALC expression toxicity

Human T and B lymphocytes were obtained upon PHA-stimulation and EBV transformation of total PBMC, respectively. Similarly to the experiments with monocytes and macrophages, transduction was optimized by using GFP.LV and flow cytometry. B lymphocytes were efficiently transduced with GALC.LV/GALC-HA.LV and control vectors at MOI 100 while two hits at MOI 100 were used for T lymphocytes. Despite sustained increase on GALC activity upon transduction, no apoptosis was detected at all the examined time points (Figure 30), thus further supporting the notion that differentiated hematopoietic cells are not detectably sensitive to GALC over-expression.

7.3 Primary oligodendroglia are resistant to GALC-induced apoptosis

Oligodendrocytes are the cells mostly affected by GALC deficiency in GLD and are, as well, the primary target of cross-correction in HSCT gene therapy. For this reason, we tested the sensitivity of oligodendroglia to GALC toxicity. Primary cultures of oligodendoglia were generated from the brain of +/+ and -/- FVB/twi mice by established protocols [267] [268]. The purity of the culture was evaluated by immunofluorescence using the specific oligodendroglia markers NG2 and GalCer [281]. Oligodendroglia constituted up to the 80% of the cells in culture, as estimated by the ratio between NG2+ plus GalCer+ cells, and the number of total cells (nuclei were stained with ToPro3) (Figure 31B). Once the transduction protocol had been optimized using GFP.LV and confocal microscopy, oligodendroglia were efficiently transduced with GALC.LV/GALC-HA.LV and control vectors at MOI 50. No apoptotic cells were detected by TUNEL assay, despite an increase in GALC activity upon transduction (Figure 31A-B). These results demonstrate that oligodendroglia are resistant to GALC *de novo* expression apoptosis and could be a safe target of GALC cross-correction in HSCT gene therapy. Moreover, this data suggests that GALC susceptibility is lineage-specific.

8. Regulation of GALC expression

Overall, our data thus far demonstrates that GALC *de novo* expression is responsible for apoptosis induction and functional impairment of HSPC, while differentiated hematopoietic cells and oligodendrocytes are not detectably sensitive to GALC overexpression. In order to develop an effective and safe gene therapy strategy for the treatment of GLD we thus tried to overcome this limitation by regulating GALC expression. We pursued two strategies toward this goal . The first strategy is based on the use of myeloid-specific promoters in order to restrict transgene expression only to differentiated macrophages and microglia, which represent the effector population in HSC gene therapy. A second strategy exploits HSC-specific microRNA regulation to suppress transgene expression only in HSPC, where GALC toxicity is higher, and to permit GALC over-expression in the differentiated cell progeny.

8.1 Trancriptional regulation of GALC expression

8.1.1 In vitro regulation of GALC expression by the CD11b promoter

Three different promoters of myeloid-specific genes, cFes [282], Gp91phox [283] and CD11b [284] were tested in vitro and in vivo for the level and the specificity of transgene expression, by using the reporter gene GFP. The promoter CD11b was selected according to its low expression in HSC and its sustained expression in myeloid cells, as assessed by flow cytometry (data not shown). The specificity of this promoter among the different hematopoietic lineages was quite low, as it was detectably expressed in B and T lymphocytes both *in vitro* and *in vivo*. However, since we demonstrated that GALC expression in these cells is not detrimental, we selected CD11b as our promoter of choice for future studies. In order to evaluate the effect of CD11b-regulated GALC

expression in HSPC, we generated CD11b_GALC.LV (Figure 32A). mHSPC were transduced with this new vector or with PGK_GFP.LV or PGK_ARSA.LV at MOI 100. After washing, cells were seeded for CFC assay or cultured in vitro for two weeks for GALC activity assay and Q-PCR analysis. Transduction with CD11b_GALC.LV allowed reconstitution of GALC activity in -/- HSPC progeny at physiological levels. Enzymatic activity measured in the CD11b_GALC.LV transduced mHSPC progeny was slight lower than the one measured in PGK_GALC.LV controls (Figure 32B). Interestingly, the number of colonies obtained from mHSPC transduced with CD11b_GALC.LV was similar to controls and was 1.5 fold higher than the PGK_GALC.LV colonies (Figure 32C), thus suggesting that the use of the CD11b promoter to drive GALC expression protects the transduced HSPC from *in vitro* functional impairment.

We then evaluated the occurrence of apoptosis in CD11b_GALC.LV transduced mHSPC. After transduction, mHSPC were seeded on matrigel-coated coverslip and TUNEL assay was performed after 2 and 5 days of culture. The level of apoptosis was evaluated by confocal microscopy. TUNEL assay on CD11b_GALC.LV transduced cells showed minor or no apoptosis at both time points (7%±10 and 9%±2 at 2 and 5 days respectively), similar to the one observed in cells transduced with control LV (Figure 33A-B), thus demonstrating that CD11b-regulation of GALC expression rescues mHSPC from GALC toxicity.

8.1.2 In vivo regulation of GALC expression by the CD11b promoter

The effect of CD11b-regulated GALC expression on mHSPC repopulation potential was evaluated in FVB/twi heterozygous mice. Lethally irradiated 8 day old +/-FVB/twi mice were transplanted with CD11b_GALC.LV transduced mHSPC (n = 3) or with PGK_GALC.LV transduced cells (n = 5). Survival was evaluated both short- and long-term. Untransplanted cells were cultured *in vitro* in order to perform Q-PCR. As expected, VCN measured on *in vitro* culture was higher in the CD11b_GALC.LV

transduced mHSPC progeny as compared to the PGK_GALC.LV control (VCN = 12 for CD11b_GALC and 2.4 for PGK_GALC). Remarkably, +/- FVB/twi mice transplanted with CD11b_GALC.LV transduced mHSPC were rescued from lethal conditioning and survived long-term, differently from PGK_GALC.LV-transplanted mice that did not survive after conditioning and died approximately two weeks after HSCT (Figure 34). One out of three mice transplanted with CD11b_GALC.LV transduced mHSPC was euthanized at the age of 80 days in order to harvest BM and perform Q-PCR analysis. We measured a VCN of 4.8, thus confirming the presence of transduced cells in the BM long-term after HSCT. Surprisingly, however, CD11b_GALC.LV transduced mHSPC failed to engraft into -/- FVB/twi mice (n = 5), which died two weeks after HSCT because of lethal conditioning.

8.2 Post-transcriptional regulation of GALC expression

Recent studies in our Institute demonstrated the possibility of regulating transgene expression by endogenous microRNAs [228 285 286]. We exploited a newly characterized microRNA (miR126) which is selectively expressed in HSPC among hematopoietic cells (Gentner et al., manuscript in preparation). We thus generated a new LV expressing GALC under the PGK promoter, and containing four target sequences of microRNA 126 (GALC.miR126T.LV)(Figure 35A). The effective suppression of GALC expression by miRNA126 in HSPC, and the use of the strong PGK promoter might allow reaching a higher level of GALC expression in macrophages and microglia, as compared to the enzyme expression levels obtained using the CD11b promoter. We generated also a proper control vector, containing four miR126 target sequences down-stream of GFP (GFP.miR126T.LV).

8.2.1 In vitro regulation on GALC expression by miRNA126

In order to evaluate the effect of miRNA126-regulated GALC expression in HSPC, we transduced mHSPC with GALC.miR126T.LV or with GFP.miR126T.LV or GALC.LV at MOI 100. After washing, cells were seeded for CFC assay or cultured in vitro for two weeks for GALC activity assay and Q-PCR analysis. Transduction with GALC.miR126T.LV allowed a reconstitution of GALC activity at supraphysiological levels in the differentiated mHSPC progeny, up to 2 fold over wild type levels (Figure 35B). Importantly, the number of colonies obtained from mHSPC transduced with GALC.miR126T.LV was similar to controls and was almost 2-fold with respect to GALC.LV colonies (figure 35C), thus suggesting that regulation of GALC expression by miRNA126 allowed preserving the clonogenic potential of transduced mHSPC. These encouraging results prompted us to evaluate if the unaffected clonogenic potential was due to the rescue from apoptosis of GALC.miR126T.LV transduced mHSPC. After transduction, mHSPC were seeded on matrigel-coated coverslip and TUNEL assay was performed after 2 and 5 days of culture. The level of apoptosis was evaluated by confocal microscopy. TUNEL assay on GALC.miR126T.LV transduced cells showed minor or no apoptosis at both the time points (1%±1 and 3%±2 at 2 and 5 days respectively), similarly to what was observed in cells transduced with the control LV (Figure 36A-B). This data demonstrated that suppression of GALC expression by miRNA126 could rescue mHSPC from GALC-induced apoptosis.

8.2.2 In vivo regulation on GALC expression by miRNA126

The effect of miRNA126-regulated GALC expression on mHSPC repopulation potential was evaluated in +/- and -/- FVB/twi mice. Lethally irradiated 8 day old mice were transplanted with GALC.miR126T.LV transduced -/- mHSPC (n = 3 for +/- and n = 8 for -/- FVB/twi mice) or with PGK_GALC.LV transduced cells (n = 3 for +/- and n = 5 for -/- FVB/twi mice) and survival was evaluated at both short- and long-term.

Similarly to what observed with CD11b_GALC.LV, +/- FVB/twi mice transplanted with GALC.miR126T.LV transduced mHSPC were rescued from lethality and survived long term (more than 3 months after HSCT), differently from PGK_GALC.LV-transplanted mice that did not survive after lethal conditioning (Figure 37). One out of three mice transplanted with GALC.miR126T.LV transduced mHSPC was euthanized at the age of 80 days and Q-PCR analysis was performed on BM. We found a VCN of 5, thus confirming the presence of transduced cells in the BM long-term after HSCT. However, also GALC.miR126T.LV transduced mHSPC were not able to rescue lethally irradiated -/-FVB/twi mice from lethal conditioning.

Overall, these results together to those observed with CD11b_GALC.LV transduced cells, show successful rescue of the GALC deficiency and protection from de novo GALC expression in HSPC by our improved regulated gene therapy strategies. However, the failure of the corrected cells to engraft in twi mice also suggest a non cell autonomous defect, which cannot be overcome by our gene replacement strategies and selectively challenges the engraftment of gene-corrected twi cells.

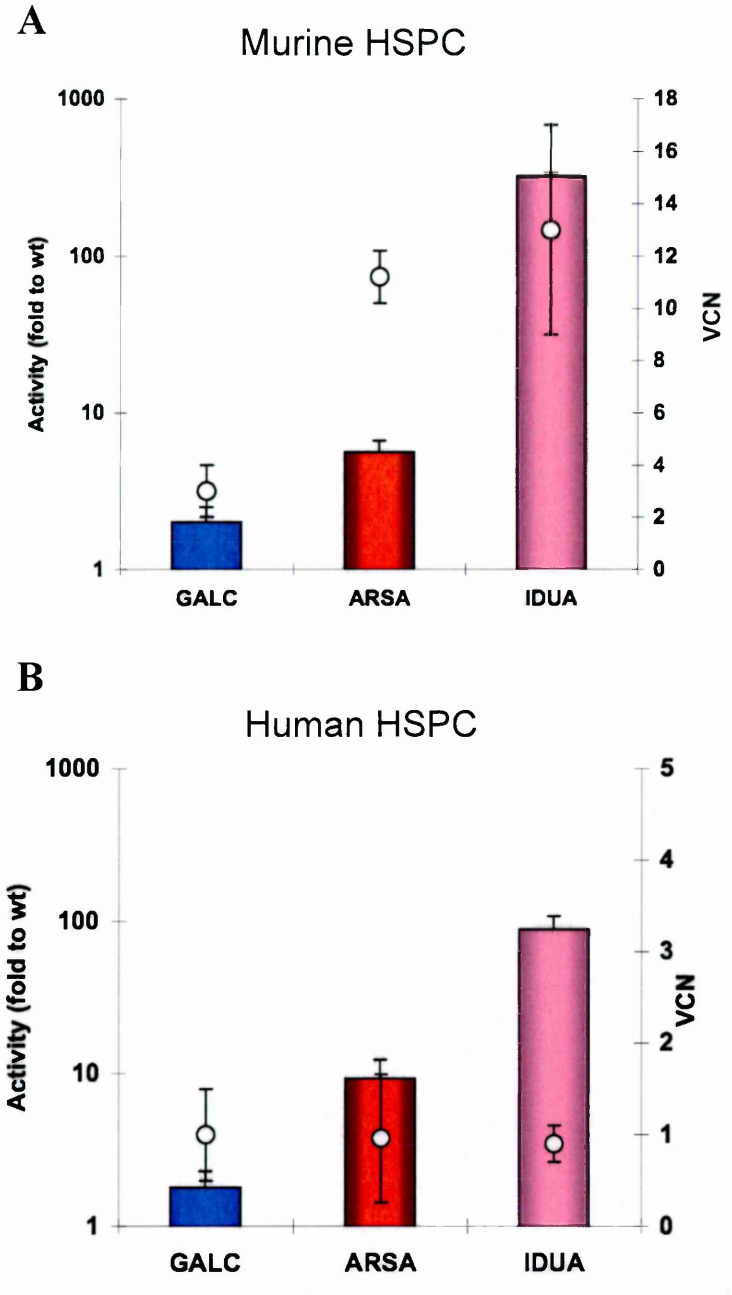

Figure 17. Lysosomal enzyme over-expression in HSPC.
Enzyme expression level, normalized to wild type, in mHSPC **(A)** and hHSPC **(B)** upon LV transduction. GALC expression was significantly lower as compared to ARSA and IDUA.

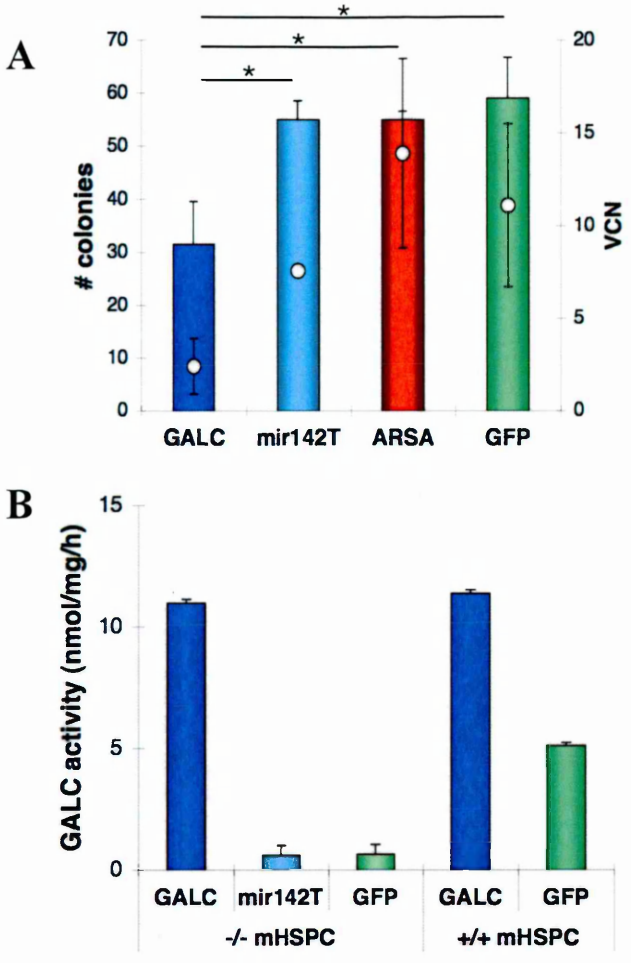

Figure 18. Impaired function of murine HSPC upon LV-mediated GALC expression.

(A) CFC assay on mHSPC transduced with GALC and control LV. The number (#) of colonies/plate (Y left axis, columns) was counted and the number of integrated LV copies/cell (VCN)(Y right axis, dots) was measured. GALC.LV transduced -/- mHSPC (n = 12 independent experiments) produced a significantly lower number of colonies as compared to GFP.LV (n = 10) and ARSA.LV (n = 8) transduced cells. This impairment was not observed when mHSPC were transduced with the mir142T GALC.LV (n = 6). * $p<0.001$ at one-Way Anova for both number of colonies/plate and VCN. Mean values ± SD are shown. Similar results were obtained with -/- and +/+ mHSPC. **(B)** GALC activity measured on transduced mHSPC. After GALC.LV transduction GALC -/- (hereon -/-) (n = 5) and GALC +/+ (hereon +/+) (n = 5) mHSPC showed a 2 fold increase in GALC activity above wild type levels (+/+ mHSPC transduced with GFP.LV, n = 5). No increase in activity was detected in mHSPC transduced with a mir142 regulated GALC.LV (mir142T) (n = 3).

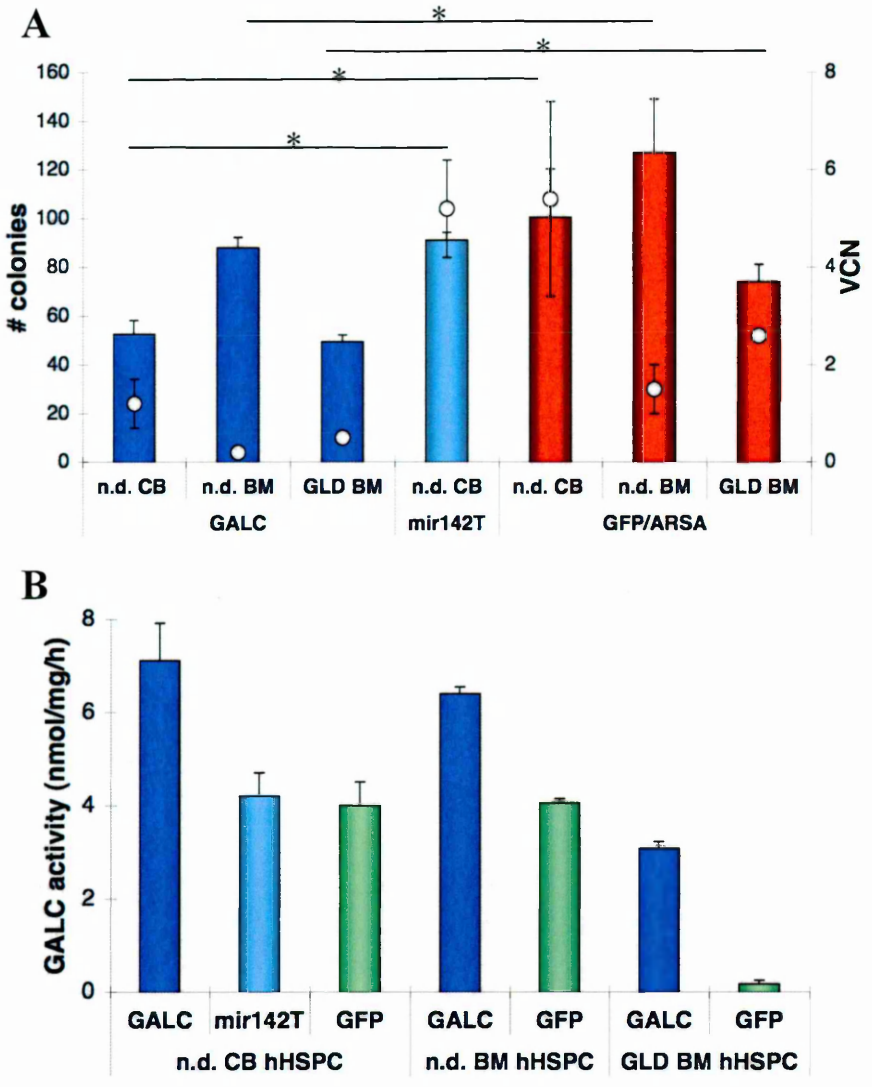

Figure 19. Impaired function of human HSPC upon LV-mediated GALC expression.

(A) CFC assay on hHSPC transduced with GALC and control LV. The number (#) of colonies/plate (Y left axis, columns) was counted and the number of integrated LV copies/cell (VCN)(Y right axis, dots) was measured. GALC.LV transduced n.d. (n = 4) and GLD hHSPC (n = 4) showed a significant impairment in colony formation as compared to control cells (n = 5), which was not observed following mir142T GALC.LV transduction (n = 4). Colonies obtained from GALC.LV transduced hHSPC showed a significantly lower vector content, when compared to GFP/ARSA/GALCmir142T.LV controls. * $p<0.001$ at One-Way Anova for both number of colonies/plate and VCN. Mean values ± SD are shown. **(B)** GALC activity measured on transduced hHSPC. GALC.LV transduction permitted the reconstitution of GALC activity at n.d. levels in GLD hHSPC (n = 3), while transduction of n.d. hHSPC (n = 4 for CB and n = 3 for BM) led to over-expression of the enzyme above GFP.LV transduced levels (n = 3). No increase in activity was detected in hHSPC transduced with a mir142 regulated GALC.LV (mir142T) (n = 3).

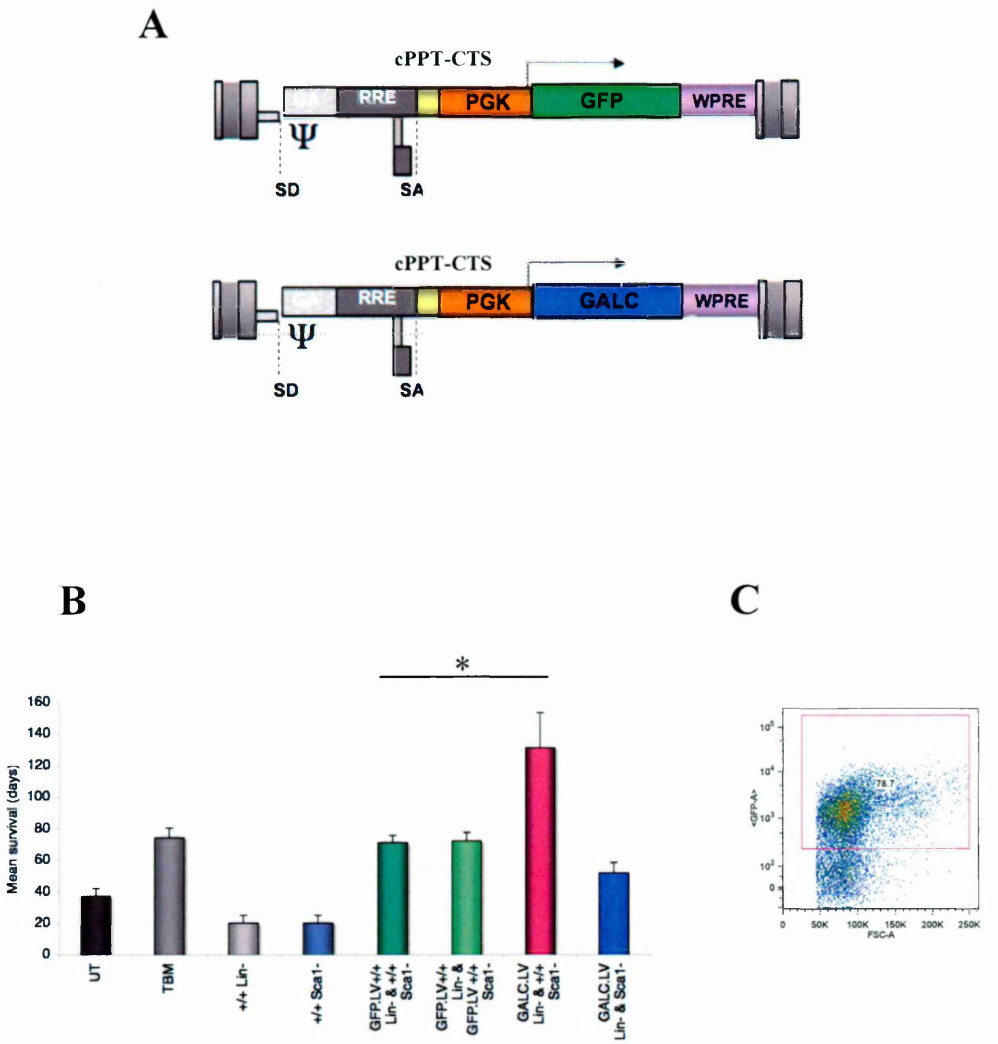

Figure 20. Survival of twi mice upon HSCT.

(**A**) Schematic representation of GFP.LV and GALC.LV. (**B**) Mean survival of twi mice receiving HSCT. Twi mice transplanted with total BM (TBM) (n = 12) or with GFP.LV transduced +/+ mHSPC and untransduced Sca1- progenitors (GFP.LV +/+ Lin- & +/+ Sca1-, n = 7) or with GFP.LV transduced +/+ mHSPC and GFP.LV transduced Sca1- progenitors (GFP.LV +/+ Lin- & GFP.LV +/+ Sca1-, n = 5) achieved longer survival as compared to untreated controls (UT) (n = 10). Mice receiving GALC.LV transduced -/- mHSPC and +/+ Sca1- progenitors (n = 7) showed a significantly higher lifespan respect to TBM or +/+ Lin- & Sca1- transplanted mice. On the contrary, transplantation with GALC.LV transduced -/- Lin- & -/- Sca1- (n = 13) did not result in a prolonged lifespan. Control groups: mice transplanted with GFP.LV transduced +/+ HSPC (+/+ Lin-) (n = 10); mice transplanted with GFP.LV transduced +/+ Sca1- progenitors (n = 8). * $p<0.01$ at one-Way Anova test. (**C**) Representative plot showing the percentage of GFP+ engrafted cells in the peripheral blood of a twi mouse transplanted with GFP.LV transduced +/+ mHSPC and Sca1- progenitors.

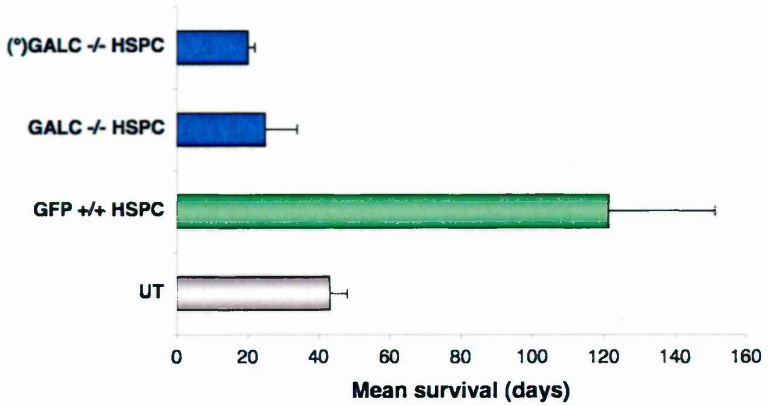

Figure 21. Impaired in vivo function of mHSPC in FVB/twi mice. Mean survival of mice receiving mHSPC transplantation, as indicated. -/- mice transplanted with GFP.LV transduced +/+ mHSPC (n = 11) achieved longer survival as compared to untreated controls (UT); on the contrary, -/- (n = 9) and +/- (°)(n = 5) mice transplanted with GALC.LV transduced -/- mHSPC did not survive after lethal irradiation.

Transplanted cells	Host	VCN (20 days)	VCN (≥120 days)
(°)GALC -/- HSPC (§)	+/-	0.01±0	-
GALC -/- HSPC (§)	-/-	0.02±0	-
GFP -/- HSPC (§)	-/-	2.3±1	2±0.5

Table 2. Mean VCN ± SD detected in the BM of -/- or +/- mice transplanted with the listed mHSPC (transduced with GALC.LV or GFP.LV) at 20 and ≥120 days post transplant (n = 3 *per* time point). (°)+/- host. (§) Similar results were obtained using +/+ mHSPC.

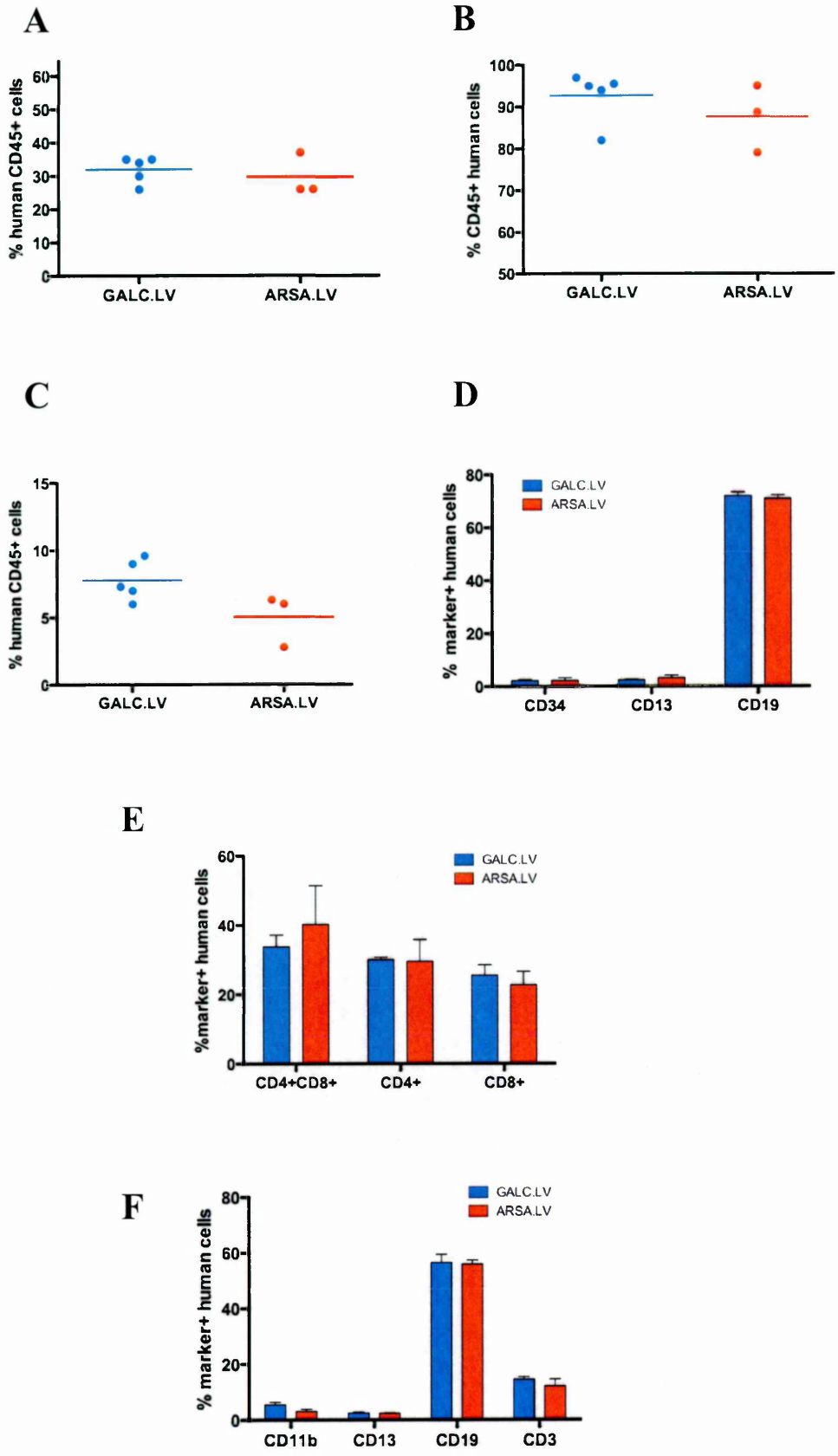
A
% human CD45+ cells
60
50
40
30
20
10
0
GALC.LV
ARSA.LV
B
% CD45+ human cells
100
90
80
70
60
50
GALC.LV
ARSA.LV
C
% human CD45+ cells
15
10
5
0
GALC.LV
ARSA.LV
D
% marker+ human cells
80
60
40
20
0
GALC.LV
ARSA.LV
CD34
CD13
CD19
E
%marker+ human cells
60
40
20
0
GALC.LV
ARSA.LV
CD4+CD8+
CD4+
CD8+
F
% marker+ human cells
80
60
40
20
0
GALC.LV
ARSA.LV
CD11b
CD13
CD19
CD3

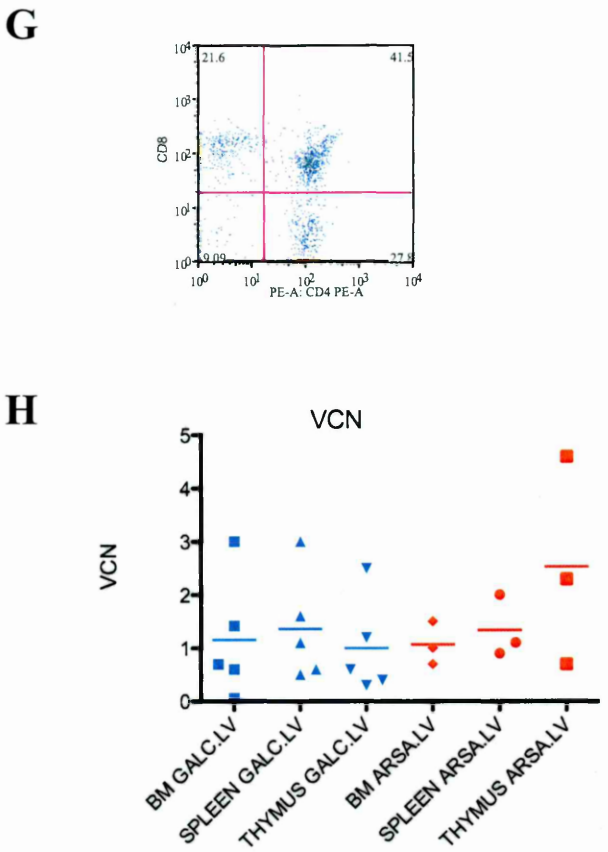

Figure 22. hHSPC engraftment and differentiation in Rag2γc mice.
(A-C) Engraftment of hHSPC in bone marrow (**A**), thymus (**B**) and spleen (**C**) of Rag2γc mice, measured as the percentage of CD45+ cells, ten weeks after transplantation. (**D-F**) Human cell differentiation in bone marrow (**D**), thymus (**E**) and spleen (**F**) of Rag2γc mice. The percentage of lineage marker positive cells is reported in the chart. (**G**) Representative plot of human lymphocyte differentiation in thymus: human lymphocytes showed a normal differentiation pattern (**H**) Number of integrated vector copies (VCN) per genome in hematopoietic tissues of repopulated mice. No significant difference between GALC.LV and ARSA.LV transduced hHSPC engraftment and differentiation was reported.

A

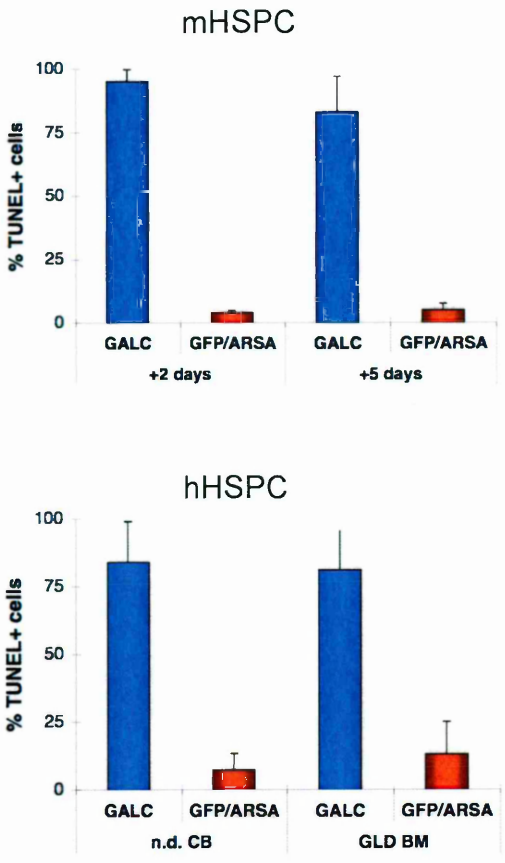
mHSPC
% TUNEL+ cells
100
75
50
25
0
GALC
GFP/ARSA
GALC
GFP/ARSA
+2 days
+5 days
hHSPC
% TUNEL+ cells
100
75
50
25
0
GALC
GFP/ARSA
GALC
GFP/ARSA
n.d. CB
GLD BM

B

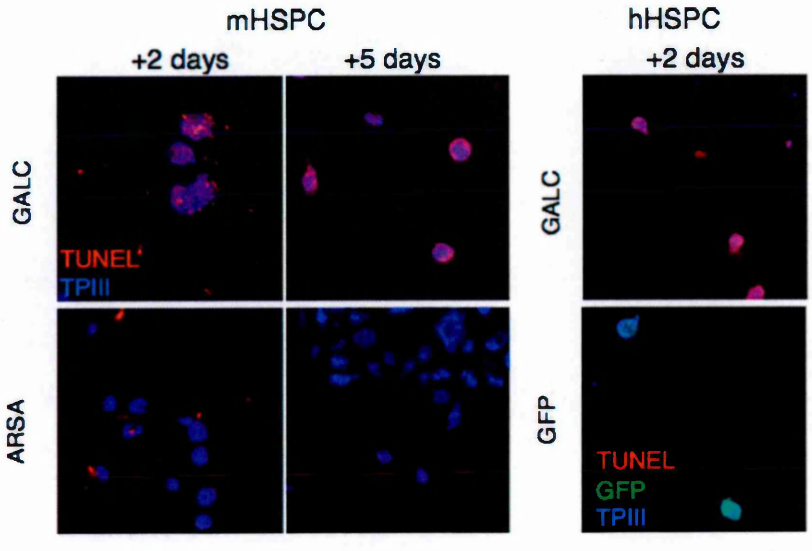
mHSPC
+2 days
+5 days
hHSPC
+2 days
GALC
ARSA
GALC
GFP
TUNEL
TPIII
TUNEL
GFP
TPIII

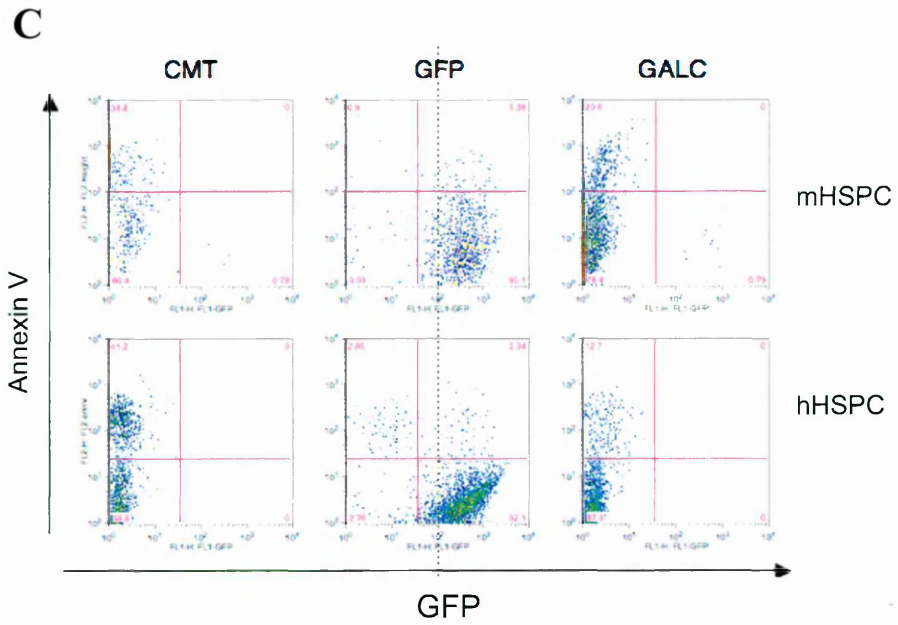

Figure 23. Apoptosis of GALC expressing murine and human HSPC.

(A-B) TUNEL assay on -/- mHSPC (left) and hHSPC (right)(from n.d. CB and GLD BM) at 2 and 5 days after gene transfer. % of TUNEL+ nuclei over the total number of nucleated cells is reported. ≥ 8 fields and ≥ 100 cells were counted *per* condition. Similar results were obtained using +/+ mHSPC. **(A)** The large majority of GALC.LV transduced m- and hHSPC were TUNEL positive both at 2 and at 5 days after transduction. **(B)** TUNEL assay (red) and ToPro3 (TPIII, blue) staining for nuclei on m- and hHSPC at 2 and 5 (mHSPC) days after transduction with the indicated LV: representative images (images were acquired by three-laser confocal microscope - Radiance 2100, BioRad; fluorescent signals from single optical sections were sequentially acquired and analyzed by Adobe Photoshop CS software; magnification 100x). **(C)** Cytofluorimetric analysis of Annexin V staining on m- (top panels)(from -/- donor mice) and hHSPC (bottom panels)(from n.d. CB). The fraction of apoptotic cells is higher among GALC.LV transduced mHSPC and hHSPC as compared to GFP-transduced controls. CMT = Camptotecin treated positive control. Acquisition was performed with FACS Calibur 2, Beckton Dickinson. At least 10,000 events were scored and data were processed by FlowJo 8.5.3 software. Data from -/- mHSPC and n.d. CB (and GLD BM for TUNEL) are shown, but similar findings were obtained following GALC transduction of +/+ mHSPC as compared to -/- cells and in n.d. BM (TUNEL and Annexin V) and GLD BM (Annexin V) hHSPC as compared to CB cells.

A

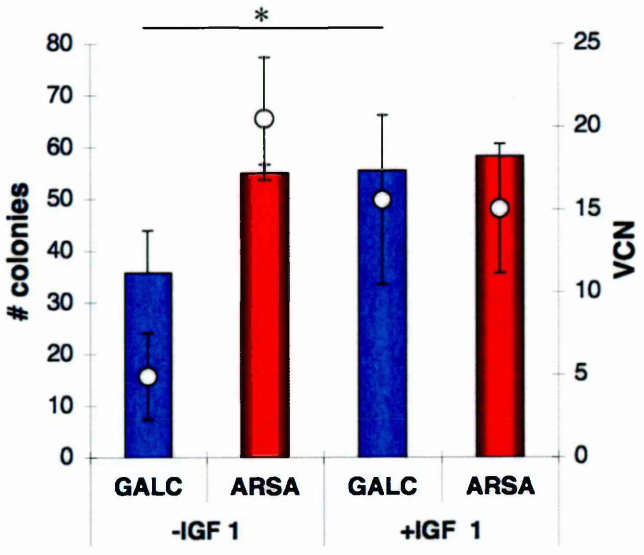
*
80
70
60
50
40
30
20
10
0
colonies
25
20
15
10
5
0
VCN
GALC
ARSA
GALC
ARSA
-IGF 1
+IGF 1

B

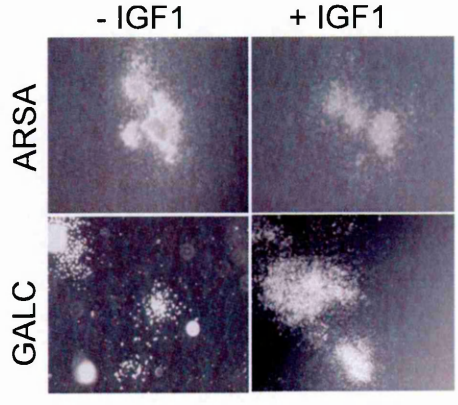
- IGF1
+ IGF1
ARSA
GALC

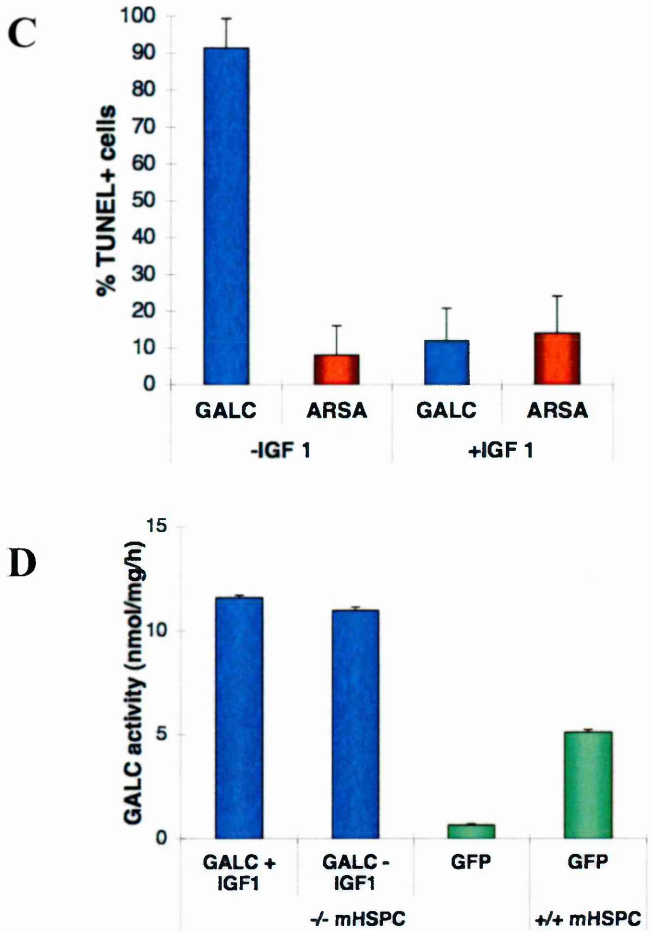

Figure 24. IGF1 treatment prevents apoptosis of GALC-expressing HSPC.
(A) CFC assay on GALC.LV and ARSA.LV transduced mHSPC treated or not with IGF1. The number (#) of colonies/plate (Y left axis, bars) was counted and the number of integrated lentiviral vector copies/cell (VCN)(Y right axis, dots) was measured. IGF1 treatment induced growth of a higher colony number, as compared to GALC.LV transduced untreated cells (n = 4 independent experiments). Upon anti-apoptotic treatment, the VCN of GALC.LV transduced cells approached that of ARSA.LV transduced control cells (for both CFC number and VCN one-Way Anova: * = $p<0.001$ for the comparison of treated GALC transduced mHSPC with untreated GALC.LV transduced cells; $p>0.05$ for the comparison of treated GALC.LV transduced mHSPC with ARSA.LV transduced cells). **(B)** The colonies grown from treated mHSPC also showed an increase in size (pictures on the right, magnification 5x). **(C)** TUNEL assay on GALC.LV and ARSA.LV-transduced mHSPC treated or not with IGF1. $\geq$ 8 fields and $\geq$ 100 cells were counted *per* condition. The large majority of treated cells were negative for TUNEL (one-Way Anova: $p<0.001$ for the comparison with untreated GALC.LV transduced cells; $p>0.05$ for the comparison with ARSA.LV transduced cells). **(D)** GALC activity measured on transduced mHSPC from -/- or +/+ mice. IGF1 treatment did not significantly affect GALC expression levels (n = 3) when compared to transduced untreated controls (n = 6). Mean values ± SD are shown.

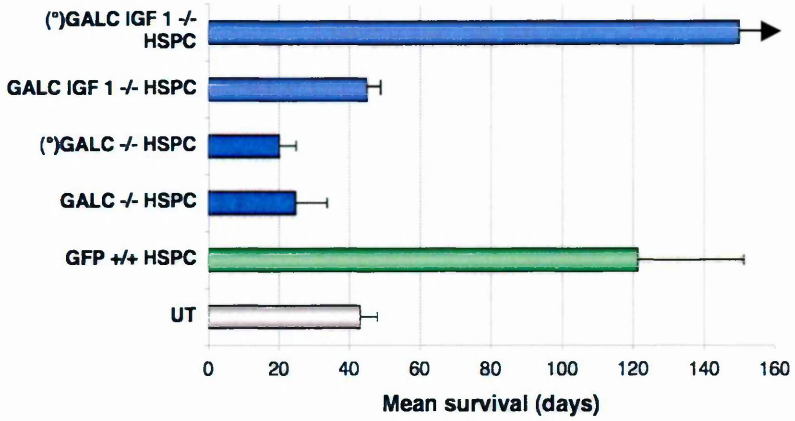

Figure 25. Survival of FVB/twi mice transplanted with IGF1- treated HSPC.
Mean survival of mice transplanted with mHSPC treated or not with IGF1 after GALC.LV transduction, as reported in the graph. -/- and +/- mice transplanted with IGF1 treated, GALC transduced -/- mHSPC survived to lethal irradiation; -/- mice (n = 3) transplanted with IGF1 treated, GALC.LV transduced died for GLD manifestation at the expected age, while transplanted +/- (°) animals (n = 3) reached long-term survival.

Transplanted cells	Host	VCN (20 days)	VCN (lomg-term)
(°)GALC IGF1 -/- HSPC	+/-	2.7±0.7	0.6±0.3
GALC IGF1 -/- HSPC	-/-	4.3±0.5	0.5±0.2
(°)GALC -/- HSPC (§)	+/-	0.01±0	-
GALC -/- HSPC (§)	-/-	0.02±0	-
GFP +/+ HSPC	-/-	2.3±1	2±0.5

Table 3. Mean VCN ± SD detected in the BM of -/- or +/- mice transplanted with the listed mHSPC (transduced with GALC.LV or GFP.LV, treated or not with IGF1) at 20 and long-term post transplant (42 days for GALC.LV IGF1 -/- HSPC in -/- recipients, 120 days for the others) (n = 3 *per* time point). (°)+/- host. (§) Similar results were obtained using +/+ mHSPC.

A

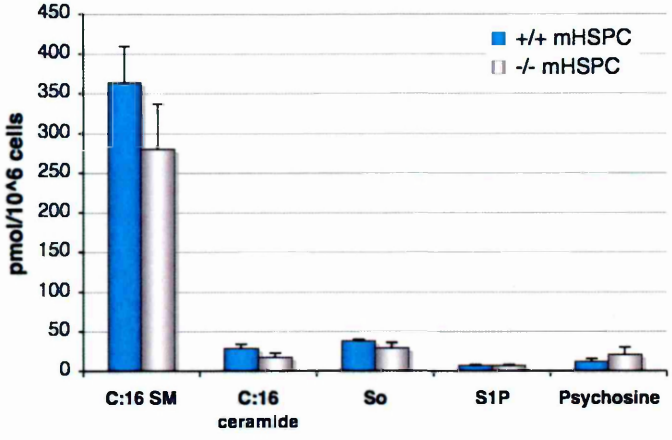
450
400
350
300
250
200
150
100
50
0
pmol/10^6 cells
+/+ mHSPC
-/- mHSPC
C:16 SM
C:16 ceramide
So
S1P
Psychosine

B

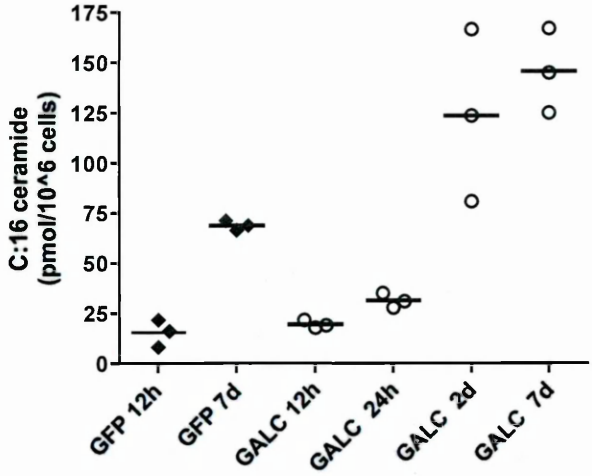
175
150
125
100
75
50
25
0
C:16 ceramide (pmol/10^6 cells)
GFP 12h
GFP 7d
GALC 12h
GALC 24h
GALC 2d
GALC 7d

C

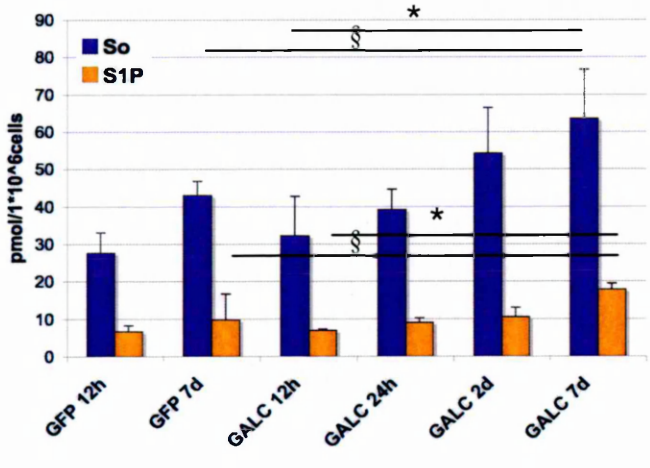
90
80
70
60
50
40
30
20
10
0
pmol/1*10^6cells
So
S1P
*
§
*
§
GFP 12h
GFP 7d
GALC 12h
GALC 24h
GALC 2d
GALC 7d

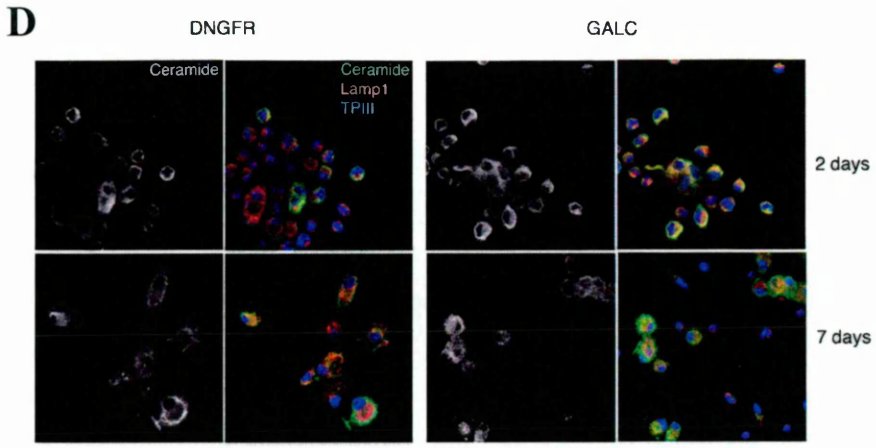

Figure 26. Sphingolipid profile of mHSPC.
Tandem mass spectrometry quantification of sphingolipids performed on mHSPC at different intervals after GALC.LV and control GFP.LV gene transfer. GFP.LV was preferred as control since ARSA expression could alter sphingolipid profile. **(A)** Sphingolipid intracellular basal content (pmol/10^6cells) in -/- (n = 6) and +/+ (n = 4) HSPC before the occurrence of transgene expression. C:16 SM, C:16 ceramide and So content are reduced in -/- cells. **(B)** C:16 ceramide quantification (pmol/10^6cells) in GALC and GFP.LV transduced -/- mHSPC at different intervals after gene transfer. A significant accumulation of ceramide occurs at 2 and 7 days after GALC.LV transduction, as compared to GFP.LV transduced cells (GALC 7d *versus* GFP 7d) and to GALC.LV transduced cells shortly after gene transfer (GALC 2d and 7d *versus* GALC 12h)(n=3). **(C)** Quantification of So and S1P in GALC.LV and GFP.LV transduced -/- HSPC at different intervals after gene transfer. A significant accumulation of So and S1P occurs at 7 days after GALC.LV transduction. **(D)** Representative images obtained after immonofluorescence staining (for ceramide and for the lysosomal marker Lamp1) and confocal analysis on the progeny of mHSPC transduced with GALC.LV and control DeltaNGFR (DNGFR).LV at 2 and 7 days after transduction (as indicated). Upon GALC gene transfer, ceramide signal co-localization with Lamp1 is more pronounced, compared to cells transduced with the control vector. DNGFR was chosen as proper control to avoid fluorescent signal interference by GFP. Mean values ± SD are shown. # = $p<0.05$ at unpaired Students' t Test; * = $p<0.001$ and § = $p< 0.05$ at one-Way Anova. In (B) and (C) data from -/- HSPC are presented, but we could detect a similar accumulation of ceramide, So and S1P in +/+ HSPC. Magnification: 100x in (D).

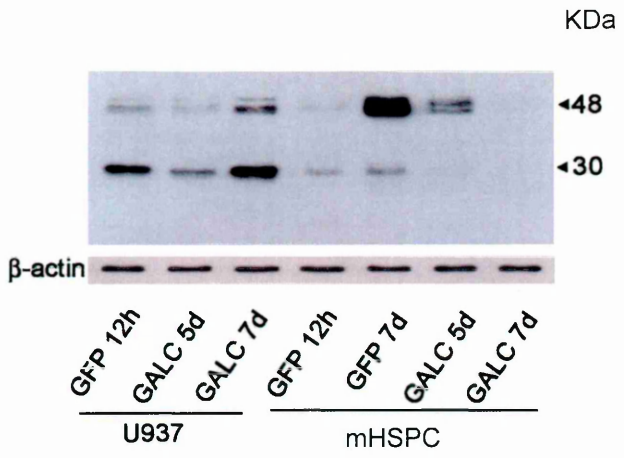

Figure 27. Analysis of Cathepsin D activation in transduced cells.
Western blot analysis for Cathepsin D on GFP.LV or GALC.LV transduced mHSPC and U937 cells at different intervals after gene transfer, as indicated. Activated form corresponds to 30kDa membrane bound isoform, as indicated by arrow. No significant accumulation of the active form of Cathepsin D was observed in GALC.LV transduced cells after gene transfer, compared to GFP.LV transduced cells. The precursor (48kDa, arrow) accumulated in GFP-transduced cells after 7 days of culture (GFP 7d), while its accumulation was less pronounced in the presence of GALC (GALC 5d), culminating with disappearance of both the precursor and mature forms after 7 days. An anti β-actin was used as control for protein loading.

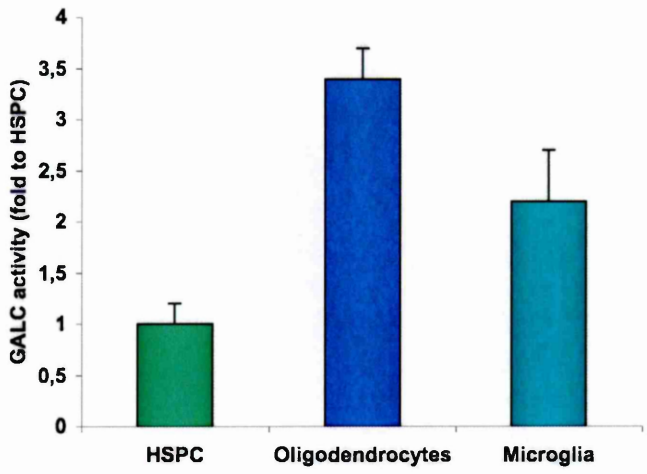

Figure 28. Basal GALC activity in different cell types.
Basal GALC activity normalized to wild type mHSPC level. Both primary wild type oligodendrocytes (n = 4) and microglia (n = 4) showed a higher GALC activity as compared to mHSPC.

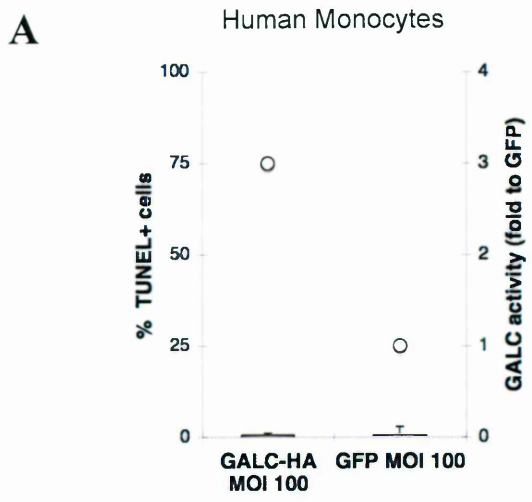
A
Human Monocytes
100
75
50
25
0
% TUNEL+ cells
4
3
2
1
0
GALC activity (fold to GFP)
GALC-HA MOI 100
GFP MOI 100

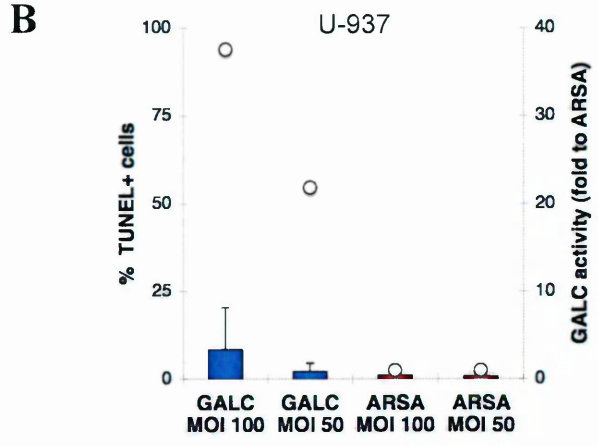
B
U-937
100
75
50
25
0
% TUNEL+ cells
40
30
20
10
0
GALC activity (fold to ARSA)
GALC MOI 100
GALC MOI 50
ARSA MOI 100
ARSA MOI 50

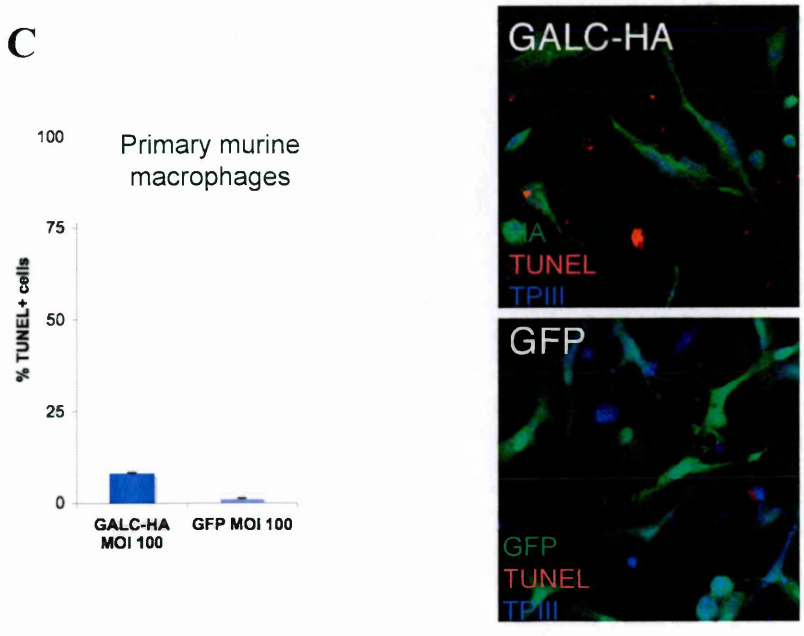
C
Primary murine macrophages
100
75
50
25
0
% TUNEL+ cells
GALC-HA MOI 100
GFP MOI 100
GALC-HA
TUNEL
GFP
GFP
TUNEL

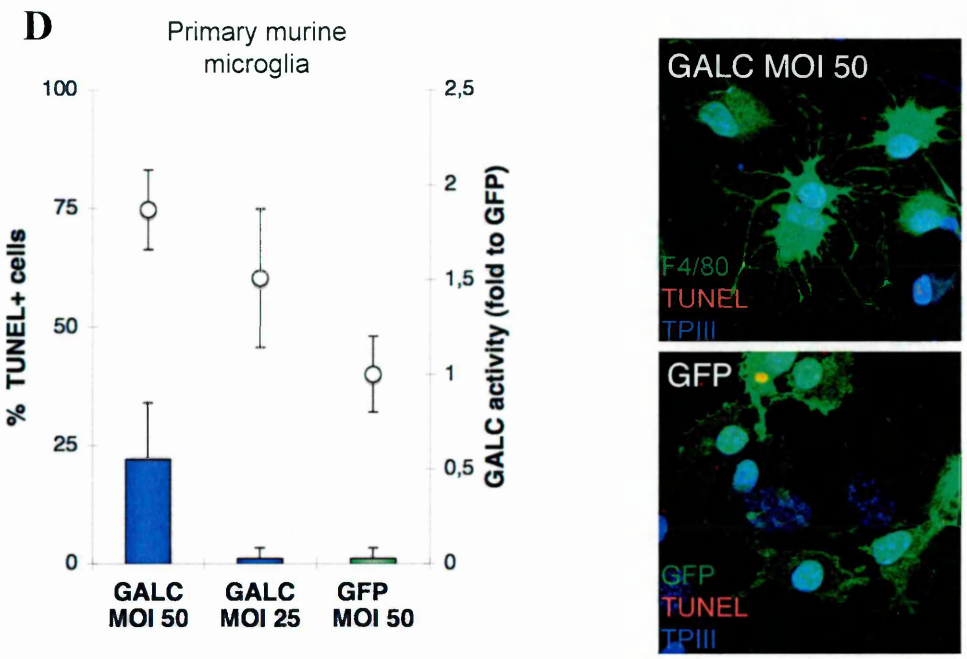

Figure 29. Sensitivity to GALC *de novo* expression in myeloid cells.
Results from TUNEL assay (% TUNEL+ cells over the total nucleated cells, on Y left axis, bars), GALC activity determination (on Y right axis, dots) and, when possible, dedicated stainings, performed on **(A)** human monocytes, **(B)** the monocytic human cell line U937, **(C)** murine macrophages and **D)** murine microglia, 5 days after transduction. In all tested conditions, TUNEL staining demonstrated the occurrence of minor/no apoptosis ($\geq$ 6 fields and $\geq$ 250 cells were counted *per* condition), despite efficient transduction (evaluated by anti-HA staining on macrophages in (C)) and sustained GALC expression above basal levels in all the other samples (ARSA.LV- or GFP.LV-transduced cells), were obtained. Mean values ± SD are shown. **(C** and **D)** Representative images of TUNEL assay on GALC/GALC-HA.LV or GFP.LV transduced macrophages **(C)** and microglia **(D)**. Images were acquired by three-laser confocal microscope (Radiance 2100, BioRad). Fluorescent signals from single optical sections were sequentially acquired and analyzed by Adobe Photoshop CS software. Magnification: 80x in C, 100x in D.

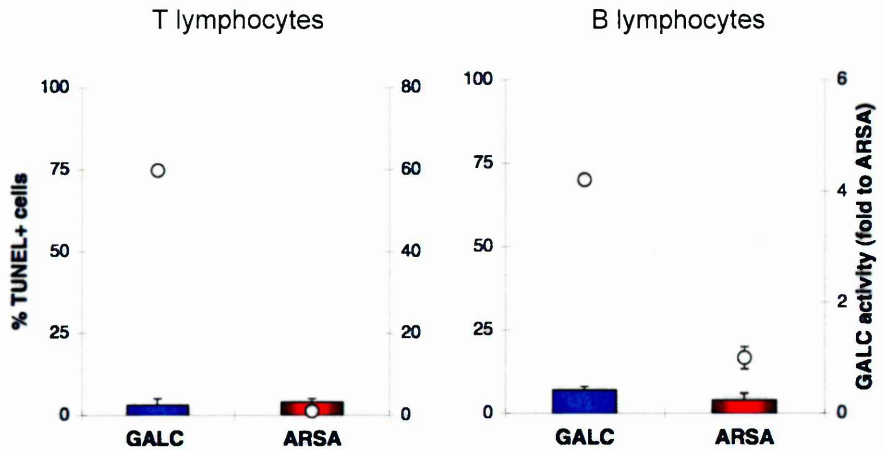

Figure 30. Sensitivity to GALC *de novo* expression in lymphocytes.
Results from TUNEL assay (% TUNEL+ cells over the total nucleated cells, on Y left axis, bars), GALC activity determination (on Y right axis, dots), performed on T and B lymphocytes, 5 days after transduction. TUNEL staining demonstrated the occurrence of minor/no apoptosis ($\geq$ 6 fields and $\geq$ 250 cells were counted *per* condition), despite efficient transduction (see the sustained GALC expression above basal levels). Mean values ± SD are shown.

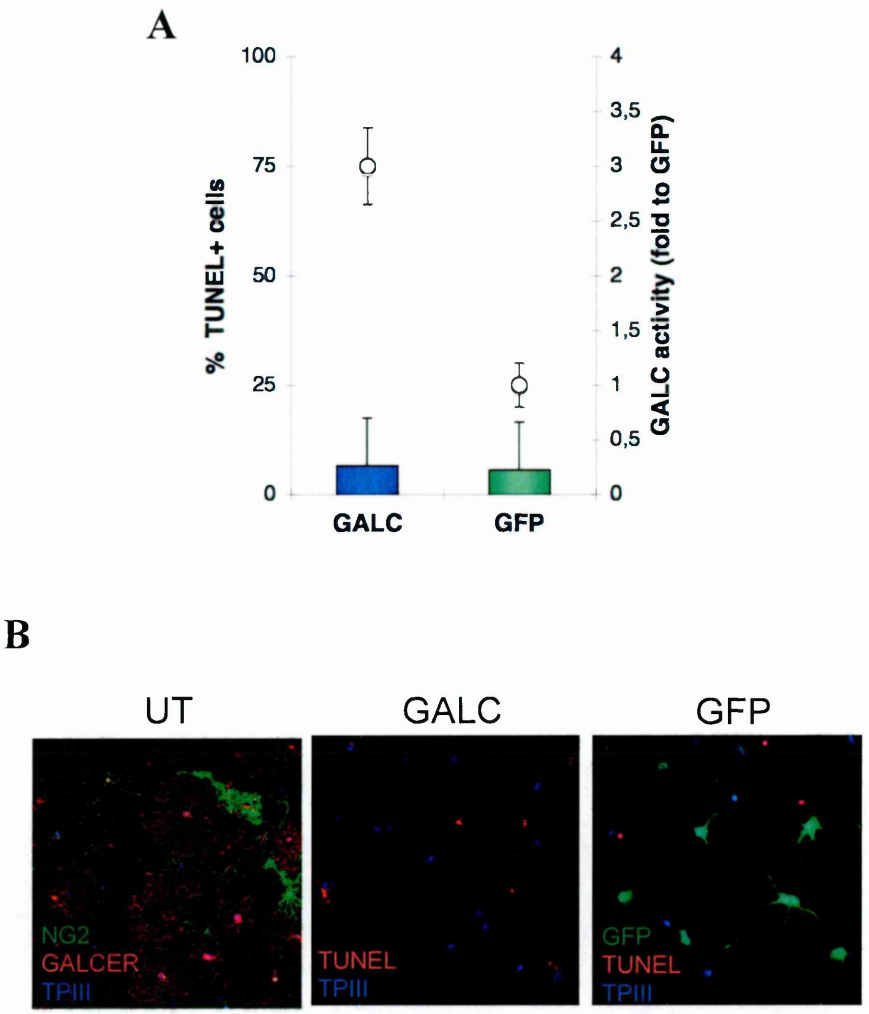

Figure 31. Sensitivity to GALC *de novo* expression in oligodendrocytes.
(A) TUNEL assay (% TUNEL+ cells over the total nucleated cells, on Y left axis, bars), GALC activity determination (on Y right axis, dots), performed 5 days after transduction. TUNEL staining demonstrated the occurrence of minor/no apoptosis (≥ 6 fields and ≥ 250 cells were counted *per* condition), despite efficient transduction (see the sustained GALC expression above basal levels). Mean values ± SD are shown. **(B)** Representative images of TUNEL assay on GALC.LV or GFP.LV transduced oligodendrocytes. The purity of the oligodendrocyte preparation was verified by NG2 and Gal-Cer staining on non-transduced cells (UT), while microglia was stained with F4/80 on GALC.LV-transduced cells; ToPro3 (TPIII) was used to stain nuclei. Images were acquired by three-laser confocal microscope (Radiance 2100, BioRad). Fluorescent signals from single optical sections were sequentially acquired and analyzed by Adobe Photoshop CS software. Magnification: 40x.

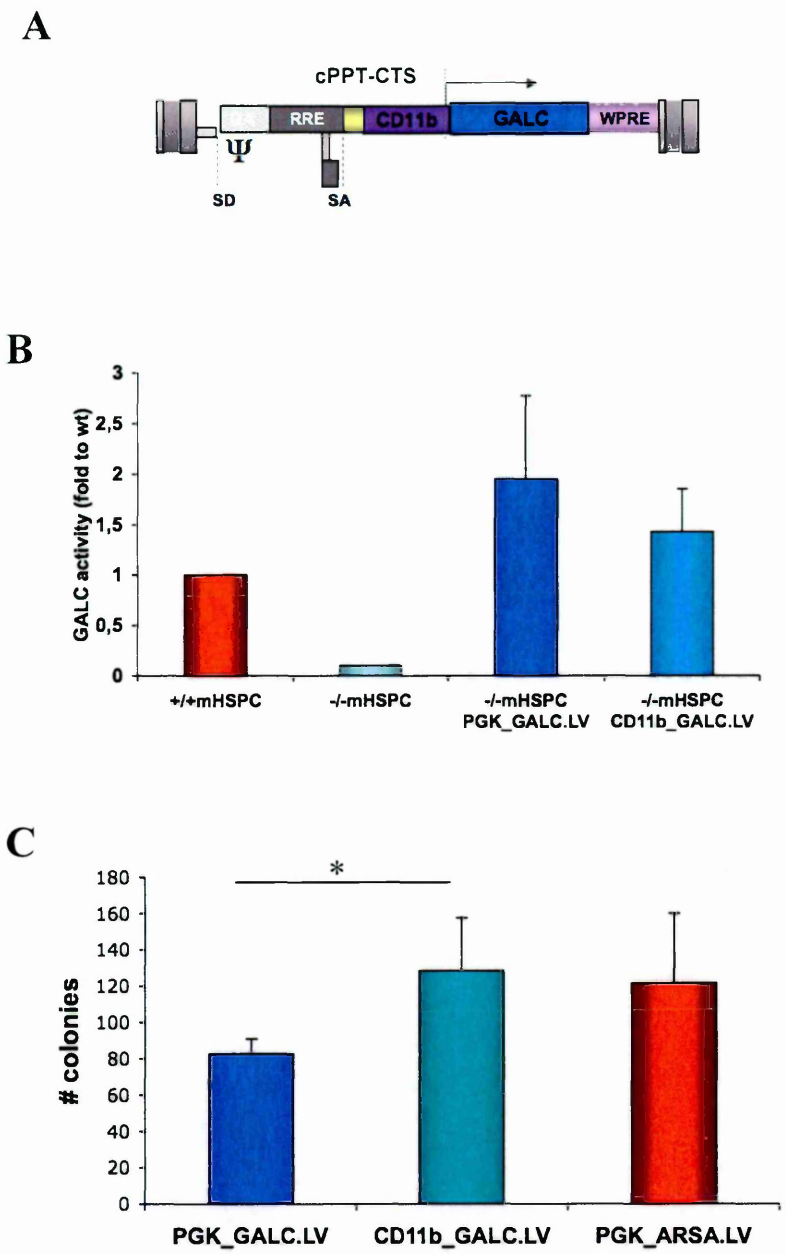

Figure 32. Regulation of GALC expression by CD11b promoter. (**A**) Schematic representation of CD11b_GALC.LV. (**B**) GALC activity assay performed on the in vitro progeny of -/- mHSPC transduced with CD11b_GALC.LV or with PGK_GALC.LV. Activity was normalized respect to +/+ Untransduced cells (first column). Cells transduced with CD11b_GALC.LV achieved a complete reconstitution of enzymatic activity. (**C**) CFC assay performed on mHSPC transduced with CD11b_GALC.LV, with PGK_GALC.LV or with PGK_ARSA.LV as a control. CD11b_GALC.LV transduced -/- mHSPC showed an intact clonongenic potential. * $p<0.01$ at one-Way Anova test.

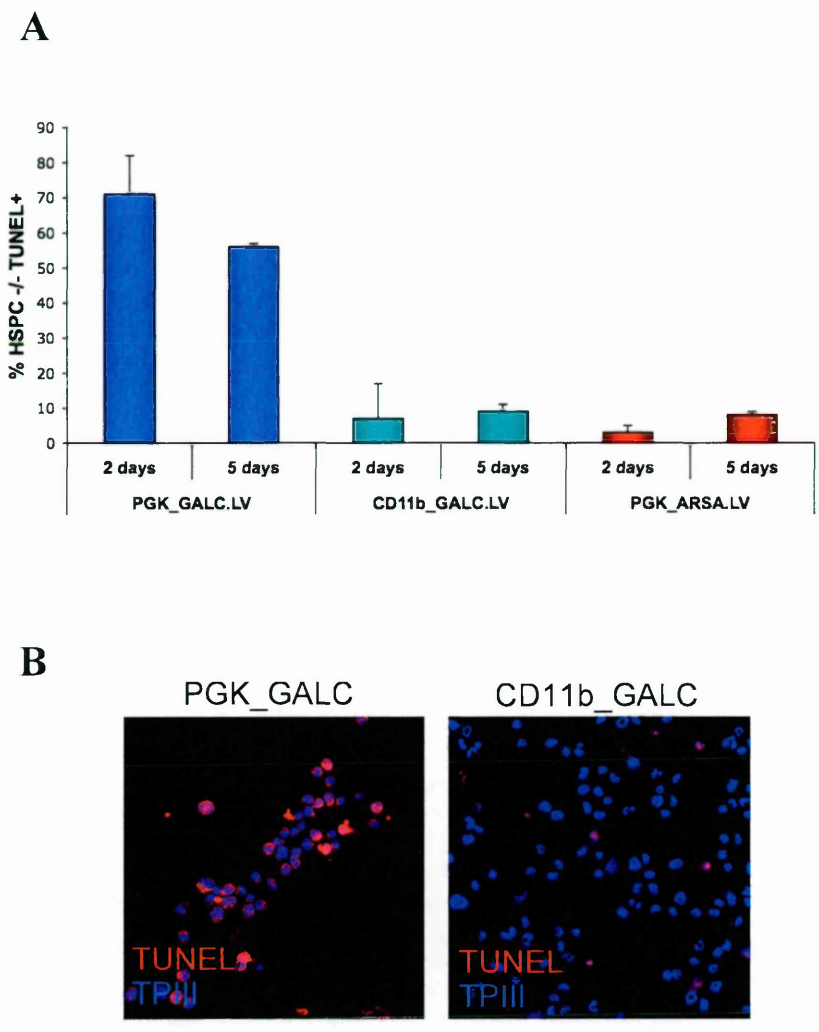

Figure 33. CD11b promoter-driven GALC expression prevents apoptosis of GALC.LV transduced mHSPC.

(A) TUNEL assay on CD11b_GALC.LV or PGK_GALC.LV and PGK_ARSA.LV - transduced mHSPC. ≥ 8 fields and ≥ 100 cells were counted per condition. The large majority of CD11b_GALC.LV transduced cells were negative for TUNEL both at 2 and 5 days after tranduction. (**B**) TUNEL assay (red) and ToPro3 (TPIII, blue) staining for nuclei on CD11b_GALC.LV or PGK_GALC.LV-transduced mHSPC-/- 5 days after transduction: representative images (images were acquired by three-laser confocal microscope - Radiance 2100, BioRad; fluorescent signals from single optical sections were sequentially acquired and analyzed by Adobe Photoshop CS software; magnification 40x).

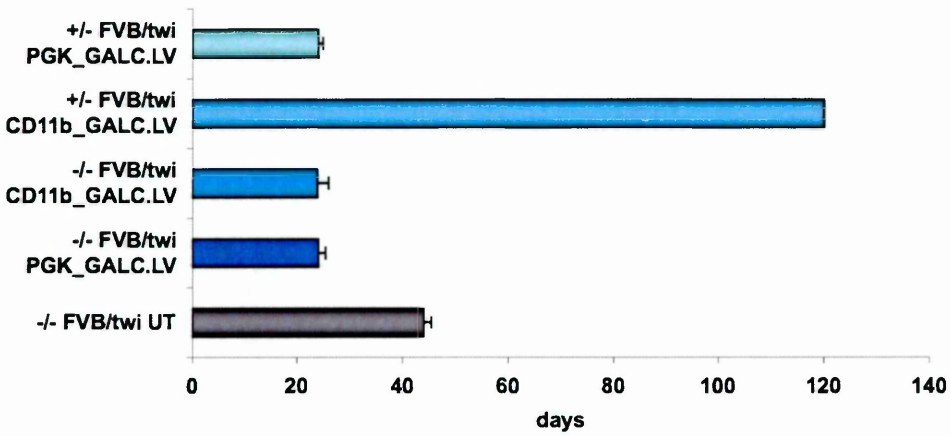

Figure 34. Survival of FVB/twi mice transplanted with CD11b_GALC.LV transduced mHSPC.

Mean survival of FVB/twi mice receiving mHSPC transplantation. +/- FVB/twi mice (n = 3) transplanted with CD11b_GALC.LV transduced mHSPC achieved long-term survival, differently from PGK_GALC.LV transplanted +/- FVB/twi mice (n = 3). Both -/- FVB/twi mice transplanted with CD11b_GALC.LV transduced mHSPC (n = 5) and mice transplanted with PGK_GALC.LV-transduced cells (n = 5) did not survive after lethal conditioning. UT = untreated controls (n = 6).

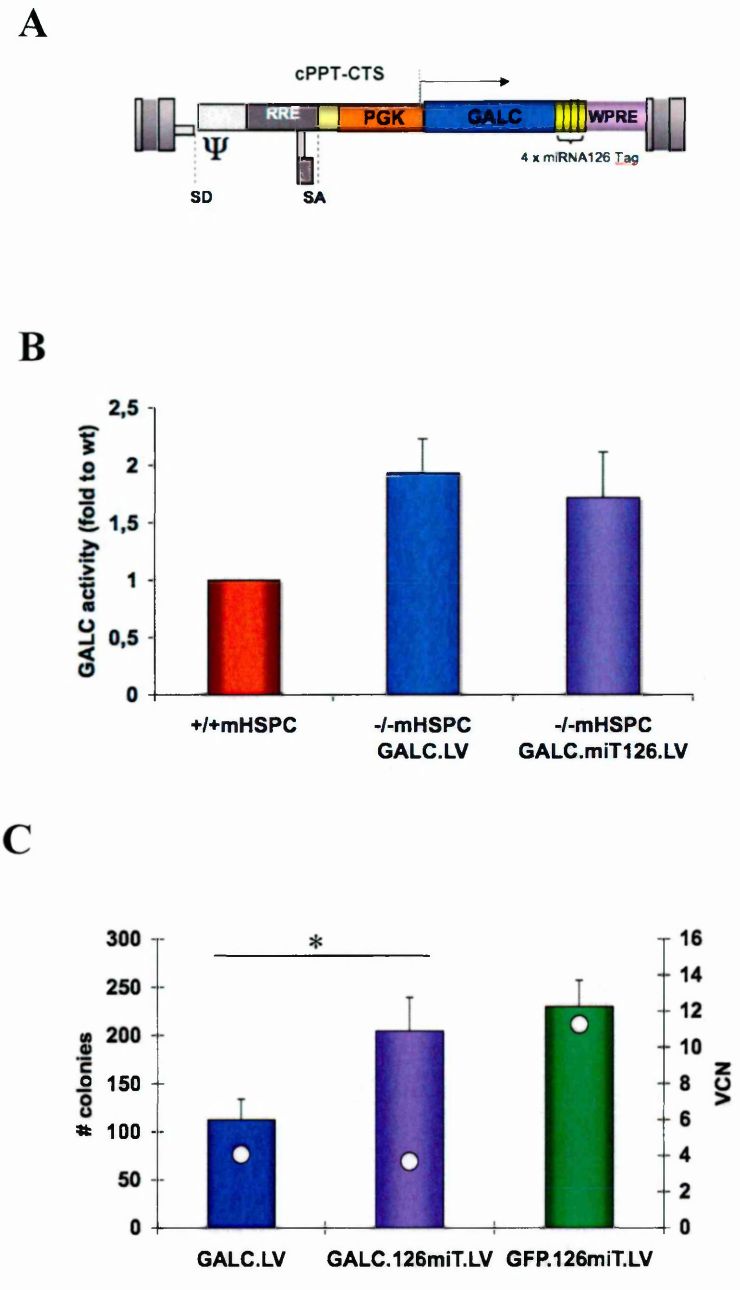

Figure 35. Regulation of GALC expression by miRNA 126.
(A) Schematic representation of GALC.miRNA126Tag.LV. (**B-C**) GALC activity assay and CFC assay performed on -/- mHSPC transduced with GALC.miRNA126Tag.LV (GALC.126miT) or with GALC.LV or GFP.miRNA126Tag.LV. (**B**) Activity was normalized respect to +/+ levels (first column). Cells transduced with GALC.miRNA126Tag.LV over-express GALC at supraphysiological levels. (**C**) The number (#) of colonies/plate (Y left axis, bars) was counted and the number of integrated lentiviral vector copies/cell (VCN)(Y right axis, dots) was measured. Repression of GALC expression by miRNA126 allowed growth of a higher colony number, as compared to GALC.LV transduced cells (n = 4 independent experiments). * $p<0.01$ at one-Way Anova test.

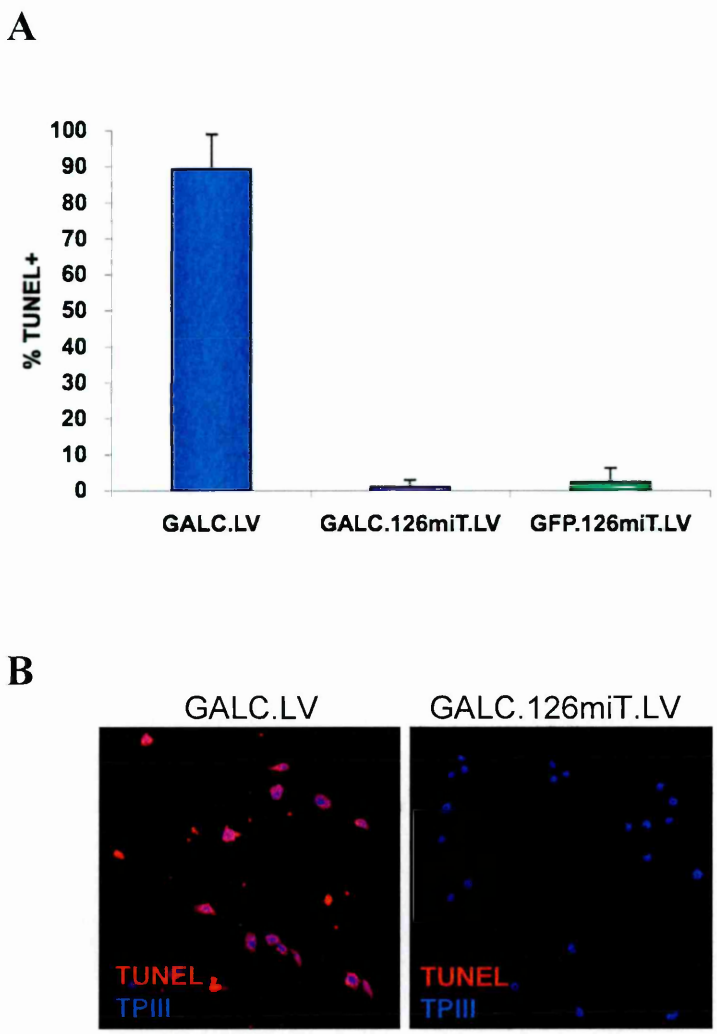

Figure 36. miRNA126 regulation of GALC expression prevents apoptosis of mHSPC.

(A) TUNEL assay on GALC.miRNA126Tag.LV or GALC.LV and GFP.miRNA126Tag.LV -transduced mHSPC. ≥ 8 fields and ≥ 100 cells were counted *per* condition. The large majority of GALC.miRNA126Tag.LV transduced cells was negative for TUNEL. **(B)** TUNEL assay (red) and ToPro3 (TPIII, blue) staining for nuclei on GALC.miRNA126Tag.LV or GALC.LV transduced mHSPC-/- 5 days after transduction: representative images (images were acquired by three-laser confocal microscope - Radiance 2100, BioRad; fluorescent signals from single optical sections were sequentially acquired and analyzed by Adobe Photoshop CS software; magnification 40x).

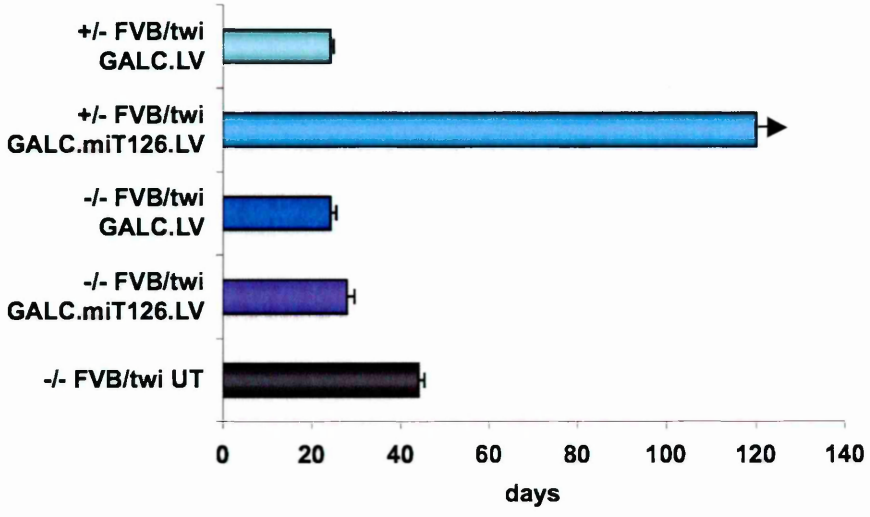

Figure 37. Survival of FVB/twi mice transplanted with GALC.miRNA126Tag.LV-transduced mHSPC.

Mean survival of FVB/twi mice receiving mHSPC transplantation. +/- FVB/twi mice (n = 3) transplanted with GALC.miRNA126Tag.LV transduced mHSPC achieved long-term survival, differently from GALC.LV transplanted +/- FVB/twi mice (n = 3). Both -/- FVB/twi mice transplanted with GALC.miRNA126Tag.LV transduced mHSPC (n = 8) and those transplanted with GALC. LV cells (n = 5) did not survive after lethal conditioning. UT = untreated controls (n = 6).

DISCUSSION

1. Toxicity of GALC de novo expression

Enzyme replacement and gene therapy applications in LSD patients [287] [288] and animal models [208] [107] [289] [290] have generally demonstrated the lack of toxicity of lysosomal enzyme administration and *de novo* expression above normal levels. In the case of Metachromatic Leukodystrophy (MLD), the safety of LV-mediated over-expression of ARSA, catalyzing the step upstream of GALC in sulfatide metabolism, was demonstrated in mHSPC, hHSPC, and transgenic mice [102] [269], prompting clinical testing of HSPC gene therapy for this disease. Here, we report the unexpected finding of overt toxicity and in vitro and in vivo functional impairment of murine and human HSPC after LV-mediated GALC gene transfer and expression. GALC.LV transduced murine HSPC showed impaired clonogenic potential and failed to engraft and long-term repopulate myeloablated transplant recipients. This was associated to negative selection *in vitro* and *in vivo* and apoptosis of highly transduced HSPC. The lack of apoptosis and functional impairment observed in murine and human HSPC, transduced with a control vector in which GALC expression is regulated by the microRNA 142 (exclusively expressed in hematopoietic lineage cells) [228], confirmed the unique role of *de novo* expressed GALC in determining the death of transduced cells.

Host influence in GALC-expressing HSPC engraftment failure

Despite the impaired clonogenic potential and apoptosis observed *in vitro* on GALC.LV transduced human HSPC, these cells displayed intact repopulation and differentiation potential when transplanted into sub-lethally irradiated Rag2γc mice. This result is in contrast with what was observed in twi and FVB/twi mice, suggesting a

fundamental role of the HSCT recipient in determining engraftment failure of GALC.LV transduced HSPC. Recent studies reported a niche defect in ko mice for the diphosphate-galactose: ceramide galactosyltransferase (CGT) gene. CGT is responsible for the production of GalCer from Cer and its deficit causes severe demyelination. In CGT ko mice, a defect in the hematopoietic niche trophism was observed, likely due to impaired sympathetic innervation. This seems to be responsible for an alteration of HSC mobilization from the niche [97]. A similar defect was observed in the thymus of twi mice: defective autonomic innervation resulted in atrophy of the thymus with consequent impaired lymphocytic maturation [291]. Specific studies of the hematopoietic bone marrow niche in twi mice are lacking. However, the engraftment failure of wild type lineage negative-selected HSPC, without the support of Sca1- progenitors, suggests the existence of a niche defect in twi mice. If so, this may represent an additional factor detrimentally affecting GALC *de novo* expressing murine HSPC engraftment in twi or FVB/twi mice.

GALC.LV transduced murine HSPC also failed to repopulate heterozygous twi and FVB/twi recipient mice, which should not be affected by the hypothesized niche defect. This indicates that while GALC *de novo* expression has a strong detrimental effect on murine HSPC, it does not appear to be sufficient, *per se,* to impair the repopulation and differentiation potential of human HSPC. This issue could be highly relevant for the clinical translation of HSCT-based gene therapy for GLD.

Protective effect of IGF1

The restored function of GALC.LV transduced HSPC upon treatment with the anti-apoptotic agent IGF1, confirmed that the GALC-induced functional impairment was due to apoptosis. IGF1 prevents cell death by activating the PI3K/Akt pathway, which is required

for the survival of a number of cell types [292] [293], including hematopoietic cells and oligodendrocytes [29] [294]. Interestingly, by acting on this pathway, IGF1 protects oligodendrocytes from psychosine-induced apoptosis [29]. Furthermore, ceramide, which can be synthesized from GalCer in the presence of functional GALC, exerts its pro-apoptotic activity, interacting with the same pathway but with an opposite effect, since it inhibits the phosphorylation and activation of Akt [295]. The protective effect of IGF1 on GALC transduced cells suggests that the PI3K/Akt pathway and possibly ceramide, may be involved in the apoptotic cell death of repopulating HSPC.

IGF1 treatment rescued mHSPC from GALC-induced functional impairment, both *in vitro* and *in vivo,* short-term after transplantation. However, the treatment was not sufficient to allow for long-term repopulation of the transplanted mice, by the transduced HSPC. This finding could either be due to the transient effect exerted by the brief *ex vivo* incubation of the transduced cells with IGF1 (only 40 minutes), or to the fact that this molecule may preferentially protect short-term repopulating committed progenitors from toxicity, but not long-term stem cells.

Interestingly, although IGF1 enabled an increase of the vector content in transduced HSPC progeny, no significant increase in GALC expression was detected in treated cells. This suggests the existence of a further regulation of GALC expression at the post-transcriptional or protein level, beyond the transcriptional control exerted by the atypical promoter and coding sequence [9] [10].

Role of bioactive sphingolipids in GALC toxicity

Recently, a novel role of Cer and other sphingolipids in regulating cell survival, senescence and apoptosis was demonstrated [21]. Hence, they have been defined as "bioactive lipids". Importantly, Cer can be considered a metabolic hub because it occupies a central position in sphingolipid biosynthesis and catabolism. Interestingly, our data suggests that GALC, as well as having a role in other relevant metabolic pathways leading to Cer

synthesis and metabolism [21], may also contribute to the regulation of the intracellular Cer levels in HSPC. In fact, lack of GALC activity in GLD HSPC is associated with a lower intracellular Cer level, compared to +/+ cells. Moreover, we observed a significant increase in the intracellular content of Cer in GALC.LV transduced *versus* GFP.LV transduced HSPC. Cer accumulation was accompanied by a significant increase in So and S1P intracellular levels. So appears to act in a similar fashion as Cer, while S1P appears to have the opposite effects to Cer in many of the pathways in which it is involved, particularly those relating to cell growth and survival. It has been suggested that the balance between survival and death of many cell types may be affected by the equilibrium between the intracellular levels of each of these inter-convertible sphingolipids. Enzymes that either produce or degrade sphingolipids, control this equilibrium. Thus, our findings suggest that an alteration of the intracellular content of Cer and other bioactive sphingolipids in HSPC following gene transfer and *de novo* GALC expression, may substantially affect this balance regulating cell survival. Indeed, the induced increase in So and Cer might exceed intracellular anti-apoptotic signals, like that of S1P, thus triggering apoptosis in both GLD and wild type, murine and human HSPC.

GALC substrates are present in HSPC

The first substrate of GALC is GalCer, which is produced in small quantities from catabolic pathways, i.e. from sulfo-GalCer by ARSA, or is synthesized by the inducible enzyme CGT. CGT is one of the key enzymes for the synthesis of galactocerebrosides (GCs), and is responsible for the galactosylation of Cer in the ER. While we previously measured basal ARSA activity in murine and human HSPC [208 269], no reports to date have demonstrated CGT activity in HSPC. However, using tandem mass spectrometry, we detected small quantities of both GalCer and GluCer in -/- HSPC in basal conditions, thus indicating the presence of GALC substrate in HSPC. We did not investigate whether

GalCer present in HSPC is derived from ARSA activity, or whether it is a product of *de novo* synthesis. More importantly, the function of this molecule in HSPC remains unclear.

PAR4 and Cathepsin D are not involved in GALC-induced apoptosis

The downstream molecular pathways activated by accumulated Cer and So, and the imbalance of Cer, So and S1P relative ratios, are not yet understood. Our data on IGF1 indicates that the PI3K/Akt pathway might be involved in GALC-induced apoptosis in a fraction of HSPC. However, other pathways, which are probably affected by the variation of Cer, So and S1P intracellular content, may be relevant for regulating HSPC survival. We were not able to demonstrate that either PAR4 (one of pathways known to participate in Cer-induced death of hematopoietic cells [279], or mature Cathepsin D (a specific target for lysosomally generated ceramide) [278] accumulate in transduced cells, thus making it unlikely that these pathways cause apoptosis of HSPC. Furthermore, the variation in intracellular content of Cathepsin D precursor in the presence of GALC, suggests that the *de novo* expressed enzyme plays a role in altering the homeostasis of molecules involved in apoptosis. Studies performed on caspase 9 ko mice confirmed that the activation of apoptotic pathways changes according to different stimuli and cell types [296]. Further studies are needed to analyze this phenomenon and the relative role of Cer and So accumulation in causing HSPC apoptosis.

Differentiated cells are less sensitive to GALC-related toxicity

We noticed that differentiated cells of the hematopoietic lineage (lymphocytes, monocytes, macrophages and microglia) and cells from other lineages (oligodendrocytes, as well as neural progenitors) (Gritti et al., personal communication), are not affected by LV-mediated GALC over-expression. Therefore, HSPC appear to have a unique sensitivity

to GALC- and sphingolipid-mediated control of cell survival, which is apparently lost during differentiation into mature myeloid, T and B cells, and which is restricted to the hematopoietic lineage. A possible explanation for this, might be the very low basal GALC activity detected in HSPC, compared to other cell types, such as microglia or oligodendrocytes. Moreover, the role of sphingolipid metabolism and the consequences of an alteration in the content of Cer and derived molecules such as So and S1P, might vary according to cell types and differentiation stages. For example, the effect of intracellular Cer accumulation in oligodendrocytes was studied in depth, with conflicting findings. A recent study reported that induction of acid sphingomyelinase, which is responsible for Cer production from sphingomyelin degradation, resulted in Cer accumulation and induction of apoptosis [297]. The same pathway seems to be involved in oligodendrocytic cell death induced by oxidative stress or by amyloid-beta peptide accumulation in Alzheimer's disease [298] [299]. However, mature oligodendrocytes were also described as being resistant to some pro-apoptotic stimuli, inducing Cer accumulation. Similarly, a differential response to pro-apoptotic TNF-α stimulation was observed in oligodendrocytic precursors, where a high level of apoptosis was observed and in mature oligodendrocytes, which appeared to be resistant to apoptotic stimulation [300]. Mature oligodendrocytes are also resistant to apoptosis induced by IL-1β administration [301]. This suggests that the increase of intracellular Cer could be managed in different ways, according to the pathways activated in that particular cell type and at that particular differentiation stage. Supporting this hypothesis, it has been reported that the increase of intracellular Cer in neural tissue, is managed by the high activity of acid ceramidase [302]. This enzyme catalyzes the degradation of Cer to So, which, in turn, is phosphorylated to S1P. S1P rescues cells from Cer-induced apoptosis [303] and induces proliferation in neural progenitor cells [304]. It could be hypothesized that a similar mechanism was responsible for the reduced sensitivity of oligodendrocytes to GALC over-expression-related apoptosis. The sphingolipid metabolic pathway is also very active in oligodendrocytes, which are involved in myelination in order

to produce the myelin glycosphingolipids (GalCer and Sulfatide). Moreover, these molecules participate in carbohydrate-carbohydrate interactions, forming glycosynapses (for a review see [305]).

The reduced sensitivity to GALC de novo expression-induced apoptosis observed in monocytes and macrophages might be explained both by the activity of ceramidase and their secretory action. Reports show that in endothelial cells and cells of the immune system, Cer is rapidly converted to So and S1P, which are secreted. In the plasma, these molecules bind albumin and act as signals for specific receptors on lymphocytes (for a review see [21 306 307].

Further studies will elucidate the actual mechanisms responsible for the peculiar sensitivity of HSPC to the toxic effect of GALC de novo expression.

2. Transcriptional and post-transcriptional regulation of GALC expression for safe and efficacious GLD gene therapy

CD11b-regulated GALC expression

The regulation of GALC expression by the myeloid promoter CD11b, has shown promising results *in vitro* and *in vivo*. Transduction of -/- HSPC with CD11b_GALC.LV allowed for the reconstitution of enzymatic activity at physiological levels without impairing the clonogenic potential of multipotent progenitors, as assessed by the CFC assay. Moreover, HSPC expressing GALC under the control of the CD11b promoter did not undergo apoptosis, despite the high VCN measured in this population. *In vivo* studies on heterozygous mice have shown that -/- HSPC expressing GALC under the CD11b promoter, could repopulate long-term, a lethally irradiated host. The absence of signs of bone marrow aplasia and pancytopenia ten weeks after bone marrow transplantation, suggests the absence of GALC-related toxicity in engrafted CD11b_GALC.LV transduced cells. The long-term presence of hematopoietic cells with high VCN in the BM after transplantation, confirms the rescue of HSC from GALC toxicity, indicating that CD11b_GALC.LV transduced HSC could repopulate the host and sustain hematopoiesis.

Although we think that the rescue of HSPC from GALC-related apoptosis by the CD11b promoter was due to the specificity of expression in myeloid cells and the reduced expression in HSPC, we cannot exclude the possibility that this result might be due to the reduced strength of CD11b, as compared to PGK promoter. Indeed, the differentiated progeny of HSPC transduced with CD11b_GALC.LV, displayed a GALC activity equal to 40% of that measured in PGK_GALC.LV transduced cells, approaching wild type levels.

We do not know if these *in vitro* measurements are predictive of GALC expression in microglia and macrophages differentiated from the engrafted cells *in vivo*. Moreover, it is difficult to know whether this enzymatic level would be adequate enough to allow cross correction of neighboring cells. The experience with the development of HSCT gene therapy for MLD, demonstrated that the therapeutic effect on the affected nervous system is directly proportional to the level of enzyme expression in HSPC and their progeny. In particular, we showed that over-expression of 4-5 fold with respect to wild type levels, is required to observe a therapeutic effect [208]. However, allogeneic HSCT in MLD patients gave poor results when compared to what was observed in GLD patients. This data might indicate that the high CNS inflammation in GLD could contribute towards enhancing the benefit of HSCT and possibly, HSC gene therapy. Neuroinflammation was reported to accelerate microglia reconstitution by cells of donor origin [107]. The neuroinflammatory environment that characterized the CNS of GLD patients and animal models, may enhance the reconstitution of brain microglia by donor-derived cells expressing GALC, thus increasing the amount of enzyme available for cross-correction. This phenomenon might result in a reduction of the enzymatic expression level *per* cell, that is required to observe a clinical benefit in transplanted subjects.

miRNA126-regulated GALC expression

The regulation of transgene expression is of great interest in the field of gene therapy. In particular, the possibility of post-transcriptional regulation by micro RNA (miRNA), has recently open new perspectives for tuning the expression level of the transgene, according to cell type and to differentiation [285]. In this study, we applied this innovative technology in order to suppress GALC expression in HSPC, which have been shown to be the most sensitive cells to GALC over-expression toxicity, while allowing enzyme over-expression in differentiated cells, which are responsible for GALC secretion and cross-correction of oligodendrocytes. In particular, we selected the microRNA126, which was reported to be

more highly expressed in HSPC, as compared to peripheral blood mononuclear cells [308]. Our data demonstrated that the regulation of GALC expression by the HSC-specific miRNA126, protects HSPC from GALC de novo-induced apoptosis in vitro and *in vivo*. Transduction of GALC -/- HSPC with GALC.miR126T.LV permitted the reconstitution of enzymatic activity in their differentiated progeny at supra-physiological levels, without impairing the clonogenic potential of the multipotent progenitors, as assessed by the CFC assay. This data confirmed that miRNA126 suppresses GALC expression only in HSPC and not in their differentiated progeny. The unaffected clonogenic potential may indicate that GALC expression is repressed not only in HSC, but also in multipotent progenitors responsible for the formation of the hematopoietic colonies in CFC assay.

Moreover, transplantation of GALC.miR126T.LV-transduced HSPC into GALC +/- FVB/twi mice, resulted in long-term survival of treated animals. This data demonstrates that the suppression of GALC activity in the more primitive HSC by miRNA126, allows their long-term repopulation and differentiation potential, to be preserved. The presence of highly transduced cells in the BM ten weeks after HSCT, further confirmed that long-term HSC were rescued from GALC over-expression apoptosis.

Importantly, the post-transcriptional regulation by HSC-specific miRNA, permitted the use of a strong promoter, such as PGK, thereby reaching the same expression level of the transgene in the differentiated HSPC progeny, as that obtained with unregulated PGK_GALC.LV. As discussed above, the level of GALC expression required for HSC gene therapy to be effective, is not known. However, even if a low enzyme expression level might be sufficient to obtain a clinical benefit, the use of a stronger promoter may allow the vector copy number(s) to be reduced, but reach the desired enzymatic expression. This issue could be relevant for the safety of clinical translation of HSC gene therapy.

Engraftment failure in GALC -/- FVB/twi mice

Although the regulation of GALC expression, either by the myeloid-specific CD11b promoter or by HSC-specific miRNA, allowed for HSC rescue from the toxic effect of GALC *de novo* expression *in vitro* and *in vivo* in heterozygous mice, both CD11b_GALC.LV and GALC.miR126T.LV transduced HSPC failed to repopulate lethally irradiated GALC -/- FVB/twi mice. All -/- FVB/twi transplanted mice died due to engraftment failure, shortly after conditioning. This poor result might be explained by the existence of a niche defect in -/-FVB/twi mice (see above). Since both CD11b_GALC.LV and GALC.miR126T.LV transduced HSPC successfully repopulated heterozygous mice long-term, the impaired repopulation observed in homozygous mice could not be exclusively cell-autonomous. Instead, is more likely that additional factors related to the BM niche affect the engraftment of CD11b_GALC.LV and GALC.miR126T.LV transduced HSPC into -/- recipients. Moreover, the good engraftment of GFP.LV-transduced wild type HSPC observed in the majority of homozygous FVB/twi recipients and the prolonged survival of these treated animals, demonstrate that if a niche defect or any other non-permissive factor was present, it may be not sufficient *per se,* to totally hamper the engraftment of HSPC with a full repopulation potential. Further experiments are needed to elucidate this hypothesis.

CONCLUDING REMARKS

Our findings demonstrate that *de novo* GALC expression affects HSPC survival by altering the delicate intracellular bioactive sphingolipid balance, showing a possible novel regulatory role for this enzyme. Moreover, the observation of a unique sensitivity of HSPC to GALC *de novo* expression toxicity, suggests that there is a need for tight regulation of GALC expression in HSPC, to permit further advances in GLD gene therapy. To this purpose, we developed two approaches to regulate GALC expression, either by myeloid specific promoters, or by exploiting post-transcriptional microRNA regulation. Despite the

poor engraftment of transduced HSPC in twi mice, we here provided the first evidence of successful application of HSPC-specific microRNA in HSC gene therapy for GLD. However, new strategies aimed at supporting the engraftment of transduced HSPC in a non-permissive host are needed.

ACKNOWLEDGEMENTS

I would like to thank Prof. Luigi Naldini and Alessandra Biffi, who supervised this project from A to Z.

Prof. Adrian Thrasher, who supervised this work and improved it with very helpful discussions and suggestions.

Dr. Sabata Martino and Dr. A. Merrill for their precious collaboration.

All the people in Biffi's lab for their brilliant suggestions, discussions and friendship; Silvia, because she shared with me the bad and the good time in these years.

BIBLIOGRAPHY

1. Meikle, P.J., Hopwood, J.J., Clague, A.E. & Carey, W.F. Prevalence of lysosomal storage disorders. *Jama* **281**, 249-254 (1999).

2. Collier, J. Prevention of Weak Legs in Experimental Chickens. *Science* **60**, 42 (1924).

3. Hagberg, B., Kollberg, H., Sourander, P. & Akesson, H.O. Infantile globoid cell leucodystrophy (Krabbe's disease). A clinical and genetic study of 32 Swedish cases 1953--1967. *Neuropadiatrie* **1**, 74-88 (1969).

4. Wenger, D.A., Rafi, M.A. & Luzi, P. Molecular genetics of Krabbe disease (globoid cell leukodystrophy): diagnostic and clinical implications. *Hum Mutat* **10**, 268-279 (1997).

5. Loonen, M.C., Van Diggelen, O.P., Janse, H.C., Kleijer, W.J. & Arts, W.F. Late-onset globoid cell leucodystrophy (Krabbe's disease). Clinical and genetic delineation of two forms and their relation to the early-infantile form. *Neuropediatrics* **16**, 137-142 (1985).

6. Kolodny, E.H., Raghavan, S. & Krivit, W. Late-onset Krabbe disease (globoid cell leukodystrophy): clinical and biochemical features of 15 cases. *Dev Neurosci* **13**, 232-239 (1991).

7. Jardim, L.B. et al. Protracted course of Krabbe disease in an adult patient bearing a novel mutation. *Arch Neurol* **56**, 1014-1017 (1999).

8. Luzi, P., Rafi, M.A. & Wenger, D. Structure and Organization of the Human Galactocerebrosidase (GALC) Gene. *Genomics* **26**, 407-409 (1995).

9. Sakai, N. et al. Human galactocerebrosidase gene: promoter analysis of the 5'-flanking region and structural organization. *Biochim Biophys Acta.* **1395**, 62-67 (1998).

10. Luzi, P., Rafi, M.A., Victoria, T., Baskin, G.B. & Wenger, D.A. Characterization of the rhesus monkey galactocerebrosidase (GALC) cDNA and gene and identification

of the mutation causing globoid cell leukodystrophy (Krabbe disease) in this primate. *Genomics* **42**, 319-324 (1997).

11. Nagano, S. et al. Expression and processing of recombinant human galactosylceramidase. *Clin Chim Acta* **276**, 53-61 (1998).

12. Harzer, K. et al. Saposins (sap) A and C activate the degradation of galactosylceramide in living cells. *FEBS Lett* **417**, 270-274 (1997).

13. Wenger, D.A., Rafi, M.A., Luzi, P., Datto, J. & Costantino-Ceccarini, E. Krabbe disease: genetic aspects and progress toward therapy. *Mol. Genet. Metab.* **70**, 1-9 (2000).

14. Norton, W.T. Some thoughts on the neurobiology of the leukodystrophies. *Neuropediatrics* **15 Suppl**, 28-31 (1984).

15. Dyer, C.A. & Benjamins, J.A. Organization of oligodendroglial membrane sheets. I: Association of myelin basic protein and 2',3'-cyclic nucleotide 3'-phosphohydrolase with cytoskeleton. *J Neurosci Res* **24**, 201-211 (1989).

16. Marcus, J. & Popko, B. Galactolipids are molecular determinants of myelin development and axo-glial organization. *Biochim Biophys Acta* **1573**, 406-413 (2002).

17. Jung, E.M., Griner, R.D., Mann-Blakeney, R. & Bollag, W.B. A potential role for ceramide in the regulation of mouse epidermal keratinocyte proliferation and differentiation. *J Invest Dermatol* **110**, 318-323 (1998).

18. Uchida, N. et al. HIV, but not murine leukemia virus, vectors mediate high efficiency gene transfer into freshly isolated G0/G1 human hematopoietic stem cells. *Proc Natl Acad Sci U S A* **95**, 11939-11944 (1998).

19. Sawada, M. et al. Molecular mechanisms of TNF-alpha-induced ceramide formation in human glioma cells: P53-mediated oxidant stress-dependent and -independent pathways. *Cell Death Differ* **11**, 997-1008 (2004).

20. Tepper, A.D., de Vries, E., van Blitterswijk, W.J. & Borst, J. Ordering of ceramide formation, caspase activation, and mitochondrial changes during CD95- and DNA damage-induced apoptosis. *J Clin Invest* **103**, 971-978 (1999).

21. Hannun, Y.A. & Obeid, L.M. Principles of bioactive lipid signalling: lessons from sphingolipids. *Nat Rev Mol Cell Biol* **9**, 139-150 (2008).

22. Spiegel, S. & Milstien, S. Exogenous and intracellularly generated sphingosine 1-phosphate can regulate cellular processes by divergent pathways. *Biochem Soc Trans* **31**, 1216-1219 (2003).

23. Austin, J. et al. Studies in globoid (Krabbe) leukodystrophy (GLD). V. Controlled enzymic studies in ten human cases. *Arch Neurol* **23**, 502-512 (1970).

24. Suzuki, K. Ultrastructural study of experimental globoid cells. *J Neuropathol Exp Neurol* **30**, 145-146 (1971).

25. Miyatake, T. & Suzuki, K. Globoid cell leukodystrophy: additional deficiency of psychosine galactosidase. *Biochem Biophys Res Commun* **48**, 539-543 (1972).

26. Suzuki, K. Twenty five years of the "psychosine hypothesis": a personal perspective of its history and present status. *Neurochem. Res.* **23**, 251-259 (1998).

27. Kobayashi, T., Shinnoh, N., Goto, I. & Kuroiwa, Y. Hydrolysis of galactosylceramide is catalyzed by two genetically distinct acid beta-galactosidases. *J Biol Chem* **260**, 14982-14987 (1985).

28. Tapasi, S., Padma, P. & Setty, O.H. Effect of psychosine on mitochondrial function. *Indian J Biochem Biophys* **35**, 161-165 (1998).

29. Zaka, M., Rafi, M.A., Rao, H.Z., Luzi, P. & Wenger, D. Insulin-like growth factor-1 provides protection against psycosine-onduced apoptosis in cultured mouse oligodendrocyte progenitor cells using primarily the P13K/Akt pathway. *Molecular and Cellular Neuroscience* **30**, 398-407 (2005).

30. Giri, S., Khan, M., Rattan, R., Singh, I. & Singh, A.K. Krabbe disease: psychosine-mediated activation of phospholipase A2 in oligodendrocyte cell death. *J Lipid Res* **47**, 1478-1492 (2006).

31. Giri, S., Khan, M., Nath, N., Singh, I. & Singh, A.K. The role of AMPK in psychosine mediated effects on oligodendrocytes and astrocytes: implication for Krabbe disease. *J Neurochem* **105**, 1820-1833 (2008).

32. Haq, E., Contreras, M.A., Giri, S., Singh, I. & Singh, A.K. Dysfunction of peroxisomes in twitcher mice brain: a possible mechanism of psychosine-induced disease. *Biochem Biophys Res Commun* **343**, 229-238 (2006).

33. Martin, J.J. et al. Fetal Krabbe leukodystrophy. A morphologic study of two cases. *Acta Neuropathol* **53**, 87-91 (1981).

34. Itoh, M. et al. Immunohistological study of globoid cell leukodystrophy. *Brain Dev* **24**, 284-290 (2002).

35. Im, D.S., Heise, C.E., Nguyen, T., O'Dowd, B.F. & Lynch, K.R. Identification of a molecular target of psychosine and its role in globoid cell formation. *J Cell Biol* **153**, 429-434 (2001).

36. Jesionek-Kupnicka, D. et al. Krabbe disease: an ultrastructural study of globoid cells and reactive astrocytes at the brain and optic nerves. *Folia Neuropathol* **35**, 155-162 (1997).

37. Formichi, P. et al. Psychosine-induced apoptosis and cytokine activation in immune peripheral cells of Krabbe patients. *J Cell Physiolo.* **212**, 737-743 (2007).

38. Matsushima, G.K. et al. Absence of MHC class II molecules reduces CNS demyelination, microglial/macrophage infiltration, and twitching in murine globoid cell leukodystrophy. *Cell* **78**, 645-656 (1994).

39. Formichi, P. et al. Human fibroblasts undergo oxidative stress-induced apoptosis without internucleosomal DNA fragmentation. *J Cell Physiol* **208**, 289-297 (2006).

40. Contreras, M.A., Haq, E., Uto, T., Singh, I. & Singh, A.K. Psychosine-induced alterations in peroxisomes of twitcher mouse liver. *Arch Biochem Biophys* **477**, 211-218 (2008).

41. Farley, T.J., Ketonen, L.M., Bodensteiner, J.B. & Wang, D.D. Serial MRI and CT findings in infantile Krabbe disease. *Pediatr Neurol* **8**, 455-458 (1992).

42. Loes, D.J., Peters, C. & Krivit, W. Globoid cell leukodystrophy: distinguishing early-onset from late-onset disease using a brain MR imaging scoring method. *AJNR Am J Neuroradiol* **20**, 316-323 (1999).

43. Percy, A.K., Odrezin, G.T., Knowles, P.D., Rouah, E. & Armstrong, D.D. Globoid cell leukodystrophy: comparison of neuropathology with magnetic resonance imaging. *Acta Neuropathol* **88**, 26-32 (1994).

44. Sabatelli, M. et al. Peripheral neuropathy with hypomyelinating features in adult-onset Krabbe's disease. *Neuromuscul Disord* **12**, 386-391 (2002).

45. Satoh, J.I. et al. Adult-onset Krabbe disease with homozygous T1853C mutation in the galactocerebrosidase gene. Unusual MRI findings of corticospinal tract demyelination. *Neurology* **49**, 1392-1399 (1997).

46. Husain, A.M., Altuwaijri, M. & Aldosari, M. Krabbe disease: neurophysiologic studies and MRI correlations. *Neurology* **63**, 617-620 (2004).

47. Callahan, J.W. & Skomorowski, M.A. Diagnosis of Krabbe disease by use of a natural substrate. *Methods Mol Biol* **347**, 321-330 (2006).

48. Farina, L. et al. MR imaging and proton MR spectroscopy in adult Krabbe disease. *AJNR Am J Neuroradiol* **21**, 1478-1482 (2000).

49. Suzuki, K. Globoid cell leukodystrophy (Krabbe's disease): update. *J Child Neurol* **18**, 595-603 (2003).

50. Kleijer, W.J. et al. Prevalent mutations in the GALC gene of patients with Krabbe disease of Dutch and other European origin. *J Inherit Metab Dis* **20**, 587-594 (1997).

51. Henderson, R.D., MacMillan, J.C. & Bradfield, J.M. Adult onset Krabbe disease may mimic motor neurone disease. *J Clin Neurosci* **10**, 638-639 (2003).

52. Meikle, P.J. et al. Diagnosis of lysosomal storage disorders: evaluation of lysosome-associated membrane protein LAMP-1 as a diagnostic marker. *Clin Chem* **43**, 1325-1335 (1997).

53. Chamoles, N.A., Blanco, M.B., Gaggioli, D. & Casentini, C. Hurler-like phenotype: enzymatic diagnosis in dried blood spots on filter paper. *Clin Chem* **47**, 2098-2102 (2001).

54. Chamoles, N.A., Blanco, M., Gaggioli, D. & Casentini, C. Tay-Sachs and Sandhoff diseases: enzymatic diagnosis in dried blood spots on filter paper: retrospective diagnoses in newborn-screening cards. *Clin Chim Acta* **318**, 133-137 (2002).

55. Umapathysivam, K., Hopwood, J.J. & Meikle, P.J. Determination of acid alpha-glucosidase activity in blood spots as a diagnostic test for Pompe disease. *Clin Chem* **47**, 1378-1383 (2001).

56. Meikle, P.J., Fuller, M. & Hopwood, J.J. Mass spectrometry in the study of lysosomal storage disorders. *Cell Mol Biol (Noisy-le-grand)* **49**, 769-777 (2003).

57. Li, Y. et al. Direct multiplex assay of lysosomal enzymes in dried blood spots for newborn screening. *Clin Chem* **50**, 1785-1796 (2004).

58. Bach, G., Zeigler, M. & Zlotogora, J. Prevention of lysosomal storage disorders in Israel. *Mol Genet Metab* **90**, 353-357 (2007).

59. Kurtz, H.J. & Fletcher, T.F. The peripheral neuropathy of canine globoid-cell leukodystrophy (krabbe-type). *Acta Neuropathol* **16**, 226-232 (1970).

60. Victoria, T., Rafi, M.A. & Wenger, D.A. Cloning of the canine GALC cDNA and identification of the mutation causing globoid cell leukodystrophy in West Highland White and Cairn terriers. *Genomics* **33**, 457-462 (1996).

61. Kobayashi, T., Yamanaka, T., Jacobs, J.M., Teixeira, F. & Suzuki, K. The Twitcher mouse: an enzymatically authentic model of human globoid cell leukodystrophy (Krabbe disease). *Brain Res* **202**, 479-483 (1980).

62. Luzi, P. et al. Generation of a mouse with low galactocerebrosidase activity by gene targeting: a new model of globoid cell leukodystrophy (Krabbe disease). *Mol. Genetics and Metab.* **73**, 211-223 (2001).

63. Pedchenko, T.V. & LeVine, S.M. IL-6 deficiency causes enhanced pathology in Twitcher (globoid cell leukodystrophy) mice. *Exp Neurol* **158**, 459-468 (1999).

64. Tominaga, K. et al. Genetic background markedly influences vulnerability of the hippocampal neuronal organization in the "twitcher" mouse model of globoid cell leukodystrophy. *J Neurosci Res* **77**, 507-516 (2004).

65. Biswas, S., Biesiada, H., Williams, T.D. & LeVine, S.M. Delayed clinical and pathological signs in Twitcher (Globoid cell leukodystrophy) mice on a C57BL/6 x CAST/Ei background. *Neurobiology of Disease* **10**, 344-357 (2002).

66. Baskin, G.B. et al. Genetic galactocerebrosidase deficiency (globoid cell leukodystrophy, Krabbe disease) in rhesus monkeys (Macaca mulatta). *Lab Anim Sci* **48**, 476-482 (1998).

67. Borda, J.T. et al. Clinical and immunopathologic alterations in rhesus macaques affected with globoid cell leukodystrophy. *Am J Pathol* **172**, 98-111 (2008).

68. Fratantoni, J.C., Hall, C.W. & Neufeld, E.F. Hurler and Hunter syndromes: mutual correction of the defect in cultured fibroblasts. *Science* **162**, 570-572 (1968).

69. Hasilik, A., Klein, U., Waheed, A., Strecker, G. & von Figura, K. Phosphorylated oligosaccharides in lysosomal enzymes: identification of alpha-N-acetylglucosamine(1)phospho(6)mannose diester groups. *Proc Natl Acad Sci U S A* **77**, 7074-7078 (1980).

70. Orchard, P.J. et al. Hematopoietic cell therapy for metabolic disease. *J Pediatr* **151**, 340-346 (2007).

71. Desnick, R.J. & Schuchman, E.H. Enzyme replacement and enhancement therapies: lessons from lysosomal disorders. *Nat Rev Genet* **3**, 954-966 (2002).

72. Grabowski, G.A., Leslie, N. & Wenstrup, R. Enzyme therapy for Gaucher disease: the first 5 years. *Blood Rev* **12**, 115-133 (1998).

73. Vellodi, A. et al. Management of neuronopathic Gaucher disease: a European consensus. *J Inherit Metab Dis* **24**, 319-327 (2001).

74. Butters, T.D. Gaucher disease. *Curr Opin Chem Biol* **11**, 412-418 (2007).

75. Burrow, T.A., Hopkin, R.J., Leslie, N.D., Tinkle, B.T. & Grabowski, G.A. Enzyme reconstitution/replacement therapy for lysosomal storage diseases. *Curr Opin Pediatr* **19**, 628-635 (2007).

76. Wenk, J., Hille, A. & von Figura, K. Quantitation of Mr 46000 and Mr 300000 mannose 6-phosphate receptors in human cells and tissues. *Biochem Int* **23**, 723-731 (1991).

77. Kakkis, E.D. et al. Enzyme-replacement therapy in mucopolysaccharidosis I. *N. Engl. J. Med.* **344**, 182-188 (2001).

78. Winkel, L.P. et al. Morphological changes in muscle tissue of patients with infantile Pompe's disease receiving enzyme replacement therapy. *Muscle Nerve* **27**, 743-751 (2003).

79. Enns, G.M. & Huhn, S.L. Central nervous system therapy for lysosomal storage disorders. *Neurosurg Focus* **24**, E12 (2008).

80. Vogler, C. et al. Overcoming the blood-brain barrier with high dose enzyme replacemnet therapy in murine mucopolysaccharidosis VII. *Proc Natl Acad Sci U S A*, 14777-17782 (2005).

81. Matzner, U. et al. Induction of tolerance to human arylsulfatase A in a mouse model of metachromatic leukodystrophy. *Mol Med* **13**, 471-479 (2007).

82. Lee, W.C. et al. Enzyme replacement therapy results in substantial improvements in early clinical phenotype in a mouse model of globoid cell leukodystrophy. *FASEB J* **19**, 1549-1551 (2005).

83. Boado, R.J., Zhang, Y., Zhang, Y. & Pardridge, W.M. Humanization of anti-human insulin receptor antibody for drug targeting across the human blood-brain barrier. *Biotechnol Bioeng* **96**, 381-391 (2007).

84. Brooks, D.A., Kakavanos, R. & Hopwood, J.J. Significance of immune response to enzyme-replacement therapy for patients with a lysosomal storage disorder. *Trends Mol Med* **9**, 450-453 (2003).

85. Brady, R.O. et al. Management of neutralizing antibody to Ceredase in a patient with type 3 Gaucher disease. *Pediatrics* **100**, E11 (1997).

86. Baum, C.M., Weissman, I.L., Tsukamoto, A.S., Buckle, A.M. & Peault, B. Isolation of a candidate human hematopoietic stem-cell population. *Proc Natl Acad Sci U S A* **89**, 2804-2808 (1992).

87. Strauss, L.C. et al. Antigenic analysis of hematopoiesis. IV. The My-11 hematopoietic cell surface antigen is expressed by myelomonocytic and lymphoid, but not erythroid, progenitor cells. *Exp Hematol* **14**, 935-945 (1986).

88. Morrison, S.J. & Weissman, I.L. The long-term repopulating subset of hematopoietic stem cells is deterministic and isolatable by phenotype. *Immunity* **1**, 661-673 (1994).

89. Meyerrose, T.E., Herrbrich, P., Hess, D.A. & Nolta, J.A. Immune-deficient mouse models for analysis of human stem cells. *Biotechniques* **35**, 1262-1272 (2003).

90. Larochelle, A. et al. Identification of primitive human hematopoietic cells capable of repopulating NOD/SCID mouse bone marrow: implications for gene therapy. *Nat Med* **2**, 1329-1337 (1996).

91. Sutherland, H.J., Lansdorp, P.M., Henkelman, D.H., Eaves, A.C. & Eaves, C.J. Functional characterization of individual human hematopoietic stem cells cultured

at limiting dilution on supportive marrow stromal layers. *Proc Natl Acad Sci U S A* **87**, 3584-3588 (1990).

92. Dick, J.E. Immune-deficient mice as models for human hematopoietic disease. *Mol Genet Med* **1**, 77-115 (1991).

93. Wilson, A. & Trumpp, A. Bone-marrow haematopoietic-stem-cell niches. *Nat Rev Immunol* **6**, 93-106 (2006).

94. Adams, G.B. & Scadden, D.T. A niche opportunity for stem cell therapeutics. *Gene Ther* **15**, 96-99 (2008).

95. Calvi, L.M. et al. Osteoblastic cells regulate the haematopoietic stem cell niche. *Nature* **425**, 841-846 (2003).

96. Whetton, A.D. & Graham, G.J. Homing and mobilization in the stem cell niche. *Trends Cell Biol* **9**, 233-238 (1999).

97. Katayama, Y. et al. Signals from the sympathetic nervous system regulate hematopoietic stem cell egress from bone marrow. *Cell* **124**, 407-421 (2006).

98. Peled, A. et al. The chemokine SDF-1 stimulates integrin-mediated arrest of CD34(+) cells on vascular endothelium under shear flow. *J Clin Invest* **104**, 1199-1211 (1999).

99. Kollet, O. et al. Rapid and efficient homing of human CD34(+)CD38(-/low)CXCR4(+) stem and progenitor cells to the bone marrow and spleen of NOD/SCID and NOD/SCID/B2m(null) mice. *Blood* **97**, 3283-3291 (2001).

100. Eglitis, M.A. & Mezey, E. Hematopoietic cells differentiate into both microglia and macroglia in the brains of adult mice. *Proc. Natl. Acad. Sci. USA* **94**, 4080-4085 (1997).

101. Hoogerbrugge, P.M. et al. Effect of bone marrow transplantation on enzyme levels and clinical course in the neurologically affected twitcher mouse. *J Clin Invest* **81**, 1790-1794 (1988).

102. Biffi, A. et al. Correction of Metachromatic Leukodystrophy in the Mouse Model by Transplantation of Genetically Modified Hematopoietic Stem Cells. *J. Clin. Invest.* **113**, 1118-1129 (2004).

103. Simard, A.R., Soulet, D., Gowing, G., Julien, J.P. & Rivest, S. Bone marrow-derived microglia play a critical role in restricting senile plaque formation in Alzheimer's disease. *Neuron* **49**, 489-502 (2006).

104. Malm, T.M. et al. Bone-marrow-derived cells contribute to the recruitment of microglial cells in response to beta-amyloid deposition in APP/PS1 double transgenic Alzheimer mice. *Neurobiol Dis* **18**, 134-142 (2005).

105. Ponomarev, E.D., Shriver, L.P., Maresz, K. & Dittel, B.N. Microglial cell activation and proliferation precedes the onset of CNS autoimmunity. *J Neurosci Res* **81**, 374-389 (2005).

106. Rodriguez, M. et al. Bone-marrow-derived cell differentiation into microglia: a study in a progressive mouse model of Parkinson's disease. *Neurobiol Dis* **28**, 316-325 (2007).

107. Sano, R., Tessitore, A., Ingrassia, A. & d'Azzo, A. Chemokine-induced recruitment of genetically modified bone marrow cells into the CNS of GM1-gangliosidosis mice corrects neuronal pathology. *Blood* **106**, 2259-2268 (2005).

108. Ajami, B., Bennett, J.L., Krieger, C., Tetzlaff, W. & Rossi, F.M. Local self-renewal can sustain CNS microglia maintenance and function throughout adult life. *Nat Neurosci* **10**, 1538-1543 (2007).

109. Li, Y., Liu, L., Barger, S.W. & Griffin, W.S. Interleukin-1 mediates pathological effects of microglia on tau phosphorylation and on synaptophysin synthesis in cortical neurons through a p38-MAPK pathway. *J Neurosci* **23**, 1605-1611 (2003).

110. Mildner, A. et al. Microglia in the adult brain arise from Ly-6ChiCCR2+ monocytes only under defined host conditions. *Nat Neurosci* **10**, 1544-1553 (2007).

111. Yeager, A.M., Shinn, C., Shinohara, M. & Pardoll, D.M. Hematopoietic cell transplantation in the twitcher mouse. The effects of pretransplant conditioning with graded doses of busulfan. *Transplantation* **56**, 185-190 (1993).

112. Krivit, W., Sung, J.H., Shapiro, E.G. & Lockman, L.A. Microglia: the effector cell for reconstitution of the central nervous system following bone marrow transplantation for lysosomal and peroxisomal storage diseases. *Cell Transplant.* **4**, 385-392 (1995).

113. Boelens, J.J. et al. Outcomes of hematopoietic stem cell transplantation for Hurler's syndrome in Europe: a risk factor analysis for graft failure. *Bone Marrow Transplant* **40**, 225-233 (2007).

114. Kogler, G. et al. A new human somatic stem cell from placental cord blood with intrinsic pluripotent differentiation potential. *J Exp Med* **200**, 123-135 (2004).

115. Chen, H.K. et al. Combined cord blood stem cells and gene therapy enhances angiogenesis and improves cardiac performance in mouse after acute myocardial infarction. *Eur J Clin Invest* **35**, 677-686 (2005).

116. Hansen, M.D. et al. Allogeneic hematopoietic cell transplantation (HCT) in Hurler's syndrome using a reduced intensity preparative regimen. *Bone Marrow Transplant* **41**, 349-353 (2008).

117. Staba, S.L. et al. Cord-Blood Transplants from Unrelated Donors in Patients with Hurler's Syndrome. *N Engl J Med.* **350**, 1960-1969 (2004).

118. Krivit, W. Stem cell bone marrow transplantation in patients with metabolic storage diseases. *Adv Pediatr* **49**, 359-378 (2002).

119. Aubourg, P. et al. The red-green visual pigment gene region in adrenoleukodystrophy. *Am J Hum Genet* **46**, 459-469 (1990).

120. Peters, C. et al. Cerebral X-linked adrenoleukodystrophy: the international hematopoietic cell transplantation experience from 1982 to 1999. *Blood* **104**, 881-888 (2004).

121. Krivit, W. Allogeneic stem cell transplantation for the treatment of lysosomal and peroxisomal metabolic diseases. *Springer Semin Immunopathol* **26**, 119-132 (2004).

122. Tolar, J. et al. Combination of enzyme replacement and hematopoietic stem cell transplantation as therapy for Hurler syndrome. *Bone Marrow Transplant* **41**, 531-535 (2008).

123. Ichioka, T., Kishimoto, Y., Brennan, S., Santos, G.W. & Yeager, A.M. Hematopoietic cell transplantation in murine globoid cell leukodystrophy (the twitcher mouse): effects on levels of galactosylceramidase, psychosine, and galactocerebrosides. *Proc Natl Acad Sci U S A* **84**, 4259-4263 (1987).

124. Suzuki, K., Hoogerbrugge, P.M., Poorthuis, B.J., Bekkum, D.W. & Suzuki, K. The twitcher mouse. Central nervous system pathology after bone marrow transplantation. *Lab Invest* **58**, 302-309 (1988).

125. Kondo, A. et al. Pathology of the peripheral nerve in the twitcher mouse following bone marrow transplantation. *Brain Res* **460**, 178-183 (1988).

126. Yeager, A.M., Brennan, S., Tiffany, C., Moser, H.W. & Santos, G.W. Prolonged survival and remyelination after hematopoietic cell transplantation in the twitcher mouse. *Science* **225**, 1052-1054 (1984).

127. Escolar, M.L. et al. Transplantation of Umbilical-Cord Blood in Babies with Infantile Krabbe's Disease. *N. Engl. J. Med.* **352**, 2069-2081 (2005).

128. Krivit, W. et al. Hematopoietic stem-cell transplantation in globoid-cell leukodystrophy. *N Engl J Med* **338**, 1119-1126 (1998).

129. Lim, Z.Y. et al. Sustained neurological improvement following reduced-intensity conditioning allogeneic haematopoietic stem cell transplantation for late-onset Krabbe disease. *Bone Marrow Transplant* **41**, 831-832 (2008).

130. Pastores, G.M. & Barnett, N.L. Substrate reduction therapy: miglustat as a remedy for symptomatic patients with Gaucher disease type 1. *Expert Opin Investig Drugs* **12**, 273-281 (2003).

131. Biswas, S., Biesiada, H., Williams, T.D. & LeVine, S.M. Substrate reduction intervention by L-cycloserine in twitcher mice (globoid cell leukodystrophy) on a B6;CAST/Ei background. *Neurosci Lett* **347**, 33-36 (2003).

132. LeVine, S.M., Pedchenko, T.V., Bronshteyn, I.G. & Pinson, D.M. L-cycloserine slows the clinical and pathological course in mice with globoid cell leukodystrophy (twitcher mice). *J Neurosci Res* **60**, 231-236 (2000).

133. Ozkara, H.A. Recent advances in the biochemistry and genetics of sphingolipidoses. *Brain Dev* **26**, 497-505 (2004).

134. Platt, F.M., Neises, G.R., Karlsson, G.B., Dwek, R.A. & Butters, T.D. N-butyldeoxygalactonojirimycin inhibits glycolipid biosynthesis but does not affect N-linked oligosaccharide processing. *J Biol Chem* **269**, 27108-27114 (1994).

135. Jeyakumar, M. et al. Delayed symptom onset and increased life expectancy in Sandhoff disease mice treated with N-butyldeoxynojirimycin. *Proc Natl Acad Sci U S A* **96**, 6388-6393 (1999).

136. Ezoe, T. et al. Biochemistry and neuropathology of mice doubly deficient in synthesis and degradation of galactosylceramide. *J Neurosci Res* **59**, 170-178 (2000).

137. Aerts, J.M., Hollak, C.E., Boot, R.G., Groener, J.E. & Maas, M. Substrate reduction therapy of glycosphingolipid storage disorders. *J Inherit Metab Dis* **29**, 449-456 (2006).

138. Kay, M.A., Glorioso, J.C. & Naldini, L. Viral vectors for gene therapy: the art of turning infectious agents into vehicles of therapeutics. *Nat Med* **7**, 33-40 (2001).

139. Hayes, M.E. et al. Genospheres: self-assembling nucleic acid-lipid nanoparticles suitable for targeted gene delivery. *Gene Ther* **13**, 646-651 (2006).

140. Fuller, D.H. et al. DNA immunization in combination with effective antiretroviral drug therapy controls viral rebound and prevents simian AIDS after treatment is discontinued. *Virology* **348**, 200-215 (2006).

141. Blomberg, P., Eskandarpour, M., Xia, S., Sylven, C. & Islam, K.B. Electroporation in combination with a plasmid vector containing SV40 enhancer elements results in increased and persistent gene expression in mouse muscle. *Biochem Biophys Res Commun* **298**, 505-510 (2002).

142. Lechardeur, D. & Lukacs, G.L. Intracellular barriers to non-viral gene transfer. *Curr Gene Ther* **2**, 183-194 (2002).

143. Hackett, P.B., Ekker, S.C., Largaespada, D.A. & McIvor, R.S. Sleeping beauty transposon-mediated gene therapy for prolonged expression. *Adv Genet* **54**, 189-232 (2005).

144. Wakabayashi, T. et al. A phase I clinical trial of interferon-beta gene therapy for high-grade glioma: novel findings from gene expression profiling and autopsy. *J Gene Med* **10**, 329-339 (2008).

145. Boorjian, S.A. et al. Phase 1/2 clinical trial of interferon alpha2b and weekly liposome-encapsulated all-trans retinoic acid in patients with advanced renal cell carcinoma. *J Immunother* **30**, 655-662 (2007).

146. Verma, I.M. & Weitzman, M.D. Gene therapy: twenty-first century medicine. *Annu Rev Biochem* **74**, 711-738 (2005).

147. Tomanin, R. & Scarpa, M. Why do we need new gene therapy viral vectors? Characteristics, limitations and future perspectives of viral vector transduction. *Curr Gene Ther* **4**, 357-372 (2004).

148. Sandrin, V. et al. Lentiviral vectors pseudotyped with a modified RD114 envelope glycoprotein show increased stability in sera and augmented transduction of primary lymphocytes and CD34+ cells derived from human and nonhuman primates. *Blood* **100**, 823-832 (2002).

149. Kelly, P.F., Vandergriff, J., Nathwani, A., Nienhuis, A.W. & Vanin, E.F. Highly efficient gene transfer into cord blood nonobese diabetic/severe combined immunodeficiency repopulating cells by oncoretroviral vector particles pseudotyped

with the feline endogenous retrovirus (RD114) envelope protein. *Blood* **96**, 1206-1214 (2000).

150. Ailles, L. et al. Molecular evidence of lentiviral vector-mediated gene transfer into human self-renewing, multi-potent, long-term NOD/SCID repopulating hematopoietic cell. *Mol Ther.* **6**, 615-626 (2002).

151. Movassagh, M. et al. High-level gene transfer to cord blood progenitors using gibbon ape leukemia virus pseudotype retroviral vectors and an improved clinically applicable protocol. *Hum Gene Ther* **9**, 225-234 (1998).

152. Dick, J.E., Magli, M.C., Huszar, D., Phillips, R.A. & Bernstein, A. Introduction of a selectable gene into primitive stem cells capable of long-term reconstitution of the hemopoietic system of W/Wv mice. *Cell* **42**, 71-79 (1985).

153. Keller, G., Paige, C., Gilboa, E. & Wagner, E.F. Expression of a foreign gene in myeloid and lymphoid cells derived from multipotent haematopoietic precursors. *Nature* **318**, 149-154 (1985).

154. Ott, M.G. et al. Correction of X-linked chronic granulomatous disease by gene therapy, augmented by insertional activation of MDS1-EVI1, PRDM16 or SETBP1. *Nat Med* **12**, 401-409 (2006).

155. Schwarzwaelder, K. et al. Gammaretrovirus-mediated correction of SCID-X1 is associated with skewed vector integration site distribution in vivo. *J Clin Invest* **117**, 2241-2249 (2007).

156. Aiuti, A. et al. Multilineage hematopoietic reconstitution without clonal selection in ADA-SCID patients treated with stem cell gene therapy. *J Clin Invest* **117**, 2233-2240 (2007).

157. Miller, D.G., Adam, M.A. & Miller, A.D. Gene transfer by retrovirus vectors occurs only in cells that are actively replicating at the time of infection. *Mol Cell Biol* **10**, 4239-4242 (1990).

158. Barquinero, J. et al. Efficient transduction of human hematopoietic repopulating cells generating stable engraftment of transgene-expressing cells in NOD/SCID mice. *Blood* **95**, 3085-3093 (2000).

159. Dao, M.A., Hashino, K., Kato, I. & Nolta, J.A. Adhesion to fibronectin maintains regenerative capacity during ex vivo culture and transduction of human hematopoietic stem and progenitor cells. *Blood* **92**, 4612-4621 (1998).

160. Glimm, H., Oh, I.H. & Eaves, C.J. Human hematopoietic stem cells stimulated to proliferate in vitro lose engraftment potential during their S/G(2)/M transit and do not reenter G(0). *Blood* **96**, 4185-4193 (2000).

161. Howe, S.J. et al. Insertional mutagenesis combined with acquired somatic mutations causes leukemogenesis following gene therapy of SCID-X1 patients. *J Clin Invest* **118**, 3143-3150 (2008).

162. Hacein-Bey-Abina, S. et al. A serious adverse event after successful gene therapy for X-linked severe combined immunodeficiency. *N Engl J Med* **348**, 255-256 (2003).

163. Hacein-Bey-Abina, S. et al. LMO2-associated clonal T cell proliferation in two patients after gene therapy for SCID-X1. *Science* **302**, 415-419 (2003).

164. Schweizer, M. et al. Markers of foamy virus infections in monkeys, apes, and accidentally infected humans: appropriate testing fails to confirm suspected foamy virus prevalence in humans. *AIDS Res Hum Retroviruses* **11**, 161-170 (1995).

165. Russell, D.W. & Miller, A.D. Foamy virus vectors. *J Virol* **70**, 217-222 (1996).

166. Trobridge, G., Vassilopoulos, G., Josephson, N. & Russell, D.W. Gene transfer with foamy virus vectors. *Methods Enzymol* **346**, 628-648 (2002).

167. Trobridge, G. & Russell, D.W. Cell cycle requirements for transduction by foamy virus vectors compared to those of oncovirus and lentivirus vectors. *J Virol* **78**, 2327-2335 (2004).

168. Anderson, J.L. & Hope, T.J. HIV accessory proteins and surviving the host cell. *Curr HIV/AIDS Rep* **1**, 47-53 (2004).

169. Peruzzi, F. The multiple functions of HIV-1 Tat: proliferation versus apoptosis. *Front Biosci* **11**, 708-717 (2006).

170. von Schwedler, U., Song, J., Aiken, C. & Trono, D. Vif is crucial for human immunodeficiency virus type 1 proviral DNA synthesis in infected cells. *J Virol* **67**, 4945-4955 (1993).

171. He, J. et al. Human immunodeficiency virus type 1 viral protein R (Vpr) arrests cells in the G2 phase of the cell cycle by inhibiting p34cdc2 activity. *J Virol* **69**, 6705-6711 (1995).

172. Mangasarian, A. et al. The HIV-1 Nef protein acts as a connector with sorting pathways in the Golgi and at the plasma membrane. *Immunity* **6**, 67-77 (1997).

173. Aiken, C. Pseudotyping human immunodeficiency virus type 1 (HIV-1) by the glycoprotein of vesicular stomatitis virus targets HIV-1 entry to an endocytic pathway and suppresses both the requirement for Nef and the sensitivity to cyclosporin A. *J Virol* **71**, 5871-5877 (1997).

174. Aiken, C. & Trono, D. Nef stimulates human immunodeficiency virus type 1 proviral DNA synthesis. *J Virol* **69**, 5048-5056 (1995).

175. Bour, S. & Strebel, K. The HIV-1 Vpu protein: a multifunctional enhancer of viral particle release. *Microbes Infect* **5**, 1029-1039 (2003).

176. Weinberg, J.B., Matthews, T.J., Cullen, B.R. & Malim, M.H. Productive human immunodeficiency virus type 1 (HIV-1) infection of nonproliferating human monocytes. *J Exp Med* **174**, 1477-1482 (1991).

177. Lewis, P.F. & Emerman, M. Passage through mitosis is required for oncoretroviruses but not for the human immunodeficiency virus. *J Virol* **68**, 510-516 (1994).

178. Fassati, A. & Goff, S.P. Characterization of intracellular reverse transcription complexes of human immunodeficiency virus type 1. *J Virol* **75**, 3626-3635 (2001).

179. Bukrinskaya, A., Brichacek, B., Mann, A. & Stevenson, M. Establishment of a functional human immunodeficiency virus type 1 (HIV-1) reverse transcription complex involves the cytoskeleton. *J Exp Med* **188**, 2113-2125 (1998).

180. Piller, S.C., Caly, L. & Jans, D.A. Nuclear import of the pre-integration complex (PIC): the Achilles heel of HIV? *Curr Drug Targets* **4**, 409-429 (2003).

181. Wu, X., Li, Y., Crise, B. & Burgess, S.M. Transcription start regions in the human genome are favored targets for MLV integration. *Science* **300**, 1749-1751 (2003).

182. Cattoglio, C. et al. Hot spots of retroviral integration in human CD34+ hematopoietic cells. *Blood* **110**, 1770-1778 (2007).

183. Deng, H. et al. Identification of a major co-receptor for primary isolates of HIV-1. *Nature* **381**, 661-666 (1996).

184. Marcello, A. et al. Nuclear organization and the control of HIV-1 transcription. *Gene* **326**, 1-11 (2004).

185. Naldini, L. et al. In vivo gene delivery and stable transduction of nondividing cells by a lentiviral vector. *Science* **272**, 263-267 (1996).

186. Dull, T. et al. A third-generation lentivirus vector with a conditional packaging system. *J Virol* **72**, 8463-8471 (1998).

187. Zufferey, R. et al. Self-inactivating lentivirus vector for safe and efficient in vivo gene delivery. *J VIrol* **72**, 9873-9880 (1998).

188. Cronin, J., Zhang, X.Y. & Reiser, J. Altering the tropism of lentiviral vectors through pseudotyping. *Curr Gene Ther* **5**, 387-398 (2005).

189. Kahl, C.A., Marsh, J., Fyffe, J., Sanders, D.A. & Cornetta, K. Human immunodeficiency virus type 1-derived lentivirus vectors pseudotyped with envelope glycoproteins derived from Ross River virus and Semliki Forest virus. *J Virol* **78**, 1421-1430 (2004).

190. Kobinger, G.P., Weiner, D.J., Yu, Q.C. & Wilson, J.M. Filovirus-pseudotyped lentiviral vector can efficiently and stably transduce airway epithelia in vivo. *Nat Biotechnol* **19**, 225-230 (2001).

191. Kappes, J.C. & Wu, X. Safety considerations in vector development. *Somat Cell Mol Genet* **26**, 147-158 (2001).

192. Kaul, M., Yu, H., Ron, Y. & Dougherty, J.P. Regulated lentiviral packaging cell line devoid of most viral cis-acting sequences. *Virology* **249**, 167-174 (1998).

193. Mautino, M.R., Ramsey, W.J., Reiser, J. & Morgan, R.A. Modified human immunodeficiency virus-based lentiviral vectors display decreased sensitivity to trans-dominant Rev. *Hum Gene Ther* **11**, 895-908 (2000).

194. Follenzi, A. & Naldini, L. HIV-based vectors. Preparation and use. *Methods Mol. Med.* **69**, 259-274 (2002).

195. Kim, V.N., Mitrophanous, K., Kingsman, S.M. & Kingsman, A.J. Minimal requirement for a lentivirus vector based on human immunodeficiency virus type 1. *J Virol* **72**, 811-816 (1998).

196. Delenda, C. Lentiviral vectors: optimization of packaging, transduction and gene expression. *J Gene Med* **6 Suppl 1**, S125-138 (2004).

197. Kraunus, J. et al. Self-inactivating retroviral vectors with improved RNA processing. *Gene Ther* **11**, 1568-1578 (2004).

198. Bodine, D.M., Karlsson, S., Papayannopoulou, T. & Nienhuis, A.W. Introduction and expression of human beta globin genes into primitive murine hematopoietic progenitor cells by retrovirus mediated gene transfer. *Prog Clin Biol Res* **319**, 589-599; discussion 600 (1989).

199. Piacibello, W. et al. Engraftment in nonobese diabetic severe combined immunodeficient mice of human CD34(+) cord blood cells after ex vivo expansion: evidence for the amplification and self-renewal of repopulating stem cells. *Blood* **93**, 3736-3749 (1999).

200. McGuckin, C.P., Forraz, N., Allouard, Q. & Pettengell, R. Umbilical cord blood stem cells can expand hematopoietic and neuroglial progenitors in vitro. *Exp Cell Res* **295**, 350-359 (2004).

201. Nolta, J.A., Smogorzewska, E.M. & Kohn, D.B. Analysis of optimal conditions for retroviral-mediated transduction of primitive human hematopoietic cells. *Blood* **86**, 101-110 (1995).

202. Hanenberg, H. et al. Colocalization of retrovirus and target cells on specific fibronectin fragments increases genetic transduction of mammalian cells. *Nat Med* **2**, 876-882 (1996).

203. Moritz, T. & Williams, D.A. Gene transfer into the hematopoietic system. *Curr Opin Hematol* **1**, 423-428 (1994).

204. Aiuti, A. et al. Correction of ADA-SCID by stem cell gene therapy combined with nonmyeloablative conditioning. *Science* **296**, 2410-2413 (2002).

205. Cavazzana-Calvo, M. et al. Gene therapy of human severe combined immunodeficiency (SCID)-X1 disease. *Science* **288**, 669-672 (2000).

206. Mazurier, F., Gan, O.I., McKenzie, J.L., Doedens, M. & Dick, J.E. Lentivector-mediated clonal tracking reveals intrinsic heterogeneity in the human hematopoietic stem cell compartment and culture-induced stem cell impairment. *Blood* **103**, 545-552 (2004).

207. Santoni de Sio, F.R., Cascio, P., Zingale, A., Gasparini, M. & Naldini, L. Proteasome activity restricts lentiviral gene transfer into hematopoietic stem cells and is down-regulated by cytokines that enhance transduction. *Blood* **107**, 4257-4265 (2006).

208. Biffi, A. et al. Gene therapy of metachromatic leukodystrophy reverses neurological damage and deficits in mice. *J. Clin. Invest.* **116**, 3070-3082 (2006).

209. May, C., Rivella, S., Chadburn, A. & Sadelain, M. Successful treatment of murine beta-thalassemia intermedia by transfer of the human beta-globin gene. *Blood* **99**, 1902-1908 (2002).

210. Pawliuk, R. et al. Correction of sickle cell disease in transgenic mouse models by gene therapy. *Science* **294**, 2368-2371 (2001).

211. Dupre, L. et al. Efficacy of gene therapy for Wiskott-Aldrich syndrome using a WAS promoter/cDNA-containing lentiviral vector and nonlethal irradiation. *Hum Gene Ther* **17**, 303-313 (2006).

212. Barese, C.N., Goebel, W.S. & Dinauer, M.C. Gene therapy for chronic granulomatous disease. *Expert Opin Biol Ther* **4**, 1423-1434 (2004).

213. Bank, A., Dorazio, R. & Leboulch, P. A phase I/II clinical trial of beta-globin gene therapy for beta-thalassemia. *Ann N Y Acad Sci* **1054**, 308-316 (2005).

214. Schroder, A.R. et al. HIV-1 integration in the human genome favors active genes and local hotspots. *Cell* **110**, 521-529 (2002).

215. Montini, E. et al. Hematopoietic stem cell gene transfer in a tumor-prone mouse model uncovers low genotoxicity of lentiviral vector integration. *Nat Biotechnol.* **24**, 687-696 (2006).

216. Sands, M.S. & Davidson, B.L. Gene therapy for lysosomal storage diseases. *Mol Ther* **13**, 839-849 (2006).

217. Reddy, P.S. et al. Sustained human factor VIII expression in hemophilia A mice following systemic delivery of a gutless adenoviral vector. *Mol Ther.* **5**, 63-73 (2002).

218. Daly, T.M. AAV-mediated gene transfer to the liver. *Methods Mol Biol* **246**, 195-199 (2004).

219. Hartung, S.D. et al. Correction of metabolic, craniofacial, and neurologic abnormalities in MPSI mice treated at birth with adeno-associated virus vector transducing the human alpha-L-iduronidase gene. *Mol Ther.* **9**, 866-875 (2004).

220. Sferra, T.J. et al. Widespread correction of lysosomal storage following intrahepatic injection of a recombinant adeno-associated virus in the adult MPS VII mouse. *Mol Ther.* **10**, 478-491 (2004).

221. McCormack, J.E. et al. Factors affecting long-term expression of a secreted transgene product after intravenous administration of a retroviral vector. *Mol Ther.* **3**, 516-525 (2001).

222. Parker Ponder, K. et al. Therapeutical neonatal hepatic gene therapy in mucopolisaccharidosis VII dogs. *Proc Natl Acad Sci U S A* **99**, 13102-13107 (2002).

223. Mango, R.L. et al. Neonatal retroviral vector-mediated hepatic gene therapy reduces bone, joint, and cartilage disease in mucopolysaccharidosis VII mice and dogs. *Mol Genet Metab* **82**, 4-19 (2004).

224. Nguyen, T.H. et al. Highly efficient lentiviral vector-mediated transduction of nondividing, fully reimplantable primary hepatocytes. *MOL Ther.* **6**, 199-209 (2002).

225. Cardone, M. et al. Correction of Hunter syndrome in the MPSII mouse model by AAV2/8-mediated gene delivery. *Hum Mol Genet* **15**, 1225-1236 (2006).

226. Di Domenico, C. et al. Gene therapy for a mucopolysaccharidosis type I murine model with lentiviral-IDUA vector. *HUm Gene Ther.* **16**, 81-90 (2005).

227. Follenzi, A. et al. Targeting lentiviral vector expression to hepatocytes limits transgene-specific immune response and establishes long-term expression of human antihemophilic factor IX in mice. *BLood* **103**, 3700-3709 (2004).

228. Brown, B.D., Venneri, M.A., Zingale, A., Sergi Sergi, L. & Naldini, L. Endogenous microRNA regulation suppresses transgene expression in hematopoietic lineages and enables stable gene transfer. *Nat Med* **12**, 585-591 (2006).

229. Naldini, L. et al. In vivo gene delivery and stable transduction of nondividing cells by a lentiviral vector. *Science* **272**, 263-267 (1996).

230. Zufferey, R., Nagy, D., Mandel, R.J., Naldini, L. & Trono, D. Multiply attenuated lentiviral vector achieves efficient gene delivery in vivo. *NAT Biotechnol* **15**, 871-875 (1997).

231. Blomer, U. et al. Highly efficient and sustained gene transfer in adult neurons with a lentivirus vector. *J Virol* **71**, 6641-6649 (1997).

232. Kordower, J.H. et al. Lentiviral gene transfer to the nonhuman primate brain. *Exp. Neurol.* **160**, 1-16 (1999).

233. Consiglio, A. et al. In vivo gene therapy of metachromatic leukodystrophy by lentiviral vectors: correction of neuropathology and protection against learning impairment in affected mice. *Nat Med* **7**, 310-316 (2001).

234. Desmaris, N. et al. Prevention of neuropathology in the mouse model of Hurler syndrome. *Ann Neurol* **56**, 68-76 (2004).

235. Ciron, C. et al. Gene therapy of the brain in the dog model of Hurler's syndrome. *Ann Neurol* **60**, 204-213 (2006).

236. Passini, M.A. et al. Intracranial delivery of CLN2 reduces brain pathology in a mouse model of classical late infantile neuronal ceroid lipofuscinosis. *J Neurosci* **26**, 1334-1342 (2006).

237. Cabrera-Salazar, M.A. et al. Timing of therapeutic intervention determines functional and survival outcomes in a mouse model of late infantile batten disease. *Mol Ther* **15**, 1782-1788 (2007).

238. Crystal, R.G. et al. Clinical protocol. Administration of a replication-deficient adeno-associated virus gene transfer vector expressing the human CLN2 cDNA to the brain of children with late infantile neuronal ceroid lipofuscinosis. *Hum Gene Ther* **15**, 1131-1154 (2004).

239. Worgall, S. et al. Treatment of late infantile neuronal ceroid lipofuscinosis by CNS administration of a serotype 2 adeno-associated virus expressing CLN2 cDNA. *Hum Gene Ther* **19**, 463-474 (2008).

240. Janson, C. et al. Clinical protocol. Gene therapy of Canavan disease: AAV-2 vector for neurosurgical delivery of aspartoacylase gene (ASPA) to the human brain. *Hum Gene Ther* **13**, 1391-1412 (2002).

241. Luca, T. et al. Axons mediate the distribution of arylsulfatase A within the mouse hippocampus upon gene delivery. *Mol Ther* **12**, 669-679 (2005).

242. Priller, J. et al. Targeting gene-modified hematopoietic cells to central nervous system; use of green fluorescent proteine uncovers microglial engraftment. *Nat. Med.* **7**, 1356-1361 (2001).

243. Ohmi, K. et al. Activated microglia in cortex of mouse models of mucopolysaccharidoses I and IIIB. *Proc. Natl. Acad. Sci. USA* **100**, 1902-1907 (2003).

244. Wada, R., Tifft, C.J. & Proia, R.L. Microglial activation precedes acute neurodegeneration in Sandhoff disease and is suppressed by bone marrow transplantation. *Proc. Natl. Acad. Sci. USA* **97**, 10954-10959 (2000).

245. Zheng, Y. et al. Treatment of the mouse model of mucopolysaccharidosis I with retrovirally tyransduced bone marrow. *Molecular Genetics and Metabolism* **79**, 233-244 (2003).

246. Taupin, P. & Gage, F.H. Adult neurogenesis and neural stem cells of the central nervous system in mammals. *J Neurosci Res* **69**, 745-749 (2002).

247. Roy, N.S. et al. In vitro neurogenesis by progenitor cells isolated from the adult human hippocampus. *Nat Med* **6**, 271-277 (2000).

248. Sanai, N. et al. Unique astrocyte ribbon in adult human brain contains neural stem cells but lacks chain migration. *Nature* **427**, 740-744 (2004).

249. Lacorazza, H.D., Flax, J.D., Snyder, E.Y. & Jendoubi, M. Expression of human beta-hexosaminidase alpha-subunit gene (the gene defect of Tay-Sachs disease) in mouse brains upon engraftment of transduced progenitor cells. *Nat Med* **2**, 424-429 (1996).

250. Buchet, D., Serguera, C., Zennou, V., Charneau, P. & Mallet, J. Long-term expression of beta-glucuronidase by genetically modified human neural progenitor cells grafted into the mouse central nervous system. *Mol Cell Neurosci* **19**, 389-401 (2002).

251. Meng, X.L. et al. Brain transplantation of genetically engineered human neural stem cells globally corrects brain lesions in the mucopolysaccharidosis type VII mouse. *J Neurosci Res* **74**, 266-277 (2003).

252. Gama Sosa, M.A. et al. Correction of the galactocerebrosidase deficiency in globoid cell leukodystrophy-cultured cells by SL3-3 retroviral-mediated gene transfer. *Biochem Biophys Res Commun* **218**, 766-771 (1996).

253. Luddi, A. et al. Retrovirus-mediated gene transfer and galactocerebrosidase uptake into twitcher glial cells results in appropriate localization and phenotype correction. *Neurobiol Dis* **8**, 600-610 (2001).

254. Rafi, M.A. et al. Retroviral vector-mediated transfer of the galactocerebrosidase (GALC) cDNA leads to overexpression and transfer of GALC activity to neighboring cells. *Biochem Mol Med* **58**, 142-150 (1996).

255. Shen, J.S., Watabe, K., Ohashi, T. & Eto, Y. Intraventricular administration of recombinant adenovirus to neonatal twitcher mouse leads to clinicopathological improvements. *Gene Ther* **8**, 1081-1087 (2001).

256. Rafi, M.A. et al. AAV-mediated expression of galactocerebrosidase in brain results in attenuated symptoms and extended life span in murine models of globoid cell leukodystrophy. *Mol Ther* **11**, 734-744 (2005).

257. Lin, D. et al. AAV2/5 vector expressing galactocerebrosidase ameliorates CNS disease in the murine model of globoid-cell leukodystrophy more efficiently than AAV2. *Mol Ther* **12**, 422-430 (2005).

258. Lin, D. et al. Central nervous system-directed AAV2/5-mediated gene therapy synergizes with bone marrow transplantation in the murine model of globoid-cell leukodystrophy. *Mol Ther* **15**, 44-52 (2007).

259. Pellegatta, S. et al. The therapeutic potential of neural stem/progenitor cells in murine globoid cell leukodystrophy is conditioned by macrophage/microglia activation. *Neurobiol Dis.* **21**, 314-323 (2006).

260. Pluchino, S. et al. Injection of adult neurospheres induces recovery in a chronic model of multiple sclerosis. *Nature* **422**, 688-694 (2003).

261. Pluchino, S., Furlan, R. & Martino, G. Cell-based remyelinating therapies in multiple sclerosis: evidence from experimental studies. *Curr Opin Neurol* **17**, 247-255 (2004).

262. Taylor, R.M. et al. Intrinsic resistance of neural stem cells to toxic metabolites may make them well suited for cell non-autonomous disorders: evidence from a mouse model of Krabbe leukodystrophy. *J Neurochem* **97**, 1585-1599 (2006).

263. Luzi, P. et al. Biochemical and pathological evaluation of long-lived mice with globoid cell leukodystrophy after bone marrow transplantation. *Mol Genetics and Metab* **86**, 150-159 (2005).

264. Follenzi, A., Ailles, L.E., Bakovic, S., Geuna, M. & Naldini, L. Gene transfer by lentiviral vectors is limited by nuclear translocation and rescued by HIV-1 pol sequences. *Nat Genet* **25**, 217-222 (2000).

265. Sakai, N. et al. Molecular cloning and expression of cDNA for murine galactocerebrosidase and mutation analysis of the twitcher mouse, a model of Krabbe's disease. *J Neurochem* **66**, 1118-1124 (1996).

266. Kumar, S., Mattan, N.S. & de Vellis, J. Canavan disease: a white matter disorder. *Ment Retard Dev Disabil Res Rev.* **12**, 157-165 (2006).

267. Armstrong, R.C. Isolation and characterization of immature oligodendrocyte lineage cells. *Methods* **16**, 282-292 (1998).

268. Gritti, A. et al. Multipotential stem cells from the adult mouse brain proliferate and self-renew in response to basic fibroblast growth factor. *J Neurosci* **16**, 1091-1100 (1996).

269. Capotondo, A. et al. Safety of Arylsulfatase A Overexpression for Gene Therapy of Metachromatic Leukodystrophy. *Hum Gene Ther* **[Epub ahead of print] PMID: 17845130** (2007).

270. Dolcetta, D. et al. Design and optimization of lentiviral vectors for transfer of GALC expression in Twitcher brain. *J Gene Med* **8**, 962-971 (2006).

271. Merrill, A.H., Jr., Sullards, M.C., Allegood, J.C., Kelly, S. & Wang, E. Sphingolipidomics: high-throughput, structure-specific, and quantitative analysis of sphingolipids by liquid chromatography tandem mass spectrometry. *Methods* **36**, 207-224 (2005).

272. Martino, S., Emiliani, C., Orlacchio, A., Hosseini, R. & Stirling, J.L. Beta-N-acetylhexosaminidases A and S have similar sub-cellular distributions in HL-60 cells. *Biochim Biophys Acta* **1243**, 489-495 (1995).

273. Wu, Y.P., Matsuda, J., Kubota, A., Suzuki, K. & Suzuki, K. Infiltration of hematogenous lineage cells into the demyelinating central nervous system of twitcher mice. *J Neuropathol Exp Neurol* **59**, 628-639 (2000).

274. Laviola, L., Natalicchio, A. & Giorgino, F. The IGF-I signaling pathway. *Curr Pharm Des.* **13**, 663-669 (2007).

275. Kurmasheva, R.T. & Houghton, P. IGF-I mediated survival pathways in normal and malignant cells. *Biochim Biophys Acta.* **1766**, 1-22 (2006).

276. Miyaji, M. et al. Role of membrane sphingomyelin and ceramide in platform formation for Fas-mediated apoptosis. *J Exp Med* **202**, 249-259 (2005).

277. Stoica, B.A., Movsesyan, V.A., Knoblach, S.M. & Faden, A.I. Ceramide induces neuronal apoptosis through mitogen-activated protein kinases and causes release of multiple mitochondrial proteins. *Mol Cell Neurosci* **29**, 355-371 (2005).

278. Heinrich, M. et al. Cathepsin D links TNF-induced acid sphingomyelinase to Bid-mediated caspase-9 and -3 activation. *Cell Death Differ* **11**, 550-563 (2004).

279. Bieberich, E., MacKinnon, S., Silva, J. & Yu, R.K. Regulation of apoptosis during neuronal differentiation by ceramide and b-series complex gangliosides. *J Biol Chem* **276**, 44396-44404 (2001).

280. Camandola, S. & Mattson, M.P. Pro-apoptotic action of PAR-4 involves inhibition of NF-kappaB activity and suppression of BCL-2 expression. *J Neurosci Res* **61**, 134-139 (2000).

281. Karram, K. et al. NG2-expressing cells in the nervous system revealed by the NG2-EYFP-knockin mouse. *Genesis* **46**, 743-757 (2008).

282. Heydemann, A. et al. A minimal c-fes cassette directs myeloid-specific expression in transgenic mice. *Blood* **96**, 3040-3048 (2000).

283. Marques, B. et al. Liposome-mediated cellular delivery of active gp91. *PLoS ONE* **2**, e856 (2007).

284. Yamada, Y. & Takakura, N. Physiological pathway of differentiation of hematopoietic stem cell population into mural cells. *J Exp Med* **203**, 1055-1065 (2006).

285. Gentner, B. et al. Stable knockdown of microRNA in vivo by lentiviral vectors. *Nat Methods* (2008).

286. Brown, B.D. et al. Endogenous microRNA can be broadly exploited to regulate transgene expression according to tissue, lineage and differentiation state. *Nat Biotechnol* **25**, 1457-1467 (2007).

287. Rohrbach, M. & Clarke, J.T. Treatment of lysosomal storage disorders : progress with enzyme replacement therapy. *Drugs* **67**, 2697-2716 (2007).

288. Brady, R.O. & Schiffmann, R. Enzyme-replacement therapy for metabolic storage disorders. *Lancet Neurol* **3**, 752-756 (2004).

289. Hofling, A.A., Devine, S., Vogler, C. & Sands, M.S. Human CD34+ hematopoietic progenitor cell-directed lentiviral-mediated gene therapy in a xenotransplantation model of lysosomal storage disease. *Mol Ther.* **9**, 856-865 (2004).

290. Sands, M.S. et al. Murine mucopolysaccharidosis type VII: long term therapeutic effects of enzyme replacement and enzyme replacement followed by bone marrow transplantation. *J Clin Invest* **99**, 1596-1605 (1997).

291. Galbiati, F. et al. Autonomic denervation of lymphoid organs leads to epigenetic immune atrophy in a mouse model of Krabbe disease. *J Neurosci.* **27**, 13730-13738 (2007).

292. Campana, W.M., Darin, S.J. & O'Brien, J.S. Phosphatidylinositol 3-kinase and Akt protein kinase mediate IGF-I- and prosaptide-induced survival in Schwann cells. . *J Neurosci Res* **57**, 332-341 (1999).

293. Lichtenwalner, R.J., Forbes, M.E., Sonntag, W.E. & Riddle, D.R. Adult-onset deficiency in growth hormone and insulin-like growth factor-I decreases survival of dentate granule neurons: insights into the regulation of adult hippocampal neurogenesis. . *J Neurosci Res* **83**, 199-210 (2006).

294. Shen, W.H. et al. Tumor necrosis factor alpha inhibits insulin-like growth factor I-induced hematopoietic cell survival and proliferation. . *Endocrinology* **145** (2004).

295. Fox, T.E. et al. Ceramide recruits and activates protein kinase C zeta (PKC zeta) within structured membrane microdomains. *J Biol Chem* **282**, 12450-12457 (2007).

296. Hakem, R. et al. Differential requirement for caspase 9 in apoptotic pathways in vivo. *Cell* **94**, 339-352 (1998).

297. Chudakova, D.A. et al. Integrin-associated Lyn kinase promotes cell survival by suppressing acid sphingomyelinase activity. *J Biol Chem* **283**, 28806-28816 (2008).

298. Jana, A. & Pahan, K. Oxidative stress kills human primary oligodendrocytes via neutral sphingomyelinase: implications for multiple sclerosis. *J Neuroimmune Pharmacol* **2**, 184-193 (2007).

299. Lee, J.T. et al. Amyloid-beta peptide induces oligodendrocyte death by activating the neutral sphingomyelinase-ceramide pathway. *J Cell Biol* **164**, 123-131 (2004).

300. Scurlock, B. & Dawson, G. Differential responses of oligodendrocytes to tumor necrosis factor and other pro-apoptotic agents: role of ceramide in apoptosis. *J Neurosci Res* **55**, 514-522 (1999).

301. Brogi, A., Strazza, M., Melli, M. & Costantino-Ceccarini, E. Induction of intracellular ceramide by interleukin-1 beta in oligodendrocytes. *J Cell Biochem* **66**, 532-541 (1997).

302. Huang, Y. et al. Elevation of the level and activity of acid ceramidase in Alzheimer's disease brain. *Eur J Neurosci* **20**, 3489-3497 (2004).

303. Betito, S. & Cuvillier, O. Regulation by sphingosine 1-phosphate of Bax and Bad activities during apoptosis in a MEK-dependent manner. *Biochem Biophys Res Commun* **340**, 1273-1277 (2006).

304. Harada, J., Foley, M., Moskowitz, M.A. & Waeber, C. Sphingosine-1-phosphate induces proliferation and morphological changes of neural progenitor cells. *J Neurochem* **88**, 1026-1039 (2004).

305. Boggs, J.M., Gao, W. & Hirahara, Y. Myelin glycosphingolipids, galactosylceramide and sulfatide, participate in carbohydrate-carbohydrate interactions between apposed membranes and may form glycosynapses between oligodendrocyte and/or myelin membranes. *Biochim Biophys Acta* **1780**, 445-455 (2008).

306. Mechtcheriakova, D. et al. Sphingosine 1-phosphate phosphatase 2 is induced during inflammatory responses. *Cell Signal* **19**, 748-760 (2007).

307. Rivera, J., Proia, R.L. & Olivera, A. The alliance of sphingosine-1-phosphate and its receptors in immunity. *Nat Rev Immunol* **8**, 753-763 (2008).

308. Jin, P. et al. Differentiation of two types of mobilized peripheral blood stem cells by microRNA and cDNA expression analysis. *J Transl Med* **6**, 39 (2008).

ABBREVIATIONS

AAV	ADENO-ASSOCIATED VECTORS
AD	ADULT
ADA-SCID	ADENOSINE DEAMINASE SEVERE COMBINED IMMUNODEFICIENCY
ADV	ADENOVIRAL VECTORS
ALD	ADRENOLEUKODYSTROPHY
ARSA	ARYLSULFATASE A
ASPA	ASPARTOACYLASE
BBB	BLOOD-BRAIN BARRIER
BM	BONE MARROW
CB	CORD BLOOD
CER	CERAMIDE
CFC	COLONY FORMING CELLS
CGD	CHRONIC GRANULOMATOUS DISEASE
CGT	CERAMIDE-GALACTOSYLTRANSFERASE
CHO	CHINESE HAMSTER OVARY
CNS	CENTRAL NERVOUS SYSTEM
CPPT	CENTRAL POLY-PURINE TRACT
CTS	CENTRAL TERMINATION SITE

CXCR4	CXC CHEMOKINE RECEPTOR 4
EBV	EPSTEIN-BARR VIRUS
EEG	ELECTROENCEPHALOGRAMS
EI	EARLY INFANTILE
ERT	ENZYME REPLACEMENT THERAPY
FN	FIBRONECTIN
FVV	HFV-DERIVED VECTORS
GAGS	GLYCOSAMINOGLYCANS
GALC	GALACTOCEREBROSIDASE
GALCER	GALACTOSYLCERAMIDE
GC	GLOBOID CELLS
GFAP	GLIAL FIBRILLARY ACIDIC PROTEIN
GLD	GLOBOID CELL LEUKODYSTROPHY
GUSB	β-GLUCURONIDASE
GvHD	GRAFT-VERSUS-HOST DISEASE
GvM	GRAFT-VERSUS-MARROW
HFV	HUMAN FOAMY VIRUS
HHSPC	HUMAN HEMATOPOIETIC STEM AND PROGENITOR CELLS
HIV-1	HUMAN IMMUNODEFICIENCY VIRUS 1
HSC	HEMATOPOIETIC STEM CELLS

HSCT	HEMATOPOIETIC STEM CELL TRANSPLANTATION
HSPC	HEMATOPOIETIC STEM AND PROGENITOR CELLS
HTERT	HUMAN TELOMERASE REVERSE TRANSCRIPTASE
IDS 2	IDURONATE 2 SULFATASE
IDUA	α-L-IDURONIDASE
IGF1	INSULINE-LIKE GROWTH FACTOR 1
J	JUVENILE
LACCER	LACTOSYLCERAMIDE
LAMP-1	LYSOSOMAL-ASSOCIATED MEMBRANE PROTEIN
LI	LATE INFANTILE
LIN-	LINEAGE NEGATIVE
LINCL	CEROID LIPOFUSCINOSIS
LSDS	LYSOSOMAL STORAGE DISORDERS
LTC-IC	LONG-TERM CULTURE-INITIATING CELLS
LT-HSC	LONG TERM HEMATOPOIETIC STEM CELLS
LTR	LONG TERMINAL REPEATS
LV	LENTIVIRAL VECTORS
M6P-R	MANNOSE-6-PHOSPHATE RECEPTOR
MAPK	AMP-ACTIVATED PROTEIN KINASE
MGD	MONOGALACTOSYLDIGLYCERIDE

mHSPC	Murine Hematopoietic stem and progenitor cells
MLD	Metachromatic leukodystrophy
MLV	Moloney murine leukemia virus
MoRV	MLV-derived vectors
MPP	Multipotent progenitors
MPS	Mucopolysaccharidosis
MRI	Magnetic resonance imaging
NPC	Niemann-Pick type C
NSC	Neural stem cells
PBMC	Peripheral blood mononuclear cells
PIC	Pre-integration complex
PNS	Peripheral nervous system
Psy	Psychosine
RFLP	Restriction fragment length polymorphism
RV	Retrovirus-based vectors
S1P	Sphingosine-1-Phosphate
SA	Splice acceptor
SapA	Saposine A
SD	Splice donor
SDF-1	Stromal cell Derived Factor 1

SIN	SELF-INACTIVATING
SM	SPHINGOMYELIN
So	SPHINGOSINE
SOR	OXYGEN-REACTIVE SPECIES
sPLA2	SECRETORY PHOSPHOLIPASE A2
SRC	SCID REPOPULATING CELLS
SRT	SUBSTRATE REDUCTION THERAPY
ST-HSC	SHORT TERM HEMATOPOIETIC STEM CELLS
TGN	TRANS GOLGI NETWORK
TPIII	TOPRO 3
TPP1	TRIPEPTIDYL PEPTIDASE 1
Twi	TWITCHER
VCN	VECTOR COPY NUMBER
VLA4	VERY LATE ANTIGEN 4
VSV-G	VESICULAR STOMATITIS VIRUS GLYCOPROTEIN
WPRE	WPRE (WOODCHUCK HEPATITIS POST-TRANSCRIPTIONAL REGULATORY ELEMENT)
X LINKED-SCID	X-LINKED SEVERE COMBINED IMMUNODEFICIENCY